

**INHIBITION OF CITRATE TRANSPORT INDUCES APOPTOSIS  
IN HEPG2 CELL LINE**



**A Thesis Submitted to the Graduate School of Naresuan University  
In Partial Fulfillment of the Requirements  
for the Master of Science Degree in Physiology  
November 2015  
Copyright 2015 by Naresuan University**

Thesis entitled "Inhibition of citrate transport induces apoptosis in HepG2 cell line"

By Miss Phornpun Phokrai

has been approved by the Graduate School as partial fulfillment of the requirements  
for the Master degree of sciences in Physiology of Naresuan University

**Oral Defense Committee**

..... Bhornprom Y. ..... Chair  
(Assistant Professor Bhornprom Yoysungnoen, Ph.D.)

..... Piyarat Srisawang ..... Advisor  
(Assistant Professor Piyarat Srisawang, Ph.D.)

..... Sukkid Yasothonreekul ..... Co – Advisor  
(Associate Professor Sukkid Yasothonreekul, Ph.D.)

..... Sutatip Pongcharoen ..... Co – Advisor  
(Associate Professor Sutatip Pongcharoen, MD. Ph.D.)

..... Damrongsak Pekthong ..... Internal Examiner  
(Damrongsak Pekthong, Ph.D.)

..... Wantanee Hanchang ..... Internal Examiner  
(Wantanee Hanchang, Ph.D.)

..... Sakchai Wittaya-areekul .....  
(Associate Professor Sakchai Wittaya-areekul, Ph.D.)  
Associate Dean for Research and International Affairs  
for Dean of the Graduate School

27 NOV 2015

## ACKNOWLEDGEMENT

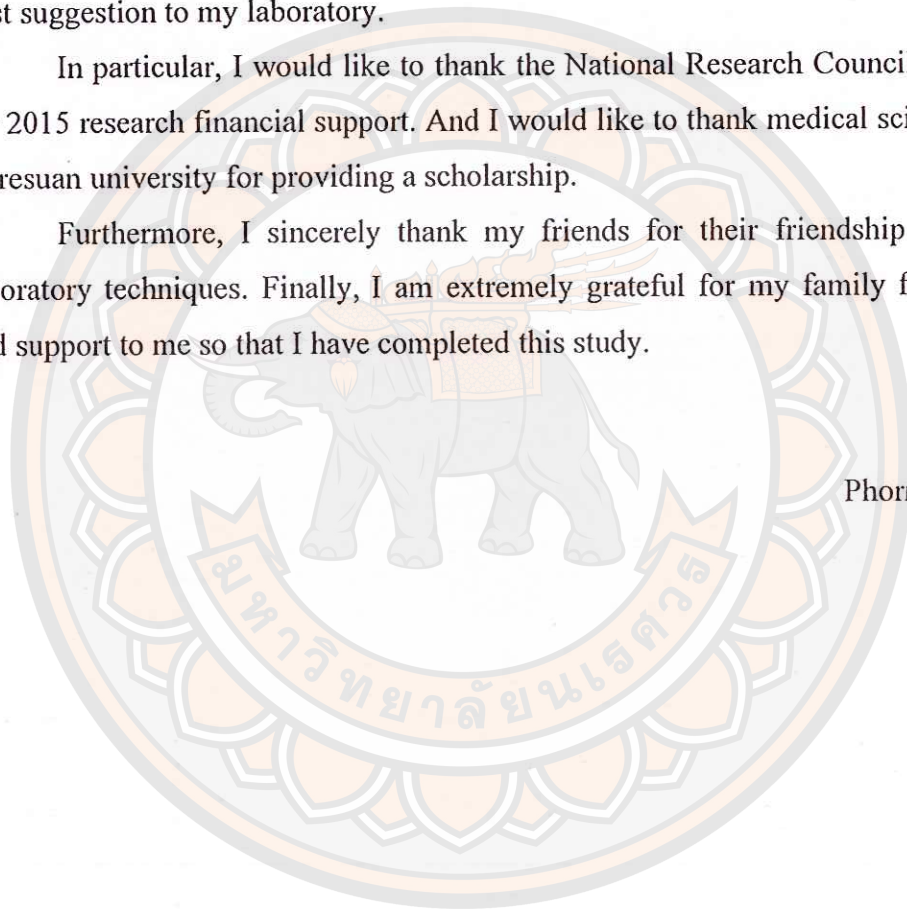
Firstly, I would like to acknowledge my major advisor, Assistant Professor Dr. Piyarat Srisawang, who is a great mentor, excellent teacher, and an ideal researcher.

I would like to special thanks my co-advisors and special teachers, Associate Professor Dr.Sukkid Yasothonsreekul, Associate Professor Dr.Sutatip Pongcharoen, Dr.Dumrongsak Pekthong and Dr.Wandhanee Hanchang for technical assistance and best suggestion to my laboratory.

In particular, I would like to thank the National Research Council of Thailand for 2015 research financial support. And I would like to thank medical science faculty, Naresuan university for providing a scholarship.

Furthermore, I sincerely thank my friends for their friendship and helpful laboratory techniques. Finally, I am extremely grateful for my family for their love and support to me so that I have completed this study.

Phornpun Phokrai





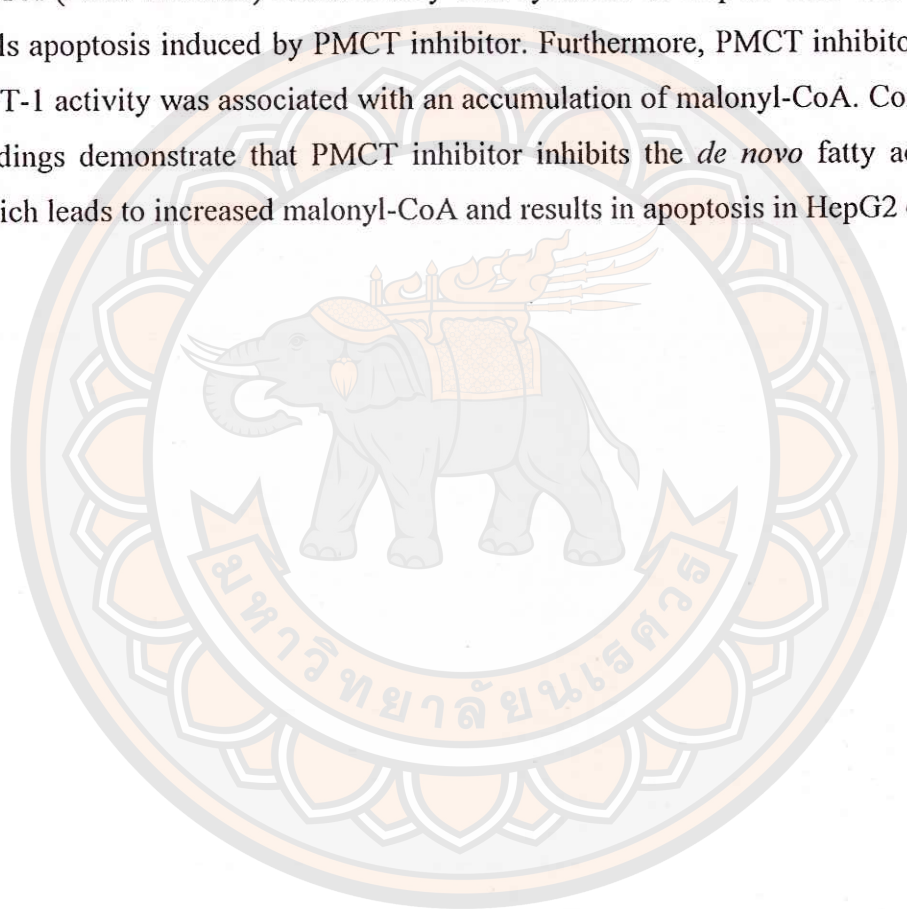
<b>Title</b>	INHIBITION OF CITRATE TRANSPORT INDUCES APOPTOSIS IN HEPG2 CELL LINE
<b>Author</b>	Phornpun Phokrai
<b>Advisor</b>	Assistant Professor Piyarat Srisawang, Ph.D.
<b>Co-Advisor</b>	Associate Professor Sukkid Yasothonsreekul, Ph.D. Associate Professor Sutatip Pongcharoen, M.D., Ph.D.
<b>Keywords</b>	Plasma membrane citrate transporter (PMCT), HepG2 cell, Apoptosis, <i>De novo</i> fatty acid synthesis

### ABSTRACT

Up-regulation of the hypoxia inducible factors (HIFs) in cancer cells switches the cellular ATP-generating system to be exclusively dependent on mitochondrial oxidative phosphorylation (OXPHOS) and rely on glycolysis and  $\beta$ -oxidation. *De novo* fatty acid synthesis, one of the cell energy metabolism, the synthesis of long chain fatty acids (LCFAs). It is highly expressed in many cancer including Hepatocellular carcinoma (HepG2). Suppression of the expression or activities of enzymes that are involved in the synthesis of *de novo* LCFAs in cancer cells causes cell apoptosis. PMCT (Plasma membrane citrate transporter) is one of citrate transporters that cotransports citrate and sodium from the circulation to the intracellular for the *de novo* LCFAs synthesis. A reduction of citrate transport via inhibition of INDY gene activity in *Drosophila* has been found to cause decreased fat content. Thus, PMCT inhibitor will become one of the potential anti-cancer agents acting by inducing apoptosis through an inhibition of citrate transport lead to inhibition of *de novo* fatty acid synthesis. The present study investigated the anti-tumor effect of PMCT inhibitor in inducing apoptosis in HepG2 cells by inhibiting the *de novo* LCFAs synthesis. The present findings showed PMCT inhibitor (0.5-3 mM) increased apoptosis in HepG2 cells. Apoptosis was detected by flow cytometry using a double staining protocol: Annexin and PI dyes. Apoptosis was associated with a dissipation of mitochondrial membrane potential ( $\Delta\Psi_m$ ) measured by a FACScalibur flow cytometer using JC-1 dye-Mitochondrial Membrane Potential Probe. Flow cytometric analysis of 5-(and-6)-chloromethyl-2',7'-dichlorodihydrofluorescein



diacetate, acetyl ester (CM-H<sub>2</sub>DCFDA) stained HepG2 cells showed increased production of reactive oxygen species in PMCT inhibitor-treated cells, indicating that PMCT inhibitor-induced cytotoxicity was mediated reactive oxygen species. PMCT inhibitor-induced apoptosis was associated with inhibition of citrate, triglyceride and free fatty acid levels without any alteration in the abundance of protein fatty acid synthase (FASN), acetyl-CoA carboxylase (ACC), and ATP-citrate lyase (ACL) expressions. However, this study showed that PMCT inhibitor treatment coupling TOFA (ACC inhibitor) reduced fatty acid synthesis in HepG2 cells and could rescue cells apoptosis induced by PMCT inhibitor. Furthermore, PMCT inhibitor-suppressed CPT-1 activity was associated with an accumulation of malonyl-CoA. Conclusion, our findings demonstrate that PMCT inhibitor inhibits the *de novo* fatty acid synthesis which leads to increased malonyl-CoA and results in apoptosis in HepG2 cells.



## LIST OF CONTENTS

Chapter	Page
<b>I INTRODUCTION.....</b>	<b>1</b>
Rational and significant of the study.....	1
Main objectives.....	4
Specific objectives.....	4
The scope of the study.....	4
Conceptual research framework.....	5
Hypothesis.....	6
Keywords.....	6
The anticipated outcomes of the study.....	6
<b>II REVIEW OF RELATED LITERATURE AND RESEARCH.....</b>	<b>7</b>
Hepatocellular carcinoma.....	7
Glucose- and non-glucose metabolism in cancer cells.....	8
Reactive oxygen species (ROS).....	17
Apoptosis.....	20
Plasma membrane citrate transporters.....	26
<b>III RESEARCH METHODOLOGY.....</b>	<b>29</b>
Chemicals and reagents.....	29
Research instrument.....	30
Materials.....	30
Methods.....	30
Statistical analysis.....	36

## LIST OF CONTENTS (CONT.)

Chapter	Page
<b>IV RESULTS.....</b>	<b>37</b>
The effect of PMCT inhibitor on apoptosis in HepG2 cells .....	37
The mechanism of PMCT inhibitor on HepG2 cell apoptosis....	47
<b>V DISCUSSION AND CONCLUSION.....</b>	<b>64</b>
The effect of PMCT inhibitor on apoptosis in HepG2 cells .....	64
The mechanism of PMCT inhibitor on HepG2 cells apoptosis ...	65
<b>REFERENCES.....</b>	<b>70</b>
<b>APPENDIX.....</b>	<b>77</b>
<b>BIOGRAPHY.....</b>	<b>87</b>



## LIST OF TABLE

Table	Page
1 Comparison of morphological features of apoptosis and necrosis.....	21

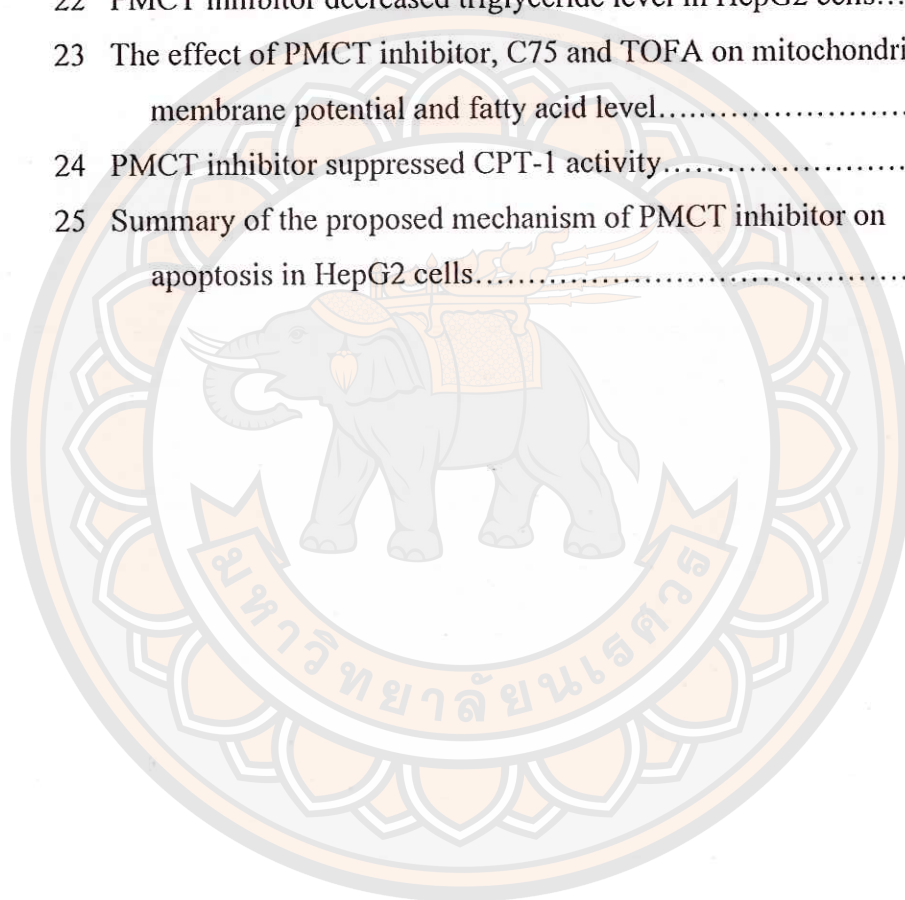


## LIST OF FIGURES

Figures	Page
1 Conceptual research framework.....	5
2 The molecular regulation of de novo fatty acid synthesis and the biochemical fate of saturated long-chain fatty acids.....	11
3 The metabolism of LCFAs.....	12
4 The coupling of elevated fatty-acid metabolism with growth factor signaling in cancer.....	14
5 A proposed apoptotic pathway induced by direct inhibition of the FAS gene.....	16
6 The generation of mitochondrial ROS.....	18
7 The role of mitochondrial ROS in cell apoptosis. ....	19
8 The mechanism of ROS production induced cell apoptosis.....	20
9 The electron micrographs show cells that have died necrosis or apoptosis .....	22
10 Induction of apoptosis by extracellular or intracellular stimuli.....	23
11 The extrinsic pathway, the DISC is the site of activation for caspase-8.....	24
12 The intrinsic and extrinsic apoptosis pathway.....	25
13 The roles of the PMCT and CTP in supplying citrate to fuel hepatic fatty acid, triacylglycerol, and sterol biosynthesis.....	27
14 Dose-dependent inhibitory affected of PMCT inhibitor on the proliferation of HepG2 cells.....	38
15 PMCT inhibitor induced apoptosis in HepG2 cells.....	39
16 PMCT inhibitor induced a damage of mitochondrial membrane potential in HepG2 cells.....	42
17 PMCT inhibitor activated caspase-8 activity in HepG2 cells.....	46
18 PMCT inhibitor increased ROS level in HepG2 cells.....	48
19 PMCT inhibitor decreased citrate level in HepG2 cells.....	51

## LIST OF FIGURES (CONT.)

Figures	Page
20 The effect of PMCT inhibitor on protein expressions in HepG2 cells.....	53
21 PMCT inhibitor decreased fatty acid level in HepG2 cells.....	56
22 PMCT inhibitor decreased triglyceride level in HepG2 cells.....	57
23 The effect of PMCT inhibitor, C75 and TOFA on mitochondrial membrane potential and fatty acid level.....	59
24 PMCT inhibitor suppressed CPT-1 activity.....	63
25 Summary of the proposed mechanism of PMCT inhibitor on apoptosis in HepG2 cells.....	68

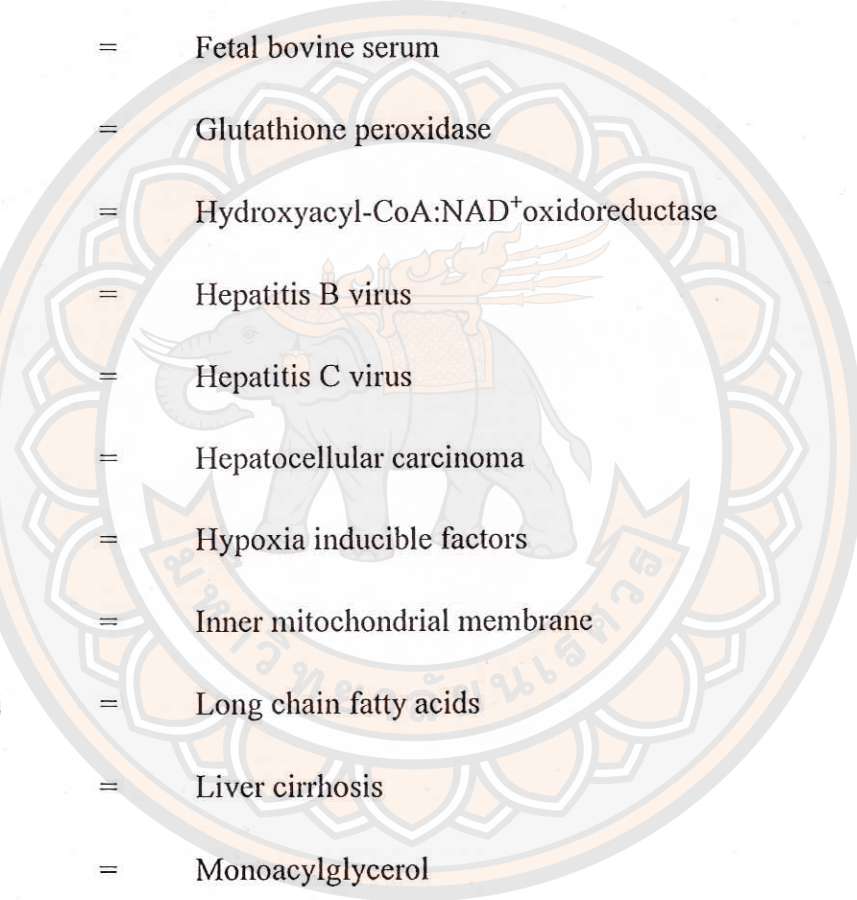




## ABBREVIATIONS

ACAA	=	Acetyl-CoA acyltransferase
ACC	=	Acetyl-CoA carboxylase
ACD	=	Acyl-CoA dehydrogenase
ACLY	=	ATP-citrate lyase
ACS	=	Acyl-CoA synthase
AR	=	Androgen receptor
ATCC	=	American Type Culture Collection
ATP	=	Adenosine triphosphate
BCA	=	Bicinchoninic acid
CCD	=	Charge-coupled device
CO <sub>2</sub>	=	Carbon dioxide
CPT-1	=	Carnitine palmitoyltransferase 1
CTP	=	Citrate transporter protein
DISC	=	Dead-inducing signaling complex
DMSO	=	Dimethyl sulfoxide
DNA	=	Deoxy-ribonucleic acid
ECH	=	Enoyl-CoA hydratase
EDTA	=	Ethylenediaminetetraacetic acid
EGFR	=	Epidermal growth factor receptor

## ABBREVIATIONS (CONT.)



ER	=	Estrogen receptor
Ex/Em	=	Excitation/Emission
FADD	=	Fas-associated dead domain
FASN	=	Fatty acid synthase
FBS	=	Fetal bovine serum
GPO	=	Glutathione peroxidase
HAD	=	Hydroxyacyl-CoA:NAD <sup>+</sup> oxidoreductase
HBV	=	Hepatitis B virus
HCV	=	Hepatitis C virus
HCC	=	Hepatocellular carcinoma
HIFs	=	Hypoxia inducible factors
IMM	=	Inner mitochondrial membrane
LCFAs	=	Long chain fatty acids
LCI	=	Liver cirrhosis
MAG	=	Monoacylglycerol
mM	=	Millimolar
MMP	=	Mitochondrial membrane potential
MPT	=	Mitochondrial permeability transition
MUFA	=	Monounsaturated fatty acid

## ABBREVIATIONS (CONT.)

NaCT	=	Sodium-citrate transporter
NADH	=	Nicotinamide adenine dinucleotide
OAA	=	Oxaloacetate
OLT	=	Orthotopic liver transplantation
OMM	=	Outer mitochondrial membrane
OXPHOS	=	Oxidative phosphorylation
PALMCoA	=	Palmitoyl-CoAs
PBS	=	Phosphate buffered saline
PDH	=	Pyruvate dehydrogenase
PMCT	=	Plasma membrane citrate transporter
PR	=	Progesterone receptor
ROS	=	Reactive oxygen species
SCD-1	=	Stearoyl-CoA desaturase 1
SD	=	Standard deviation
SOD	=	Superoxide dismutase
TCA	=	Tricarboxylic acid
USP2a	=	Ubiquitin-specific-protase 2a



## CHAPTER I

### INTRODUCTION

#### **Rational and significant of the study**

The hepatocellular carcinoma (HCC), the most common form of liver cancer, is one of the leading causes of cancer deaths worldwide. HCC is the cancer that begins in the main type of liver cells (hepatocytes). It is not the same as metastatic liver cancer, which starts in another organ (such as the colon) and spreads out to the liver. In most cases, the risk cause of liver cancer is usually scarring of the liver (cirrhosis)(El-Serag, 2011). Cirrhosis may be caused by alcohol abuse, autoimmune diseases of the liver, and hepatitis B or C virus infection. Patients with hepatitis B or C are at risk of HCC, even if they have not developed cirrhosis. The incidence of epidemic prevalence of HCC is highest in Africa and Asia. Presently, several treatment modalities of this disease are available, including liver resection, orthotopic liver transplantation (OLT), radiotherapy, and chemotherapy. Treatment options of HCC and prognosis are dependent on many factors but especially on tumor size and staging. However, aggressive liver surgery cannot completely remove the cancer and the outcome and prognosis are generally very poor. OLT outcome is also very poor because of it is difficult to find a compatible donor. Chemotherapy and radiation therapy remain largely ineffective. Many research studies testing new treatments are an important option for patients with all stages of liver cancer. Thus, new targeted molecular therapies are emerging and appear to be potential novel chemotherapy (Wörns and Galle, 2010).

Many research studies have proposed that altering energy metabolism especially fatty acid metabolism in cancer cells may afford the possibility of cancer chemotherapy that does not substantially affect normal cells. It has been reported that the energy metabolism of mammalian cancer cell is reprogrammed from aerobic metabolism of glucose, glycolysis and oxidative phosphorylation (OXPHOS) pathways which are demonstrated in normal untransformed cells to be more dominant on *de novo* fatty acid synthesis. The up-regulation of signaling pathways in cancer cell

induces fatty acid metabolism enzyme overexpression in cancer cells. The endogenous synthesis of fatty acid is usually minimal in normal cells because it is dependent of nutritional supply. Fatty acid synthesis is exceptionally high in normal cells including lactating breast, cycling endometrium, liver, and adipose tissues (Fiorentino, et al., 2008). Fatty acid synthesis is implicated in special biological functions including the promotion of cellular processes during cell growth and cell proliferation. The synthesis of fatty acid starts with citrate which is the intermediate from OXPHOS pathway within the mitochondria. Citrate is exported from mitochondria to cytoplasm and is metabolized to acetyl-CoA by ATP-citrate lyase (ACLY) enzyme. The following process is that acetyl-CoA is converted to malonyl CoA by an acetyl-CoA carboxylase (ACC) enzyme. The production of *de novo* fatty acid is catalyzed by the multifunctional lipogenic enzymes called fatty acid synthase (FASN) by the condensation of acetyl-CoA and malonyl-CoA. FASN enzyme then metabolizes malonyl CoA to be saturated long chain fatty acids (LCFAs), such as a palmitate. Palmitate, a 16-carbon saturated long-chain length fatty acids (16:0), are the primary and most abundant end product of FASN activity. After that LCFA is metabolized to monounsaturated fatty acid (MUFA) by stearoyl-CoA desaturase (SCD-1) enzyme. MUFA is the most important constituent of phospholipid cell membrane (Biswas, et al., 2012). MUFA is important for two cellular pathways. The first is the transient storage of cytoplasmic glycerolipid monoacylglycerol (MAG) which prevents lipotoxicity from the high levels of fatty acid synthesis. The other important role of MUFA involves the metabolization of MUFA to be acyl-CoA derivatives for mitochondrial  $\beta$ -oxidation.

Consequently, acetyl CoA production from  $\beta$ -oxidation is imported to TCA cycle to replenish citrate for facilitating the TCA and fatty acid synthesis (Biswas, 2012). It has been reported that the inhibition of fatty acid synthesis causes cell apoptosis, either because there is a lack of the end product fatty acids *per se*, or because there is downstream toxic effects of the activation of malonyl-CoA synthesis pathway (Mason, et al., 2012). An inhibition of fatty acid synthesis in cancer cell may induce apoptosis by increasing ceramide levels that up-regulate proapoptotic gene such as *BNIP3*, *TRAIL*, and *DAPK2* (Bandyopadhyay, et al., 2006). The inhibition of FASN is unable to suppress proliferation of normal cells that have low levels of FASN



expression, suggesting FASN is the selective target of anti-cancer therapeutic drugs (De Schrijver, et al., 2003).

The intracellular citrate is the starting material for the *de novo* fatty acid, triglycerol, and cholesterol synthesis in cancer cells. Two sources of intracellular citrate are identified which are a mitochondrial citrate and an extracellular citrate. Citrate derived from a mitochondrial matrix is an important constituent of OXPHOS or TCA cycle pathway. Mitochondrial citrate is translocated to the cytosol via citrate transporter protein (CTP). A second source of citrate is the extracellular citrate that is imported to the cytosol via plasma membrane citrate transporter (PMCT). This PMCT transports sodium which is coupled to cotransport of citrate and is named NaCT (Sun, et al., 2010). PMCT is found to express in the liver and brain. PMCT in the brain plays a role in producing neurotransmitter. PMCT in the liver is a glucose metabolism controller, acting as an inhibitor of phosphokinase enzyme that plays important roles in fatty acid, triacylglycerol, and cholesterol synthesis (Wang, et al., 2009). Once in the cytoplasm, citrate is metabolized to acetyl-CoA for *de novo* fatty acid synthesis. NaCT was originally discovered in *Drosophila* known as INDY (I'm not dead yet). In *Drosophila*, a reduction of INDY activity causes an increase of average life-span, with a decrease of body size and fat content, without an alteration of either physical activity or fertility. The further mechanism that explains the PMCT inhibition extends life-span involves a caloric restriction, a decrease fatty acid and cholesterol biosynthesis that leads to obesity prevention (Sun, 2010).

Taken together, this present work proposed the mechanism of PMCT inhibition that might apparently be involved the deficiency of the fatty acid levels leading to induction of cancer cell apoptosis. This study is aimed to examine the cytotoxic effect of PMCT inhibitor on intracellular *de novo* fatty acid synthesis pathway that induces apoptosis in HepG2 cells.



### **Main objective**

To investigate the effects and mechanisms of plasma membrane citrate transporter (PMCT) inhibitor on apoptosis in HepG2 cell

### **Specific objectives**

1. To investigate the effect of PMCT inhibitor on HepG2 cell growth and proliferation.
2. To study the effect of PMCT inhibitor on apoptosis in HepG2 cells.
3. To study the effect of PMCT inhibitor on lipid biosynthesis in HepG2 cells

### **The scope of the study**

This study used the HCC cell line (HepG2 cell) to investigate the effects of PMCT inhibitor on cell apoptosis. PMCT inhibitor at the dose of 0.5-3 mM for the 24 hours of incubation period were used. Cell proliferation was determined by MTT assay. Cell apoptosis was evaluated by Alexa Fluor®488 annexin V/propidium iodide (PI) staining. The mitochondrial membrane potential detection was performed using 5,5',6,6'-tetrachloro-1,1',3,3' tetraethylbenzimidazol- carbocyanine iodide (JC-1) dye and determined by using flow cytometric analysis. The cellular events that lead to apoptosis were detected, including the generation of reactive oxygen species (ROS) using the fluorescent dye 5-(and-6)-chloromethyl-2',7'-dichlorodihydrofluorescein diacetate, acetyl ester (CM-H<sub>2</sub>DCFDA) and determined by using flow cytometry and confocal microscopy analysis. The caspase -8 activity, which indicates extrinsic pathway of apoptosis was performed by using fluorometric assay kits. The expression of FASN was detected by immunoblotting assay and confocal microscopy analysis. The activity of FASN was determined by detecting the level of intracellular free fatty acid, triglyceride, and citrate. CPT-1 activity was evaluated by using fluorescence detection. Malonyl-CoA level was detected by using JC-1 dye, which was analyzed by flow cytometry.

### Conceptual research framework

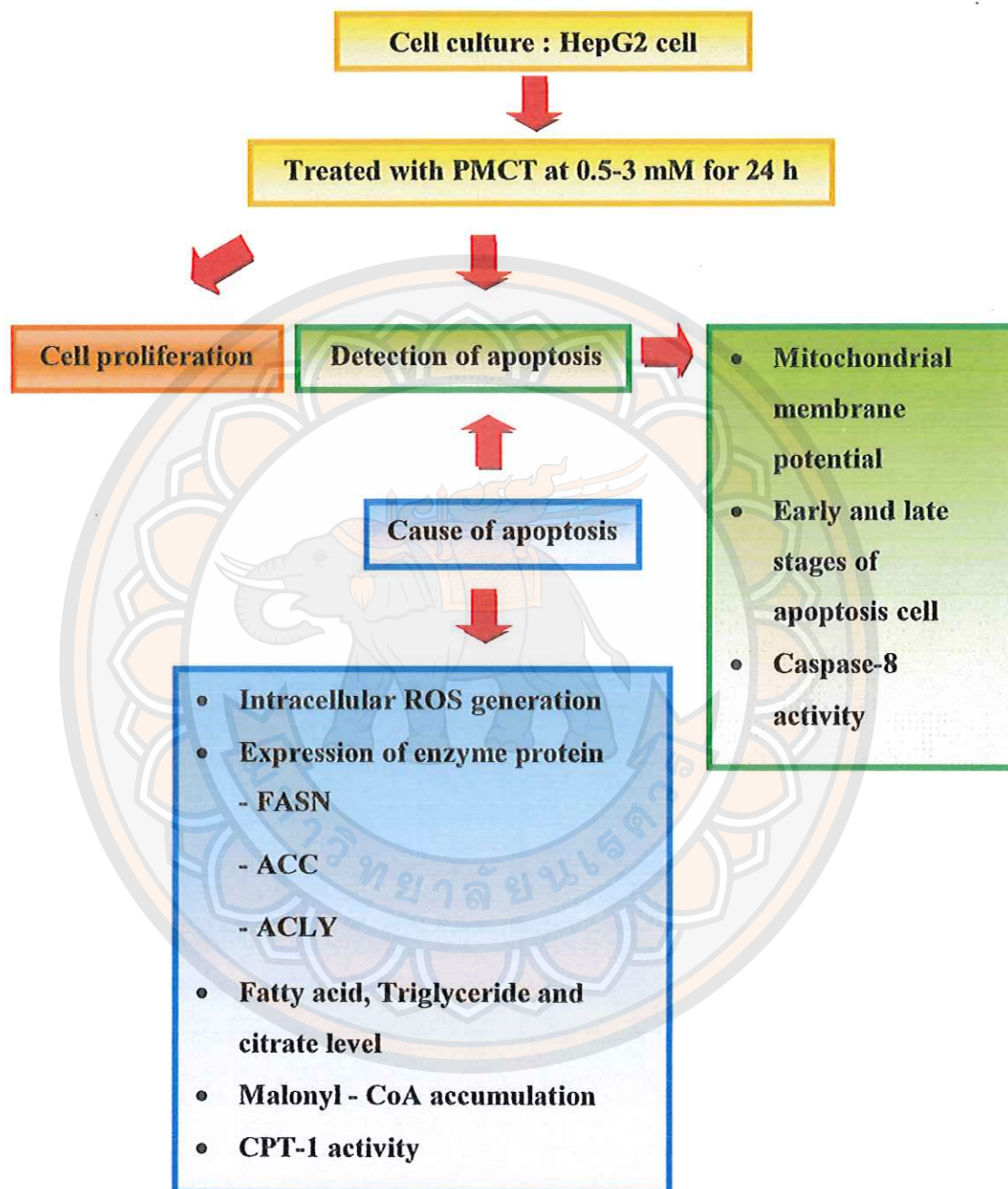


Figure 1 Conceptual research framework

## Hypothesis

PMCT inhibitor couldl inhibit the citrate influx from extracellular to cytosol. Citrate is the starting material for *de novo* fatty acid synthesis, thus decreasing of substrate of *de novo* fatty acid synthesis would cause apoptosis of HepG2 cells that overexpressed enzyme FASN. The mechanism of apoptotic effect of PMCT inhibitor would be possibly involved either the deficiency of the final product LCFA levels *per se* or the downstream steps of the metabolism of fatty acid that builds up toxic intermediates such as malonyl-CoA, or both.

## Keywords

Plasma membrane citrate transporter (PMCT), HepG2 cell, Apoptosis, *De novo* fatty acid synthesis

## The anticipated outcomes of the study

The results from this study would demonstrate the effects and mechanisms of PMCT inhibitor on apoptosis of HepG2 cells which is induced by a decrease of *de novo* fatty acid synthesis in these cells. The inhibition of PMCT would be selective to suppress proliferation in cancer cells that have overexpression of fatty acid synthesis but not in normal cells. The inhibition of fatty acid synthesis would lead to either deficiency in fatty acid available for cell proliferation or accumulation of toxic intermediates of this pathway or both, which in turn would enhance apoptosis in cancer cells. Base on these results, we will propose a model for the apoptotic pathway induced by suppression of cancer energy metabolism which is resulted from PMCT inhibition. The information from this study would outline an important link between fatty acid synthesis and cancer cell survival. It will be interesting to test this proposed pathway in an animal model and will provide the useful insights into the clinical studies as a new drug cancer chemotherapy.



## CHAPTER II

### REVIEW OF RELATED LITERATURE AND RESEARCH

#### Hepatocellular carcinoma

The hepatocellular carcinoma (HCC) or liver cancer is responsible for a large proportion of cancer deaths worldwide. The major etiologies and risk factor of this disease is usually the scarring of the liver or liver cirrhosis (LCI) or a chronic liver disease, such as hepatitis B and hepatitis C infection and aflatoxin B1. The incident rate of this disease is more common in parts of Africa and Asia than in North or South America and Europe. Patients with hepatitis B or C are at risk for liver cancer, even if they have not developed cirrhosis (Bialecki and Di Bisceglie, 2005). Chronic hepatitis virus B (HBV) infection is the leading cause of HCC in Asia and Africa and hepatitis virus C (HCV) infection is the leading cause of HCC in Europe, Japan, and North America. Aflatoxin B1 is produced by fungi of the *Aspergillus* species and is a common contaminant of grain, nuts, and vegetables in some parts of Asia and Africa. Aflatoxin B1 has also been implicated as a cofactor in the etiology of primary liver cancer in HBV carriers because it enhances the neoplastic risk. The life expectancy of patients with HCC is poor, with a mean survival of 6–20 months and likely reflects the mortality/incidence ratio, which is close to 1. At present, several treatment modalities are available, including resection, orthotopic liver transplantation (OLT), chemotherapy, and radiotherapy. The treatment options are dictated by the stage of liver cancer and the overall condition of the patient.

Surgical removal of HCC offers the best chance for possible cure. Resection can involve removing anything from a small wedge of liver but is limited by a high rate of recurrence. Many patients who undergo hepatic resections will develop a recurrence of liver cancer elsewhere in the liver within several years. The success of local ablation is usually about 80% of the case with localized HCC or in lesions < 3 cm and survival rates are about 50% in 5 years of recurrence. However, most patients with liver cancer also have cirrhosis of the liver and would not tolerate liver resection surgery. Orthotopic liver transplantation (OLT) is suitable for patients with



one tumor nodule less than 5 cm without macrovascular invasion but it is hard to find the matching between donor and patient. Chemotherapy and radiation therapy remain largely ineffective. However, chemotherapy may cause more severe side effects in people with cirrhosis because the drug damages both cancer and normal cell, this is known as systemic treatment (Wörns, 2010).

### **Glucose and non-glucose metabolism in cancer cells**

The energy metabolism of cancer cells is defined to be different from normal cell. The well-oxygenated untransformed cells rely primarily on both glycolysis and mitochondrial oxidative phosphorylation (OXPHOS) pathways for their energy production which is probably dependent on oxygen available and energy demand in the cells. The contribution ratio of glycolysis and OXPHOS varies in different conditions of cells in order to maintain the cellular energy balance or the constant of ATP production. Under aerobic condition, cell is supplied by 70% ATP production from OXPHOS, while under hypoxic condition, glycolysis plays a major role to contribute cellular ATP production with the weakened function of OXPHOS. In contrast to normal cells, the glycolysis pathway becomes enhanced regardless of the presence of oxygen. This refers to the aerobic glycolysis or Warburg effect which was first discovered by Otto Warburg in 1920s (Warburg, 1956). It was proposed that aerobic glycolysis in tumor cells resulted from the defect of OXPHOS. However, this conclusion has been challenged by an observation that aerobic glycolysis in cancer cells is one of common energy metabolism pathways that contributes to ATP production even the function of OXPHOS is intact. It has been found that OXPHOS is suppressed under the enhanced glycolysis rather than the defective of this pathway (Jose, et al., 2011), (Smolkova, et al., 2011). On the other hand, OXPHOS is still enhanced and contributes for more than 50-90% of ATP supply in various cancer cells under the aerobic condition. This contribution is found to be reduced to less than 40% in hypoxic condition (Rodriguez-Enriquez, et al., 2010). Thus, in order to meet their energy demands, the balance of cellular energy production in cancer cells is reserved and compensated under the changes of microenvironmental conditions. The glycolytic pathway in cancer cells may be primarily regulated by the hypoxic condition. However, the oncogene-mediated signaling and the hypoxia inducible factors (HIFs)

have been proposed to control the switching of OXPHOS into glycolytic pathways. Furthermore, during the past 20 years, the knowledge about the biology of tumor metabolism have demonstrated the importance of other non-glucose metabolisms, the *de novo* fatty acid synthesis and  $\beta$ -oxidation (Biswas, 2012).

Glucose metabolism is not the only one energy fuel in cancer cells. Importantly, these anaerobic-glucose and non-glucose metabolisms may be as important as OXPHOS and occur concurrently in tumor cells. The switching of aerobic OXPHOS metabolism to anaerobic pathways for ATP production in cancer cells occurs to adapt to unfavorable microenvironmental changes especially under the suboptimal oxygen availability. However, cancer cells have a tendency to turn to anaerobic glycolysis and non-glucose metabolism pathways even in the presence of high oxygen tension. The proportions of ATP generating systems of tumor cells depend on both their genetic background and microenvironment (Koukourakis, et al., 2006). The key transcription, namely HIFs, have been suggested to control the expression of genes responsible to control glucose- and non-glucose metabolisms in cancer cells (Koukourakis, et al., 2006). The Akt oncogene is known to activate HIFs and in turn upregulates enzymes involved in anaerobic glycolysis and non-glucose metabolism as well as suppresses the activity of enzymes involved in the oxidation of pyruvate for OXPHOS pathway. Consequently, the glucose oxidative metabolism is partially inhibited and the cytoplasmic pyruvate is converted to lactate. The expression of OXPHOS enzymes and transporters as well as the amount of mitochondria per cell found to be suppressed in certain cancer cells.

Since cancer cells have a higher proliferation than normal cells. ATP generation from an aerobic glycolysis is suitable for cancer cells energy demands because of the higher speed of ATP generation offers growth advantage, despite the less of ATP production is found in glycolysis. The acidity of extracellular environment which is produced from lactate product of glycolysis provides the good environment for cancer cell growth, invasion, and metastasis. The OXPHOS is retained to serve the intermediates for the biosynthesis of macromolecules, such as lipids, proteins, and nucleic acids. The metabolism of glutamine to  $\alpha$ -ketoglutarate ( $\alpha$ -KG) is one of alternative pathways that offer cells able to use OXPHOS pathway for ATP production in certain cancer cells by supplying intermediates for OXPHOS pathway (Scott, et al.,



2011). In addition, glutamine provides precursor, citrate, for the synthesis of lipid in the *de novo* fatty acid pathway.

In order to meet their requirement of growth and proliferation, glucose is not the only dominant energy fuel for most cancer cells. The *de novo* fatty acid synthesis pathway is widely accepted as a better pathway for energy production under an inefficient ATP generation from glycolysis.

The synthesis of fatty acid begins with citrate which is the intermediate from OXPHOS pathway within the mitochondria. Under aerobic conditions, the end product of glycolysis is pyruvate that enters the mitochondria where it is oxidized to acetyl-CoA for starting the tricarboxylic acid (TCA) cycle (Zheng, 2012). Citrate, the first intermediate of TCA cycle, is formed by the catalyzation reaction of acetyl-CoA with oxaloacetate (OAA) (Mashima, et al., 2009). It is translocated to the cytosol and exerts negative feed back on glycolysis (Pasteur effect) and the TCA cycle. The cytosolic citrate is cleaved by enzyme ATP-citrate lyase (ACLY) to be acetyl-CoA and OAA (Icard, et al., 2012). The carboxylation of acetyl-CoA to form malonyl-CoA is catalyzed by the acetyl-CoA carboxylase enzyme (ACC). The active form of ACC is activated by citrate. The product of this pathway, the long-chain fatty acyl-CoA inactivates this enzyme. The production of *de novo* fatty acid is catalyzed by the multifunctional dimeric lipogenic enzymes called fatty acid synthase (FASN) by the condensation of acetyl-CoA and malonyl-CoA. Palmitate, a 16-carbon saturated long-chain length fatty acids (16:0) or LCFAs, are the primarily and most abundant end product of FASN activity. Palmitate is desaturated by steroyl-CoA desaturase (SCD-1) to monounsaturated fatty acid (MUFA) which is the most important constituent of phospholipid in cell membrane structure (Figure 2).



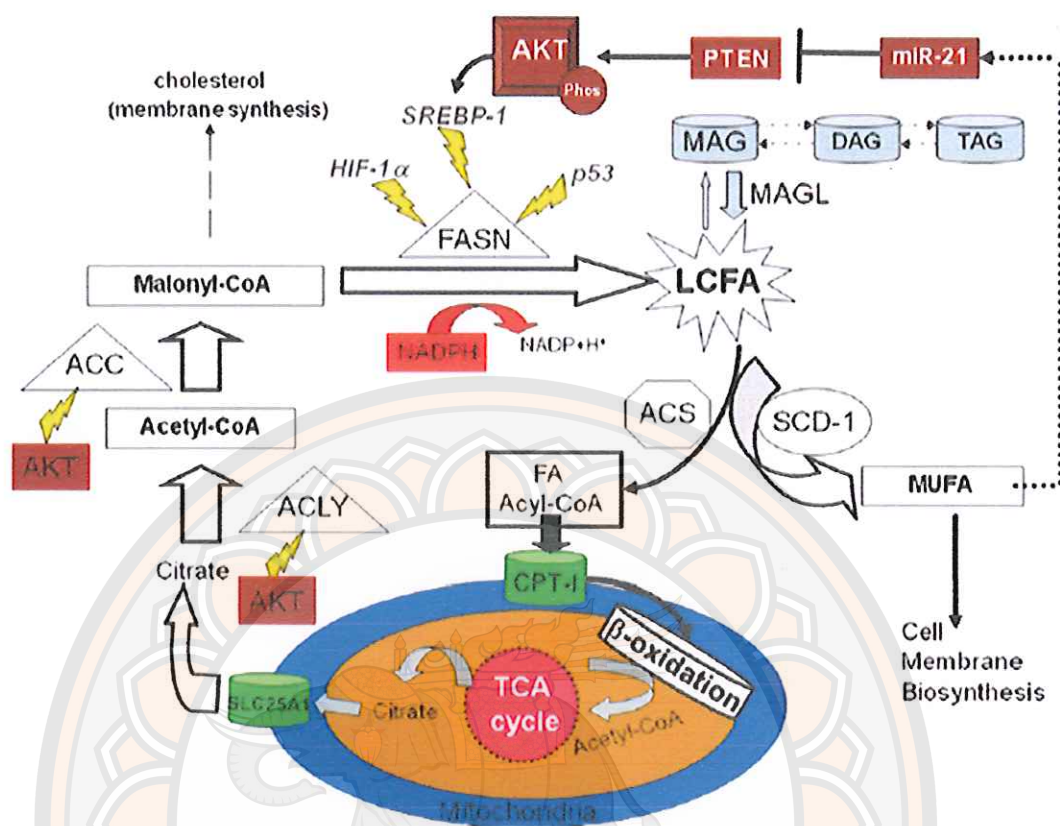


**Figure 2 The molecular regulation of de novo fatty acid synthesis and the biochemical fate of saturated long-chain fatty acids**

Source: <http://www.ncbi.nlm.nih.gov/pubmed/22706846>

The fatty acid content in normal cells is derived from the diet and from the *de novo* fatty acid synthesis pathway. The large proportion of fatty acids in cells is supplied by the diet. The excess of body's needs for carbohydrates and proteins obtained from the diet can be converted to fatty acid in the form of storage triacylglycerols. However, the *de novo* fatty acid synthesis occurs minimally in most normal cells with the exception of the liver, adipose tissues, and the lactating mammary glands. In humans, the cytosolic LCFAs are imported into mitochondria for  $\beta$ -oxidation.

The first reaction of this pathway is the metabolism of LCFAs to acyl-CoA derivatives by acyl-CoA synthase (ACS). Fatty acyl-CoAs, such as palmitoyl-CoAs (PALMCoA) are subsequently esterified to their L-carnitine derivatives by carnitine palmitoyltransferase 1 (CPT-1) on the surface of the outer mitochondrial membrane. They are imported into mitochondria for  $\beta$ -oxidation. Fatty acyl-CoA is then metabolized by 4 enzymes which are acyl-CoA dehydrogenase (ACD), hydroxyacyl-CoA:NAD<sup>+</sup> oxidoreductase (HAD), enoyl-CoA hydratase (ECH) and acetyl-CoA acyltransferase (ACAA2) to produce Fatty acetyl CoA and are translocated to TCA cycle to replenish citrate (Biswas, 2012) (Figure 3).

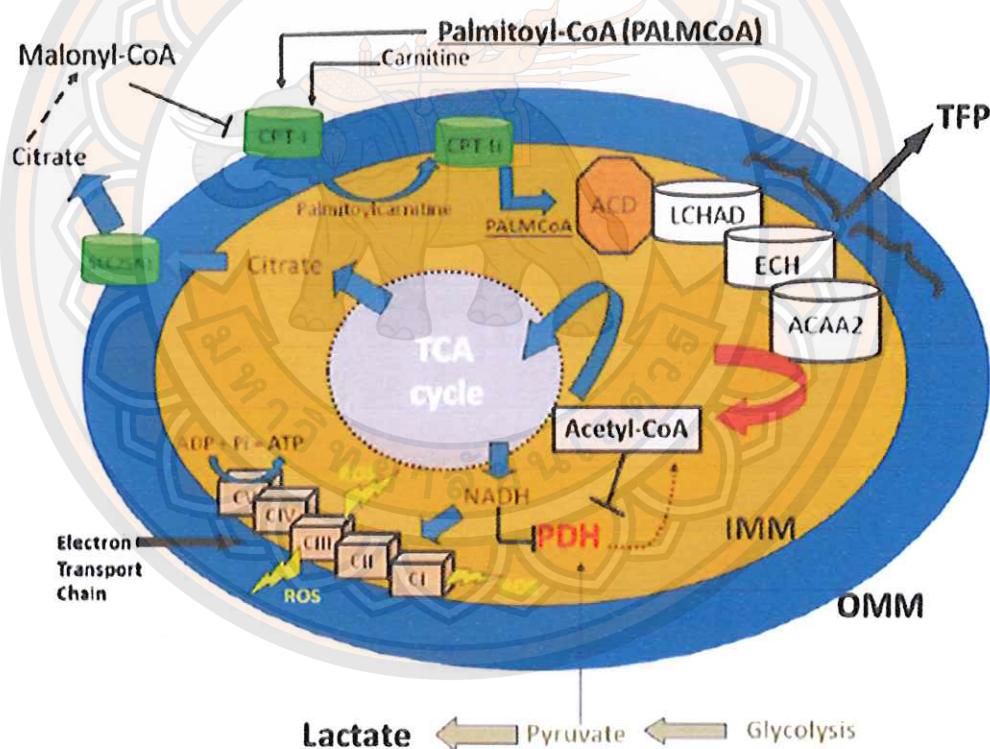
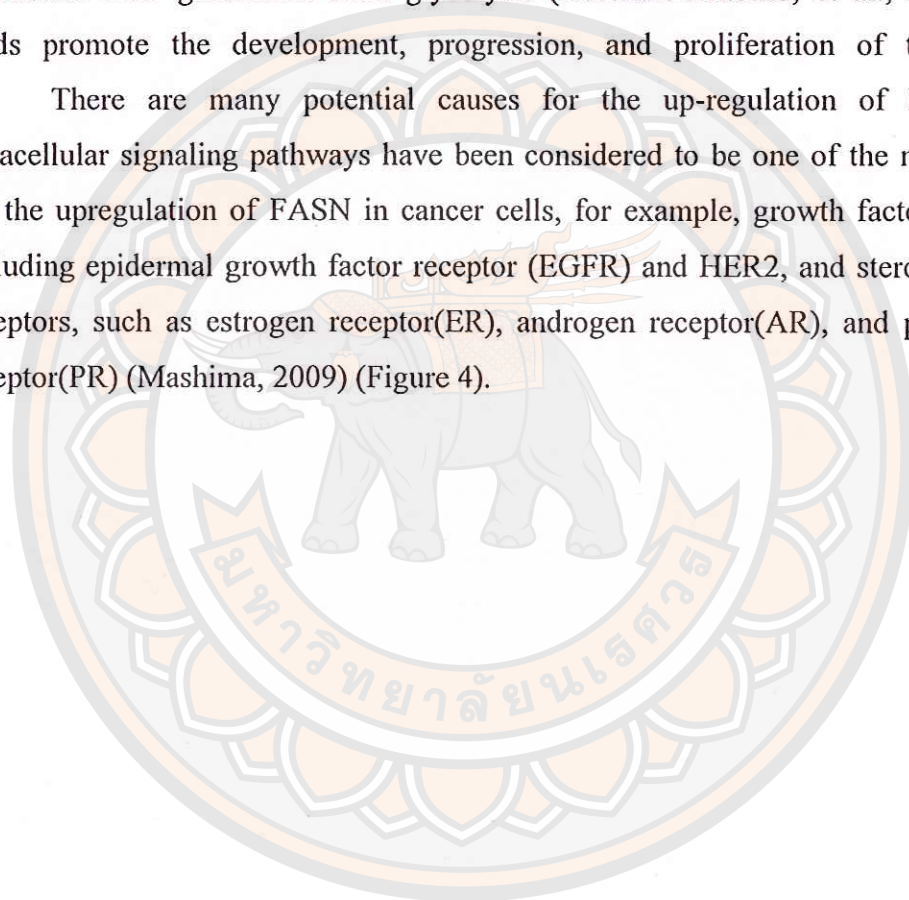


**Figure 3 The metabolism of LCFAs**

Source: <http://www.ncbi.nlm.nih.gov/pubmed/22706846>

It has been reported that FASN expression is undetectable in most normal cells. In contrast, in a variety of cancer cells, the *de novo* fatty acid synthesis is elevated. It has been reported that FASN is overexpressed and correlated with tumorigenesis. An elevated rate of *de novo* fatty acid synthesis than dietary supplementation is defined as one of the major adaptive hallmark mechanisms which provide fatty acid precursors for membrane lipid and signaling molecules synthesis, and lipid  $\beta$ -oxidation pathway to overcome the restriction of microenvironment and an inefficient ATP generation from glycolysis (Resendis-Antonio, et al., 2010). Fatty acids promote the development, progression, and proliferation of tumor cells.

There are many potential causes for the up-regulation of FASN. The intracellular signaling pathways have been considered to be one of the major causes for the upregulation of FASN in cancer cells, for example, growth factor receptors, including epidermal growth factor receptor (EGFR) and HER2, and steroid hormone receptors, such as estrogen receptor(ER), androgen receptor(AR), and progesterone receptor(PR) (Mashima, 2009) (Figure 4).





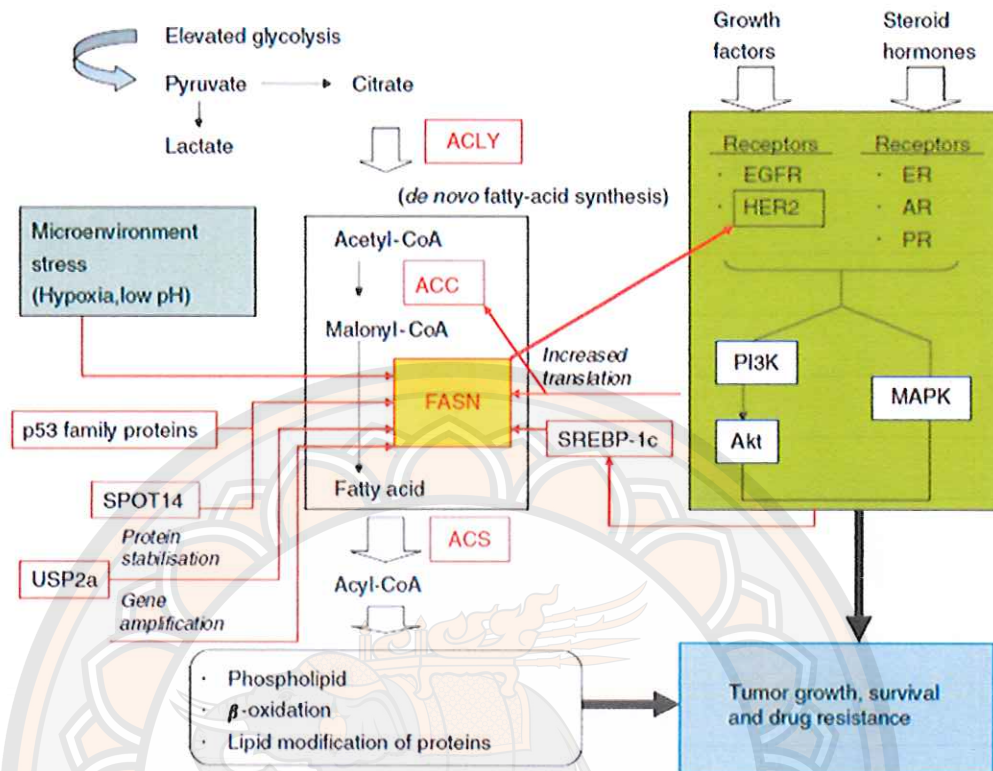


**Figure 4 Coupling of elevated fatty-acid metabolism with growth factor signaling in cancer**

Source: <http://www.ncbi.nlm.nih.gov/pubmed/19352381>

The regulation of protein stability and degradation by a signaling protein  $\beta$ -catenin (Gelebart, et al., 2012) as well as post-transcriptional regulation by ubiquitin-specific-protase 2a (USP2a) and isopeptidase proteins (Yoon, et al., 2007) have been reported to play a role in upregulating FASN expression in cancer cells. Hypoxic-inducible factor-1 $\alpha$  (HIF-1 $\alpha$ ) has recently been known to be activated by a single oncogene *Akt*, which up-regulates downstream enzymes responsible for energy metabolism of cancer cells, the aerobic glycolysis and *de novo* fatty acid synthesis pathways (Koukourakis, 2006).

Many experimental studies have suggested that the treatment of cancer cells with the pharmacologic inhibitor of FASN (Zhou, et al., 2003) or siRNAs against the *FAS* gene (Mason, 2012 and Bandyopadhyay, 2006) causes cell growth inhibition and

apoptosis. The cytotoxic effect of the depletion of FASN in cancer cells is rescued by palmitate, stearate, or oleate, suggesting fatty acid synthesis is required for cell viability (Mason, et al., 2012). The novel pharmacologic FASN inhibitor is C75 which exerts a selective apoptosis induction by blocking of the covalent reaction of acetate with malonate at the  $\beta$ -ketoacyl condensation step of fatty acid biosynthesis. It also has unfavorable side effects, including anorexia and body weight loss as a result of its direct stimulation on CPT-1 activity (Zhou, et al., 2007). These drawbacks apparently limit any potential clinical application and development of C75. The inhibition of FASN is unable to suppress proliferation of normal cells that have low levels of FASN expression, suggesting FASN is the selective target of anti-cancer therapeutic drugs (De Schrijver, 2003).

The mechanism of cytotoxic effect of FASN inhibitors is apparently involved the deficiency of the final product LCFA levels *per se* or the downstream steps of the metabolism of fatty acids. An increase of malonyl-CoA which is resulted from FAS inhibition is responsible for cytotoxicity and induces apoptosis in cancer cells. Application of ACC inhibitor activity by 5-(tetradecyloxy)-2-furoic acid (TOFA), the competitive inhibitor of ACC enzyme that catalyzes the synthesis of malonyl-CoA, rescues cancer cells from the apoptotic effect of the inhibition of fatty acid synthesis (Mason, 2012). This evidence suggests that additional mechanisms apart from the depletion of fatty acid may be necessary for the cytotoxicity following FASN inhibition (Lin, et al., 2012). As a result of FASN inhibition, malonyl-CoA levels are continuously produced by ACC action and that malonyl-CoA exerts a concomitant inhibition of carnitine palmitoyltransferase-1 (CPT-1) activity. Thus, a high level of malonyl-CoA is one of major causes of apoptosis in cancer cell (Pizer, et al., 2000).



CPT-1 allows the entry of fatty acid into mitochondrial for fatty acid  $\beta$ -oxidation to replenish intermediaries in Krebs cycle. Interestingly, inhibition of CPT-1 lead to accumulation of fatty acyl-CoA which subsequently increases the levels of the toxic sphingolipid product, ceramide. This sphingolipid is known to implicate in apoptosis (Paumen, et al., 1997). Thus, this indicates that FASN inhibition and its downstream accumulation of malonyl-CoA account for cytotoxicity by inducing apoptosis cell death (Wang, 2009). (Figure 5) In addition, FASN inhibition may lead to the up-regulation of proapoptotic gene *BNIP3*, *TRAIL*, *DAPK2* expression that augment apoptosis in MCF-7 (Bandyopadhyay, 2006).

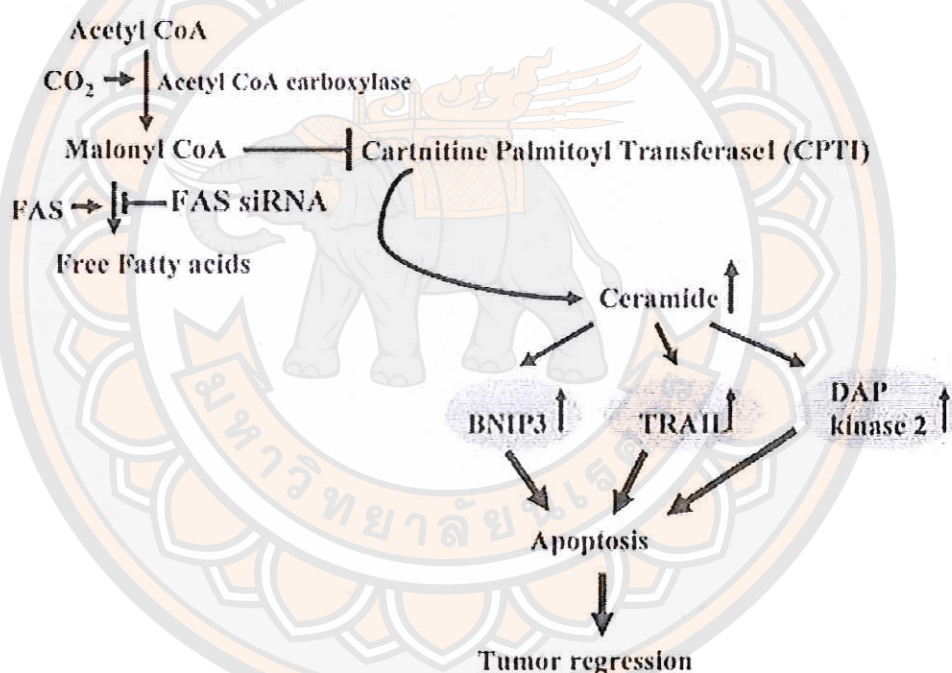


**Figure 5** A proposed apoptotic pathway induced by direct inhibition of the FAS gene

Source: <http://www.ncbi.nlm.nih.gov/pubmed/16740734>



This finding therefore provides evidence supports the suggestion that FASN is considered to be a potential therapeutic target of cancer cells which are mediated via fatty acid depletion, malonyl-CoA accumulation, and fatty acid  $\beta$ -oxidation inhibition and in turn induce apoptosis (Pandey, et al., 2011).

### Reactive oxygen species (ROS)

Reactive oxygen species (ROS) contain oxygen ion and the chemical activity of the peroxidase molecule. ROS including hydroxyl radicals, superoxide anions, singlet oxygen and hydrogen peroxide are generated by product of cellular metabolism (Crack and Taylor, 2005). ROS are generated by inflammatory cells and cause both DNA and protein damage (Simon, et al., 2000). Normally, the cellular redox balance is maintain by antioxidant enzymes, including catalase, superoxide dismutases and reduced glutathione usually protect tissue damage (Yaffe, et al., 2013).

Figure 6 shows that mitochondria are the major site of ROS production. The ubiquinone site in complex III in the respiratory chain appears as the major site of mitochondrial ROS production. This site catalyzes the conversion of molecular oxygen to the superoxide anion radical ( $O_2^-$ ) by a single electron transfer to molecular oxygen (Fleury, et al., 2002). A major pathway of ROS generation occurs is through the reduction of molecular oxygen to  $H_2O$ . The reduction of the dioxygen molecule produces the superoxide anion radical ( $O_2^-$ ) and hydrogen peroxide. The transition metals such as  $Fe^{2+}$ ,  $H_2O_2$  can suffer the Fenton reaction, which leads to enhanced levels of the hydroxyl radical. The hydroxyl radical is the most responsible for oxidative damage (Crack, 2005). Superoxide production by mitochondria in the presence of nitric oxide results in peroxynitrite ( $ONOO^-$ ). A number of antioxidant enzymes including superoxide dismutase (SOD) reduce oxygen free radical concentrations. SOD converts  $O_2^-$  to  $H_2O_2$ , whereas glutathione peroxidase (GPO) convert  $H_2O_2$  to  $H_2O$  resulting in reduce levels of ROS (Fleury, 2002). Increasing free radical formation or decreasing antioxidant defenses results in oxidative stress, leading to lipid, protein, and DNA damage. Finally, this leads to cell death via apoptotic or necrotic pathways (Crack, 2005).

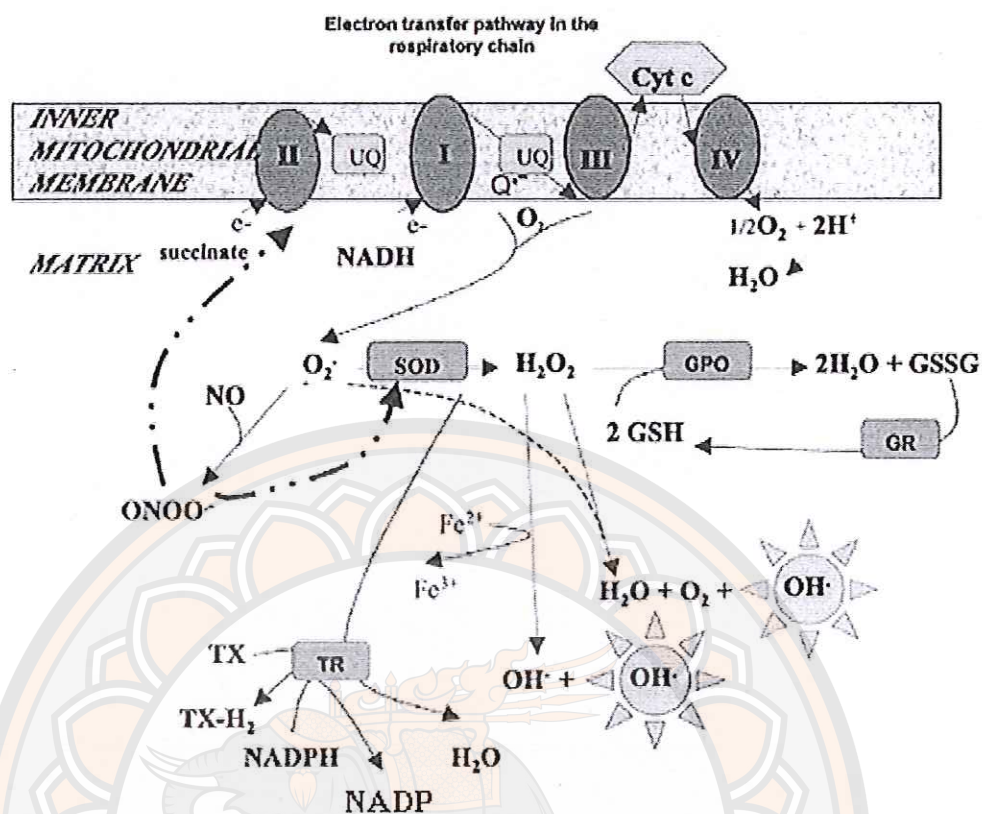
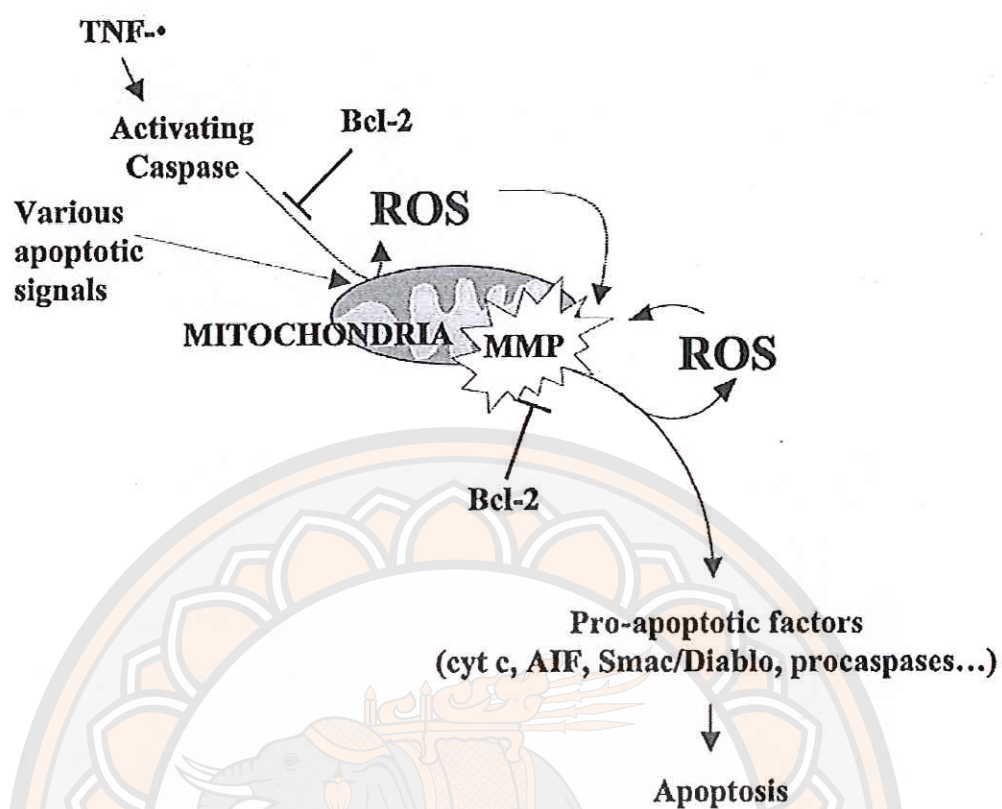


Figure 6 The generation of mitochondrial ROS

Source: <http://www.ncbi.nlm.nih.gov/pubmed/12022944>.

As shown in figure 7, accumulation of ROS induced mitochondrial membrane alteration. Mitochondria can induce cell death by releasing of pro-apoptotic factors such as pro-caspase, caspase activator or caspase-independent factor such as AIF (Fleury, 2002). Figure 8 shows that ROS production caused the loss of mitochondrial membrane potential ( $\Delta\Psi_m$ ), which induces cytochrome c release and caspase-9/-3 activation. Furthermore, p53-mediates ROS production, which activates p38 kinase, and the activated p38 can stimulate the p53 (Huang, et al., 2008).



**Figure 7** The role of mitochondrial ROS in apoptosis. (TNF- $\alpha$  and mitochondrial ROS production can induces apoptosis by acting on MMP and release pro-apoptotic factor)

Source: <http://www.ncbi.nlm.nih.gov/pubmed/12022944>



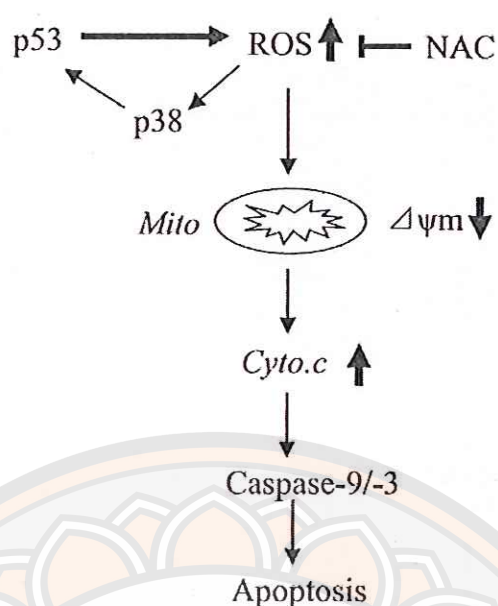


**Figure 8 The mechanism of ROS production induced cell apoptosis**

Source: <http://www.ncbi.nlm.nih.gov/pubmed/18719315>

### Apoptosis

Apoptosis normally occurs as a homeostatic mechanism to maintain the number of cells by balancing the rate of cell division and cell death. Apoptosis also occurs when immune reactions or cells are damaged by disease or many stimuli, such as heat, radiation, hypoxia and toxic chemicals. There are many conditions that trigger apoptosis for example, the damage of DNA in some cells, which can lead to activate *p53*-dependent pathway. Apoptosis can be identified by investigating various morphological changes in cells. The apoptotic cell is round or oval shape. During the early apoptosis, cell shrinkage and pyknosis are observed which is resulted from the nuclear envelope disassembles, DNA breaks into fragments, and chromatin condensation. When cell shrinkage, the size of cells is smaller, the cytoplasm is condensed and the organelles are more cramped. The organelles are enclosed within an intact plasma membrane that is blebbing. This process is called “budding”. The apoptotic cell is digested by macrophages, parenchymal cells, or neoplastic cells.

As shown in table 1 and figure 9 below, morphological changes of apoptosis are different from necrosis. Cells that undergo necrosis are injured and die as a result of inflammatory responses. The necrotic cells will be swelling, formation of cytoplasmic blebs, ruptured mitochondria, disrupted organelle membrane and cell membrane, and cell burst. Necrotic cells release their cytoplasmic content to all over surrounding tissues. In contrast, cells undergo apoptosis die without releasing of their cellular constituents into tissue and damaging their neighbors (Elmore, 2007).

**Table 1 Comparison of morphological features of apoptosis and necrosis**

Apoptosis	Necrosis
Single cells or small clusters of cells	Often contiguous cells
Cell shrinkage and convolution	Cell swelling
Pyknosis and karyorrhexis	Karyolysis, pyknosis and karyorrhexis
Intact cell membrane	Disrupted cell membrane
Cytoplasm retained in apoptotic bodies	Cytoplasm released
No inflammation	Inflammation usually present

**Source:** <http://www.ncbi.nlm.nih.gov/pmc/articles/PMC2117903/>



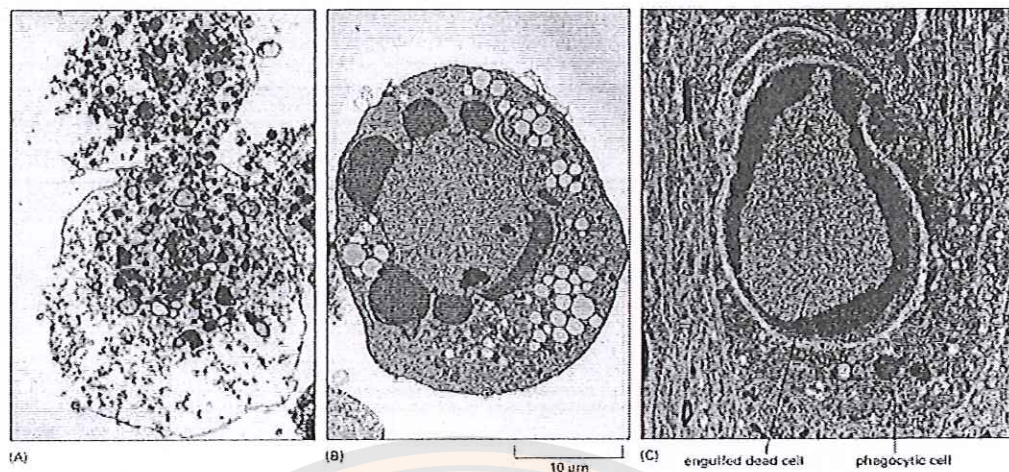


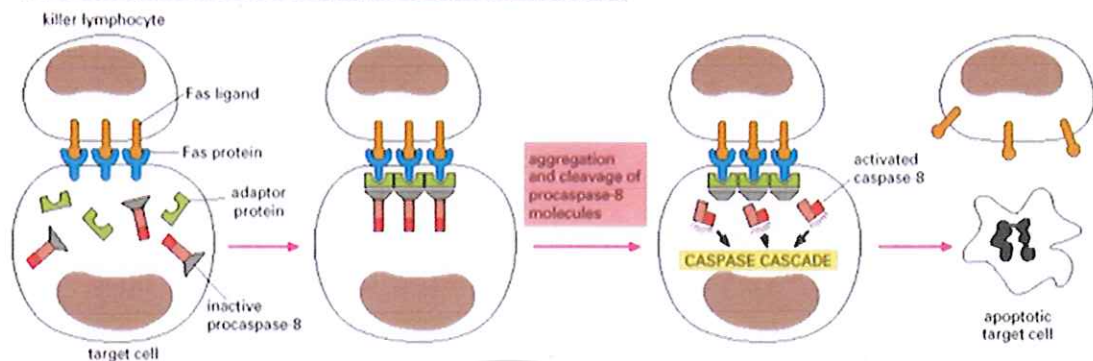
**Figure 9** The electron micrographs show cells that have died necrosis or apoptosis. (Note that the cell in (A) apoptotic cell seems to have exploded, whereas those in (B,C) necrotic cell have condensed but seem relatively intact. The large vacuoles visible in the cytoplasm of the cell in (B) are a variable feature of apoptosis.)

**Source:** <http://www.ncbi.nlm.nih.gov/books/NBK26873/figure/A3249/>

The apoptotic mechanism have two main pathways which are extrinsic and intrinsic pathways (Figure 10). The extrinsic pathway is initiated by cytoplasmic adaptor proteins (Fas-associated dead domain, FADD) or (TNF receptor-associated death domain, TRADD) is recruited to the ligand-activated dead receptor (Figure 12). The transmembrane dead receptors are the members of the tumor necrosis factor (TNF) receptor gene super family. The best characterized death receptors are CD95 (APO-1/Fas), TNF receptor 1 (TNFR1), TNF-related apoptosis-inducing ligand-receptor 1 (TRAIL-R1) and TRAIL-R2. The binding of the ligand, such as Fas to the dead receptor results in recruitment of the adapter protein which in turn results in the association of procaspase-8 to FADD (Elmore, 2007).



(A) **ACTIVATION OF APOPTOSIS FROM OUTSIDE THE CELL (EXTRINSIC PATHWAY)**



(B) **ACTIVATION OF APOPTOSIS FROM INSIDE THE CELL (INTRINSIC PATHWAY)**

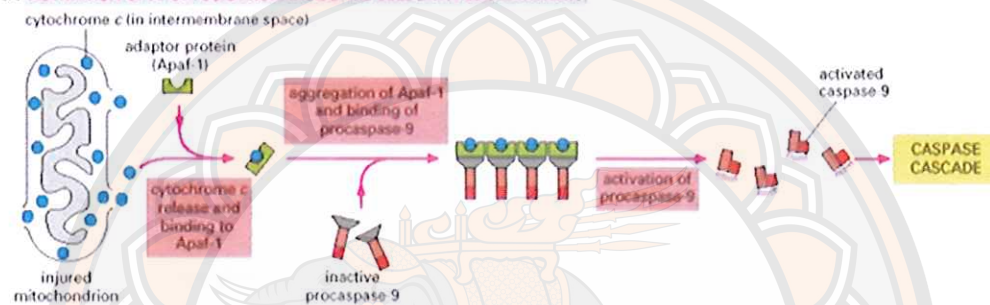


**Figure 10 Induction of apoptosis by extracellular or intracellular stimuli. ((A) Extrinsic pathway; adaptor proteins bind to the intracellular region of aggregated Fas proteins, causing the aggregation of procaspase-8 molecules. These then cleave one another to initiate the caspase cascade. (B) Intrinsic pathway; mitochondria release cytochrome *c*, which binds to and causes the aggregation of the adaptor protein Apaf-1. Apaf-1 binds and aggregates procaspase-9 molecules, which triggers a caspase cascade.)**

Source: <http://www.ncbi.nlm.nih.gov/books/NBK26873/>

As shown in figure 11, the sequence of events are the formation of a death-inducing signaling complex (DISC) which leads to the activation of caspase-8. Then, the activated caspase-8 activates caspase-3, and -7. (Boatright and Salvesen, 2003).

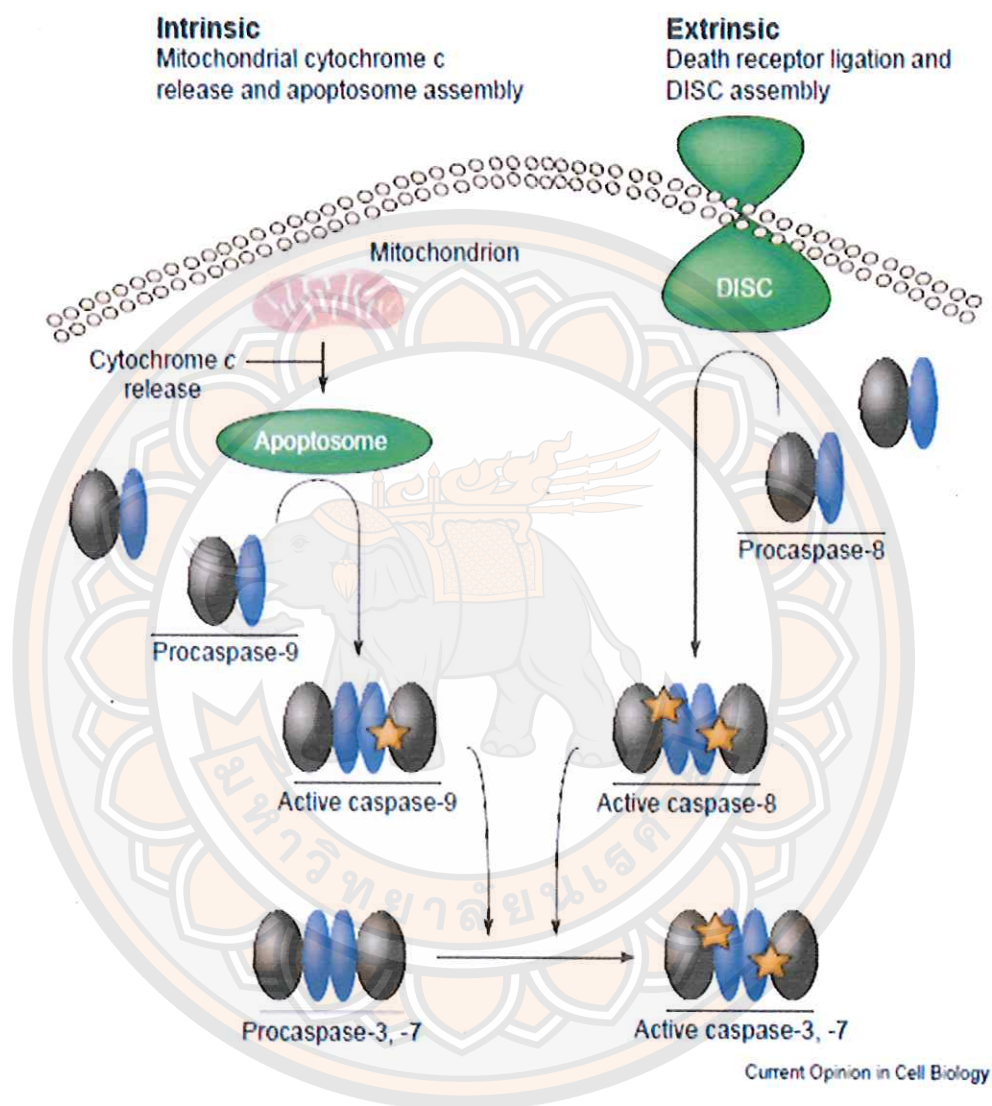


**Figure 11** The extrinsic pathway, the DISC is the site of activation for caspase-8

Source: <http://www.ncbi.nlm.nih.gov/pubmed/14644197>

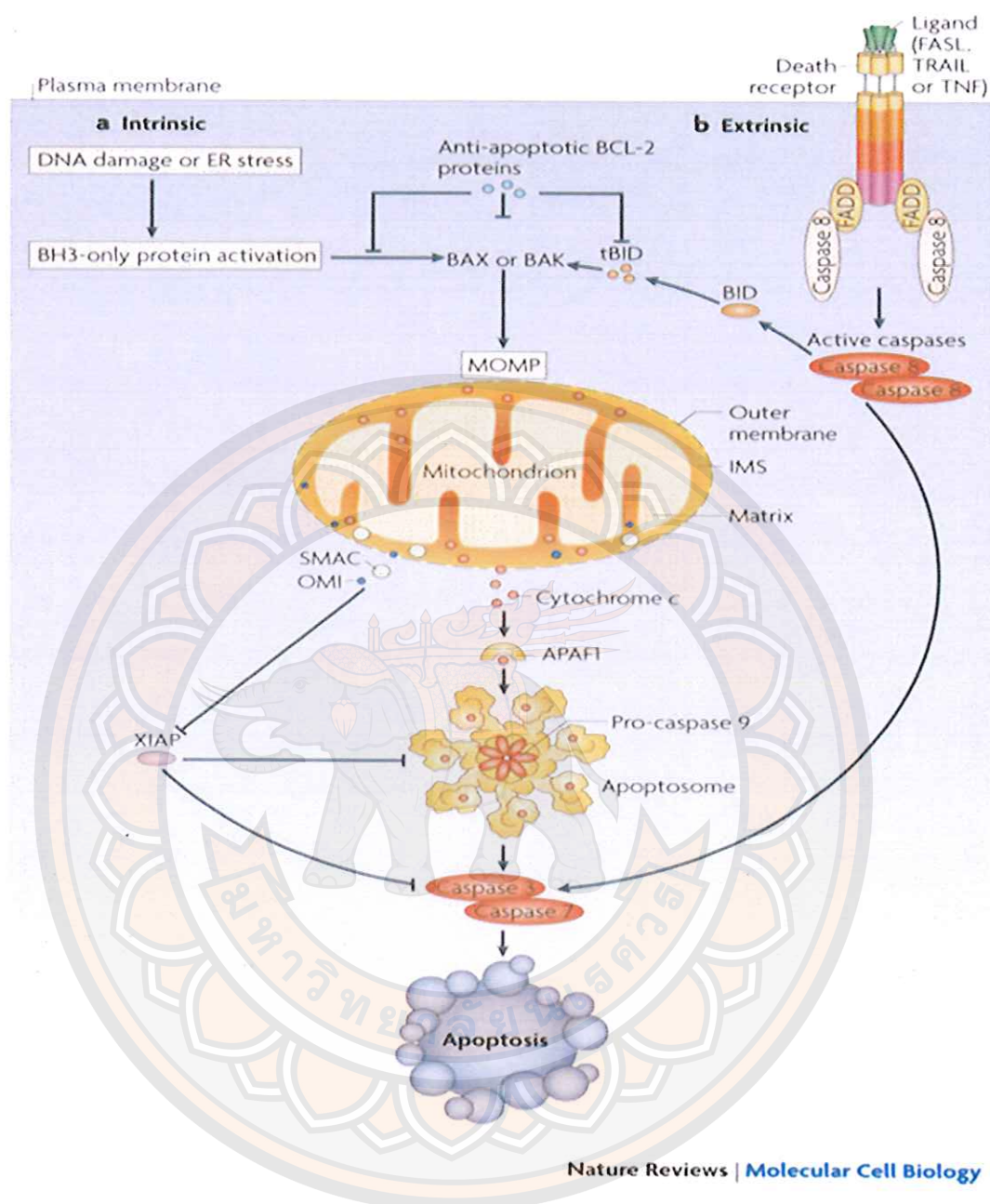


**Figure 12** The intrinsic and extrinsic apoptosis pathway.

Source: [http://www.nature.com/nrm/journal/v11/n9/fig\\_tab/nrm2952\\_F1.html](http://www.nature.com/nrm/journal/v11/n9/fig_tab/nrm2952_F1.html)



The intrinsic apoptosis pathway is initiated by stimulating intracellular signals that involve growth factors, hormones and cytokines that can lead to apoptosis triggering. All of stimuli can change the potential and integrity of the inner mitochondrial membrane leading to opening of the mitochondrial permeability transition (MPT) pore which in turn results in loss of mitochondrial transmembrane potential and release of pro-apoptotic protein from the intermembrane space into the cytosol. The Bcl-2 family is protein that controls and regulates apoptotic mitochondrial events by regulation of cytochrome c release. Cytochrome c binds and activates Apaf-1 protein which then binds to pro-caspase 9 to form an “apoptosome”. Consequently, the caspase-3 and -7 are activated and induce apoptosis. Caspase-3 activates the endonuclease CAD which leads to degrade the chromosomal DNA within the nuclei and results in chromatin condensation and DNA fragmentation. Finally, cytoskeleton is disrupted and then phagolytic events are triggered to uptake of apoptotic cells (Elmore, 2007)(Figure 12).

#### **Plasma membrane citrate transporters**

Citrate is an important substrate for cellular metabolism to produce fatty acid, triacylglycerol and cholesterol. Citrate is broken down to acetyl-CoA for *de novo* fatty acid synthesis. Two sources of intracellular citrate remain such as citrate within mitochondria and citrate from extracellular. Citrate within mitochondrial matrix is an important constituent of TCA cycle. Citrate is oxidized to NADH, FADH<sub>2</sub> and then is imported to the oxidative phosphorylation pathway to produce ATP. Mitochondria exports citrate to cytosol via citrate transporter protein (CTP) by catalyzing citrate/malate moving across the inner membrane and then it diffuses to cytosol via anion selective channel on outer mitochondrial membrane. In cytosol, citrate is metabolized to acetyl CoA and oxaloacetate (OAA), the immediate carbon source to fuel fatty acid, triglycerol and cholesterol biosynthesis.

The second source of citrate is extracellular citrate that is imported to cytosol via plasma membrane citrate transporter (PMCT) that catalyzes a sodium-couple citrate import. It has been shown that sodium-citrate transporter (NaCT) imports Na and citrate to cytosol at 4:1 ratio. CTP and PMCT transport citrate but PMCT are significantly larger in size and less polar compared to the CTP. PMCT structure is like a leucine transporter. The PMCT consists of 12 transmembrane domains and four arginine, which can simultaneously bind to a citrate molecule (Sun, 2010)(Figure 13).

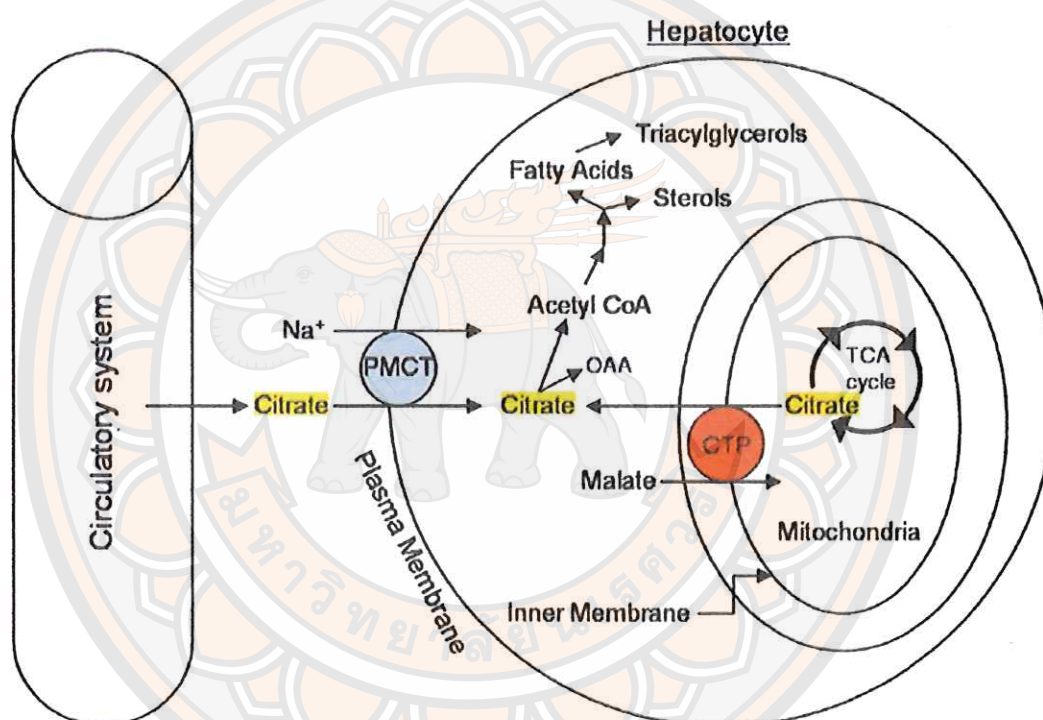


**Figure 13 The roles of the PMCT and CTP in supplying citrate to fuel hepatic fatty acid, triacylglycerol, and sterol biosynthesis**

Source: <http://www.ncbi.nlm.nih.gov/pmc/articles/PMC2913483/>



PMCT is located within the liver and brain. PMCT in brain functions in production of neurotransmitter. PMCT in liver is a glucose metabolism controller acting by inhibition of phosphokinase enzyme and affecting fatty acid, triacylglycerol and cholesterol synthesis (Inoue, et al., 2002). NaCT was originally discovered in *Drosophila* known as INDY (I'm not dead yet). In adult *Drosophila*, *Indy* is expressed in organs that are sites of intermediary metabolism, absorption, and metabolic storage, including the fat body, mid gut and oenocytes. The fat body is involved in the metabolism and storage of fat glycogen and is found mostly in the liver of vertebrates. A reduction of INDY activity by insertion of P element in the *Indy* gene causes an increase in average life-span, with a decrease of body size and fat content, without an alteration of either physical activity or fertility (Rogina, 2000).

$\text{Na}^+$ -coupled citrate transporter from *Caenorhabditis elegans* (ceNAC-2) has sequence homology to *Drosophila* Indy and the mammalian  $\text{Na}^+$ -coupled citrate transporter NaCT (NAC-2). Mammalian NaCT, expressed in the liver, is involved in the utilization of extracellular citrate for the hepatic synthesis of fat. Knockdown of *nac-2* in *C. elegans* leads to life span extension and decrease in body size and fat content. It is likely that NAC-2 utilizes extracellular citrate and other TCA cycle intermediates for the generation of metabolic energy and for the synthesis of fatty acids and cholesterol (Fei, et al., 2004).

In 2010, It found that the discovery of selective inhibitors of PMCT via *in silico*. The PMCT inhibitor has reported  $K_i$  value is 0.34 mM. It is hydrophobic compound and unchanged molecule, that specific for PMCT. The mechanism of PMCT inhibitor is a non-competitive inhibition pattern, indicating it does not combine to the substrate binding site. In contrast, the inhibitor can bind to citrate normally and leads to the conformation changes, which interrupt citrate transport to the cytoplasm.

Therefore, PMCT-selective inhibitor may be decrease fatty acid and cholesterol biosynthesis and a novel approach to the pharmacologic treatment of metabolic disorders resulting from the synthesis of excess lipid, cholesterol, and glucose, including human obesity, hyperlipidemia, hypercholesterolemia, and type 2 diabetes (Sun, 2010).



## CHAPTER III

### RESEARCH METHODOLOGY

#### Chemicals and reagents

EMEM were purchased from Corning (Manassas, VA, USA) and other culture reagent were purchased from Gibco BRL (Grand Island, NY, USA).

Plasma membrane citrate transporter (PMCT) inhibitor was purchased from TimTec (Harmony Business Park, Newark, DE)

3-(4,5-Dimethylthiazol-2-yl)-2,5-diphenyl-2H-tetrazolium Bromide (MTT), Dimethyl sulfoxide (DMSO) were purchased from AMRESCO (Solon, OH, USA).

Alexa Fluor<sup>®</sup>488 Annexin V/Dead cell Apoptosis kit, Mito Probe<sup>™</sup> JC-1 Assay kit and CM-H2DCFDA were purchased from Molecular Probes (Eugene, OR, USA).

Free Fatty acid, citrate and Triglyceride Quantification BioAssay<sup>™</sup> kit were purchased from US Biological (Swampscott, MA, USA).

M-PER<sup>®</sup> Mammalian Protein Extraction Reagent and BCA Protein Assay kit were obtained from Pierce (Rockford, IL, USA).

TOFA(5-(tetradecyloxy)-2-furoic acid) was purchased from abcam Biochemicals (Cambridge science Park, FL, UK).

C75 was purchased from Cayman Chemical company (Michigan, USA).

### Research instrument

Bio clean bench (Sanyo, MCV-B131F)  
 CO<sub>2</sub> incubator (Sanyo, MCO-20AIC)  
 Inverted microscope (Olympus, 1x71)  
 High speed refrigerated centrifuge (Scanspeed, 2236R)  
 Microplate reader (Biotek, Synergy HT)  
 Sonicator (Sonice, VCX130)  
 FACScalibur flow cytometer (Becton Dickinson(BD))  
 CCD camera (Bio-Rad, ChemiDoc XRS<sup>+</sup>)  
 Confocal Laser Scanning Microscopy (OLYMPUS, FV1000))  
 Mini PROTEAN® Tetra cell and Trans-blot semi-dry cell (Bio-rad)

### Materials

75 cm<sup>2</sup> and 25 cm<sup>2</sup> Cell culture flask (Corning, NY, USA)  
 15 ml and 50 ml centrifuge tube (Corning, NY, USA)  
 96 well tissue culture testplate (SPL, Korea)  
 35 mm and 60 mm Cell culture dish (Corning, NY, USA)  
 5 ml Polystyrene round-bottom tube (Falcon, NY, USA)  
 0.5 ml and 1.7 ml Microcentrifuge tube (Costar, NY, USA)  
 Silane-Prep Slides(glass slides coated with silane) (Sigma, MO, USA)

### Methods

#### 1. Cell culture

HB8065 Human hepatocellular carcinoma (HepG2 cells) were obtained from American Type Culture Collection (ATTC) (Manassas,VA,USA). Cells were cultured in EMEM with 1.5 g/L sodium bicarbonate, non-essential aminoacids, L-glutamine , sodium pyruvate supplemented with 10% fetal bovine serum and 10,000 ug/ml streptomycin and 10,000 units/ml penicillin. Cells were incubated at 37°C in 5% CO<sub>2</sub> and 100% humidity. The cultures were passaged at least two times per week. The cell culture passage number 78 - 90 were used for all experimental.

## 2. Determination of cell viability by MTT assay

Cell viability was determined in HepG2 cells. The cells were plated in 96-well plates at  $1 \times 10^4$  cells/well and incubated overnight. After overnight culture, cells were incubated with fresh EMEM medium containing different concentrations (0-3mM) of PMCT inhibitor for 24 h and vehicle controls were included for each plate. After incubation, medium was removed and then MTT solution (5 mg/ml) was added into each well and cells were incubated for 2 h at 37 °C. The reagent was removed carefully and MTT-formazan crystals were dissolved in 0.2% DMSO for 15 minutes at room temperature. Then, the absorbance was measured at wavelength of 595 nm by spectrophotometer (Program Gen 5 version 2.00.18 Biotek Reader Photometer).

## 3. Determination of apoptosis using AnnexinV - Alexa Fluor®488 / PI staining

HepG2 cells were seed on 60 mm<sup>3</sup> culture dish. After vehicle and 2.5 mM PMCT inhibitor treatment an overnight,  $1 \times 10^6$  cells were harvested with 0.25% Trypsin EDTA (Gibco, NY, USA) and resuspended in 1X annexin-binding buffer. The pellets were stained with the Alexa® Fluor 488 conjugated annexin V and 100 µg/mL PI working solution to each cell suspension. Cells were incubated in the dark for 15 min at room temperature and then the stained cells were analyzed by flow cytometry, to measure the fluorescence emission by FACScalibur flow cytometry (Becton Dickinson (BD), Franklin Lakes, New Jersey, USA). The data was analyzed using CellQuestPro software (BD).



#### 4. Determination of mitochondrial membrane potential ( $\Delta\Psi_m$ ) by flow cytometry and fluorescence microscopy

The level of  $\Delta\Psi_m$  in HepG2 cells were measured by flow cytometry using 5,5',6,6'-tetrachloro-1,1',3,3'-tetraethylbenzimidazolcarbocyanine iodide (JC-1) Dye Mitochondrial Membrane Potential Probe in accordance with the manufacturer's suggest protocol. Briefly, cells were plated at  $3 \times 10^5$  cells in cell culture dish 35 mm<sup>3</sup>. After incubation 24 h, cells were treated with 2.5 mM PMCT inhibitor and then washed in PBS and resuspended with warm PBS. JC-1 Dye was prepared in DMSO to 200  $\mu$ M. The control tubes, were including complete EMEM medium and 0.2% DMSO. The sample tube, JC-1 dye (2 $\mu$ M) was added to each tube and incubated at 37 °C, 5% CO<sub>2</sub> for 45 min. The 50  $\mu$ M CCCP were used as a positive control of the loss of  $\Delta\Psi_m$  and to verify the response of JC-1 to alteration of  $\Delta\Psi_m$  and depolarization of  $\Delta\Psi_m$ . After labeled with JC-1 dye, cells were analyzed by FACScalibur flow cytometry. A monomeric JC-1 form existed in cytoplasm emits green fluorescence intensity (~529 nm). An aggregated JC-1 form accumulated in mitochondria emitted red fluorescence intensity (~590 nm). Data were analyzed using CellQuestPro software (BD).

In a part of fluorescence microscopy, the treated and untreated cells at  $4 \times 10^4$  cells were stained 2 $\mu$ M JC-1 dye for 45 min in CO<sub>2</sub> incubator. JC-1 dye was removed by centrifugation and then cells were add with 4% papaformaldehyde fixative and incubated at room temperature for 20 min. Cells were dropped to silane coated slides and dried on hotplate at 41 °C for 20 min. The fixative was removed and stained nucleus with 2 $\mu$ g/ml DAPI (4',6-Diamidino-2-Phenylindole, Dihydrochloride) (Molecular Probes®,OR,USA). The mitochondrial membrane potential ( $\Delta\Psi_m$ ) was determined under fluorescence microscope.( Confocal Laser Scanning Microscopy (OLYMPUS FV1000))

### 5. Determination on Caspase-8 activity

Caspase -8 activity was measured by caspase -8/FLICE Fluorometric assay kit from Promokine (Heidelberg, Germany). The assay is based on detection of cleavage of substrate IETD-AFC (AFC: 7-amino-4-trifluoromethyl coumarin). IETD-AFC emits blue light (~400nm), upon cleavage of the substrate by FLICE or related caspases, free AFC emits a yellow-green fluorescence (~505nm). HepG2 cells were plated on 60 mm at  $2 \times 10^6$  cells per dish. After treatment with 2.5 PMCT inhibitor for 24 h, proteins were extracted by cell lysis buffer for 10 min. Then, the sample was added with 2x reaction buffer containing 10 mM DTT and IETD-AFC substrate (50  $\mu$ M) added to each sample. After incubation for 2 h, the sample was quantified using a fluorescence microplate reader at Ex/Em 360/460 nm.

### 6. Determination of ROS production by Flow cytometry and fluorescence microscopy

The intracellular ROS generation was measured by fluorescent dye 5-(and-6)-chloromethyl-2',7'-dichlorodihydrofluorescein diacetate, acetyl ester (CM-H<sub>2</sub>DCFDA) (Molecular probe, Oregon, USA) staining. CM-H<sub>2</sub>DCFDA is a chloromethyl derivative of H<sub>2</sub>DCFDA, can diffuse into cells, where its acetate groups are cleaved by intracellular esterase, resulting in a changed a compound to be a H<sub>2</sub>DCF. ROS oxidizes H<sub>2</sub>DCF to DCF(2',7' dichlorodihydrofluorescein), which is highly fluorescent. HepG2 cells were plated in culture dish at  $5 \times 10^5$  cells and incubated overnight. Then, cells were treated with 2.5mM PMCT inhibitor, 0.1mM C75 or 0.2% DMSO (control group) for 24 h. After treatment, cells were incubated with 10 $\mu$ M CM-H<sub>2</sub>DCFDA in CO<sub>2</sub> incubator for 45 min in the dark and then incubated with EMEM (10% FBS) for 20 min at 37 °C. The cells were analyzed by flow cytometry at Ex/Em ~492–495/517–527 nm. The data was analyzed using CellQuestPro software (BD).

For fluorescence microscopy, HepG2 cells ( $4 \times 10^4$  cells) were stained with 10 $\mu$ M CM-H<sub>2</sub>DCFDA and incubated for 45 mins in the dark and then incubated with EMEM for 20 mins at 37 °C. Cells were fixed with 4% paraformaldehyde and incubated at room temperature for 20 mins. Cells were dropped to silane coated slides and dried on hotplate at 41 °C for 20 min. The fixative was removed by PBS and then



stained nucleus with 2 $\mu$ g/ml DAPI. The ROS production was measured by increasing fluorescence intensity using confocal laser scanning microscope.

#### **7. Quantification of intracellular citrate**

Intracellular citrate levels were detected by the citrate assay kit. Briefly, HepG2 cells were seeded at a density of 2x10<sup>6</sup> cells per 60 mm<sup>3</sup>. Citrate was formed by the addition of oxaloacetate to the acetyl group of acetyl-CoA derived from the glycolysis. Citrate was converted to pyruvate via oxaloacetate. The pyruvate was quantified by fluorescence intensity measured at Ex/Em 535/590 nm using Synergy HT Microplate Reader (BioTek) with Gen5 Data Analysis software. Results were expressed as a percentage of intracellular citrate compared with the control.

#### **8. Detection of protein expression by Western blotting**

After treatment with 0.5 and 2.5mM PMCT inhibitor for 24 h, HepG2 cells were trypsinized and lysed with lysis buffer (MPER<sup>®</sup>), containing protease inhibitors (Cell Signaling Technology, MA,USA). Protein content was determined by the BCA protein assay. Proteins (10  $\mu$ g) was load on 8% SDS-polyacrylamide gel and transferred to PVDF membrane. After blocking of non-specific binding, the membrane was subsequently incubated an overnight at 4 °C with primary antibodies anti-Fatty acid synthase antibody(abcam Biochemicals, FL ,UK), anti-Acetyl CoA Carboxylase (Rabbit Monoclonal) (Merck Millipore, Darmstadt, Germany) anti-ATP-citrate Lyase Rabbit Antibody (Cell signaling Technology,MA,USA) and anti- $\beta$ -actin with dilution 1:1000 in 2% BSA in PBS containing 0.2% sodium azide overnight at 4 °C. After washed with 0.2% Tween20 PBS solution, the membrane was incubated with horseradish peroxidase-conjugated goat anti-Rabbit IgG secondary antibody (invitrogen,CA,USA) diluted 1:5000 in 5% skim milk with 0.2% Tween20 PBS solution for 2h at 4°C. The blots were developed using Clarity<sup>™</sup> Western ECL Chemiluminescent Substrate Reagent Kit (Bio-Rad ,Florida, USA). The intensity of each band was determined using CCD camera (Bio-Rad, ChemiDoc XRS<sup>+</sup>).



### 9. Detection of protein expression by immunofluorescence

HepG2 cells at  $4 \times 10^4$  cells/10  $\mu$ L were diluted with EMEM (non FBS). 4% paraformaldehyde fixative was added to the sample and incubated at room temperature for 20 min. Cells were dropped to silane coated slides and dried on hotplate at 41 °C. Cells were permeabilized with 0.5% Triton X-100 in PBS for 10 min and washed with PBS. The blocking solution (1% Bovine serum albumin (BSA) in 0.1M PBST) was added to slide for 30 min. The blocking reagent was removed and primary antibody (anti-FASN)(1:200) was added to slide and incubated overnight at 4 °C in moist chamber. The slide was washed with 0.1 M PBS and secondary antibody Alexa 488® (Life Technologies, OR, USA)(1:200) was then added for 2 h in moist chamber (protect light). After washing to the slide, nucleus was stained with 2  $\mu$ g/ml DAPI (4',6-Diamidino-2-Phenylindole, Dihydrochloride) (Molecular Probes®, OR, USA). The protein expression was determined under fluorescence microscope (Confocal Laser Scanning Microscopy (OLYMPUS FV1000)).

### 10. Quantification of intracellular free fatty acid

FASN activity was determined by the production of the *de novo* fatty acid synthesis, long chain free fatty acids, using the Free fatty acid quantification kit. HepG2 cells ( $1 \times 10^6$  cells) were plated for 24 h. Then, cells were harvested and homogenized with 200  $\mu$ L of chloroform-Triton-X 100 solution. After that, acyl-CoA synthase reagent was added to the sample to convert LCFAs to CoA derivatives. Then the reaction mix containing assay buffer, enzyme mix, enhancer, and fluorescence probe was added to measure the fluorescence at Ex/Em 535/590 nm using Synergy HT Microplate Reader.

### 11. Quantification of Triglyceride

HepG2 cells were seeded at a density of  $1 \times 10^6$  cells. The cells were homogenized in triglyceride buffer and slowly heat the sample until the buffer becomes cloudy and centrifuged to remove any insoluble material. Lipase was added to each sample to convert triglyceride to glycerol and fatty acid. Then the reaction mix, containing assay buffer, probe and enzyme mix were added to sample. The glycerol was oxidized to generate a product which measured the fluorometric at Ex/Em 535/590 nm by Synergy HT Microplate Reader.

## 12. Measurement of CPT-1 activity

The CPT-1 activity was determined following a method described by Kant (Kant, 2012). Cells were lysed in lysis buffer containing Tris-HCl buffer, 0.25 M sucrose and 1 mM EDTA. The pellet was centrifuged at 500×g for 10 min to keep supernatant and mitochondrial pellet was obtained by centrifugation at 13,000×g. The pellet was resuspend in lysis buffer and measured protein content by a BCA assay. The reaction mixture containing 100mM Tris buffer, 1 mM EDTA, 0.1% Triton X-100 and 0.5 mM DTNB. 0.01 mM palmitoyl CoA was added to the sample before measurement of absorbance at 412 nm. After mixed 5 mM L-carnitine to the sample, Absorbance was measured over period of 5 min.

## Statistical analysis

The results were analyzed by *t*-test and one-way ANOVA using a Turkey's test as a post-test.  $P < 0.05$  versus the control was considered statistically significant using Graph Prism Software, version 5. Three independent experiments were performed for statistical analysis and expressed as mean±SEM.

## CHAPTER IV

### RESULTS

#### Part I: The effect of PMCT inhibitor on apoptosis in HepG2 cells

##### 1. The effect of PMCT inhibitor on HepG2 cell viability

This study aimed to investigate whether PMCT inhibitor can decrease suppressed proliferation and viability of HepG2 cells. MTT assay performed after cells were treated with 0.5 to 3 mM of PMCT inhibitor for 24 h. The result showed that PMCT inhibitor induced a significant reduction in the number of viable cells in a dose-dependent manner. Cell viability was reduced to 60.47 % with 2 mM and 39.02 % with 3 mM of PMCT inhibitor, when compared to the control group (Figure 14A). As shown in figure 14B, the graph showed that Log IC<sub>50</sub> values to 0.3844 ( IC<sub>50</sub> = 2.5 mM ) of PMCT inhibitor at 24 h treatment. Moreover, we chose a specific concentration at 2.5 mM for further mechanistic studies.



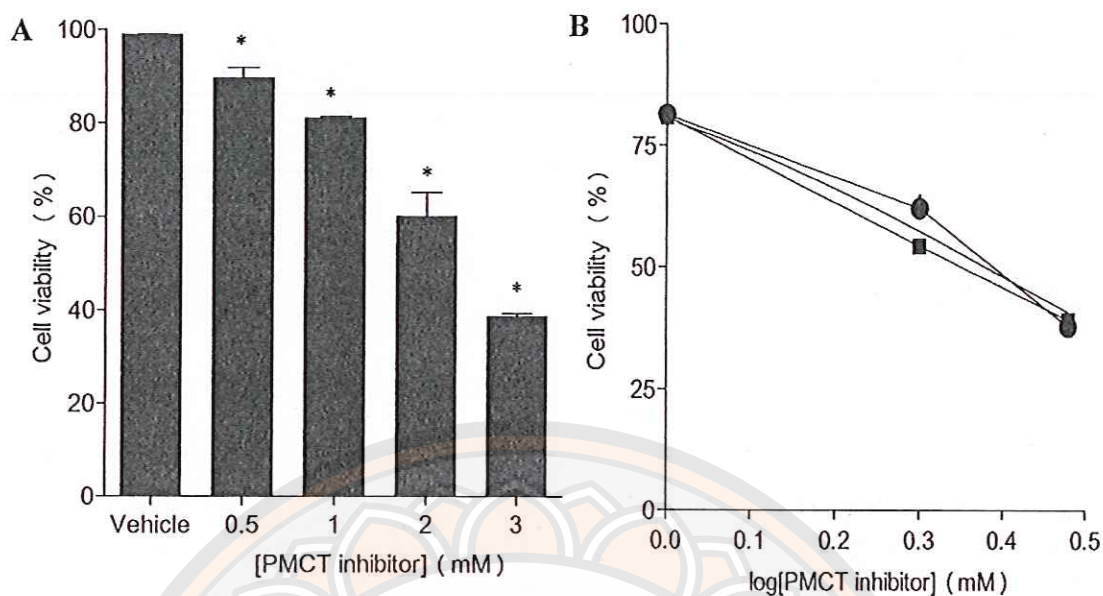


**Figure 14** Dose-dependent inhibitory affected of PMCT inhibitor on the proliferation of HepG2 cells. ((A) Cells were incubated with difference concentrations (0–3 mM) of PMCT inhibitor for 24 h, MTT assay performed to determine a number of viable cells compared with 100% of the control. The control defined as cells treated with a medium or vehicle without an inhibitor.(B) The linear graph showed a IC<sub>50</sub> value of PMCT inhibitor after 24 h treatment. Data indicated mean  $\pm$  SEM from at least three independent experiments performed in triplicates. \*  $p < 0.05$  denotes significantly different from the control.)

## 2. The effect of PMCT inhibitor on HepG2 cell apoptosis

To examine the mechanism of PMCT inhibitor-induced HepG2 cell death was due to apoptosis pathway. HepG2 cells were treated with C75 (0.1 mM) as positive control of apoptosis. HepG2 cells were incubated with 2.5 mM PMCT inhibitor for 24 h. Then, cells were stained with Alexa Fluor<sup>®</sup>488 annexin V and PI and detected by flow cytometric analysis. As shown in figure 15A. The viability cells are decreasing, the early apoptotic cell was assessed by cell having a positive staining with Annexin V but a negative staining with PI. The late apoptotic cell was observed to be stained with both Annexin V and PI. Figure 15B showed that PMCT inhibitor (2.5 mM) and C75 (0.1 mM) significantly induced apoptosis in HepG2 cells both of early and late stages when compared to the control group. This result demonstrated that PMCT inhibitor induced HepG2 cells apoptosis.

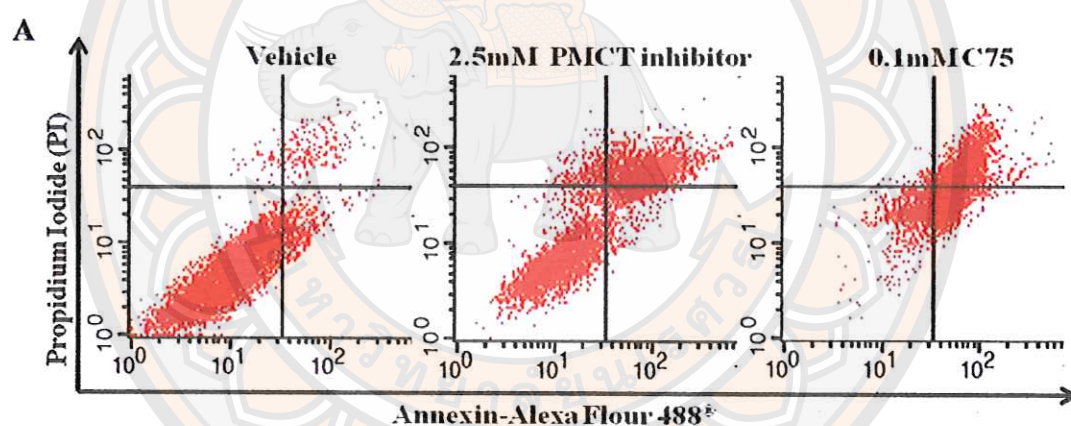
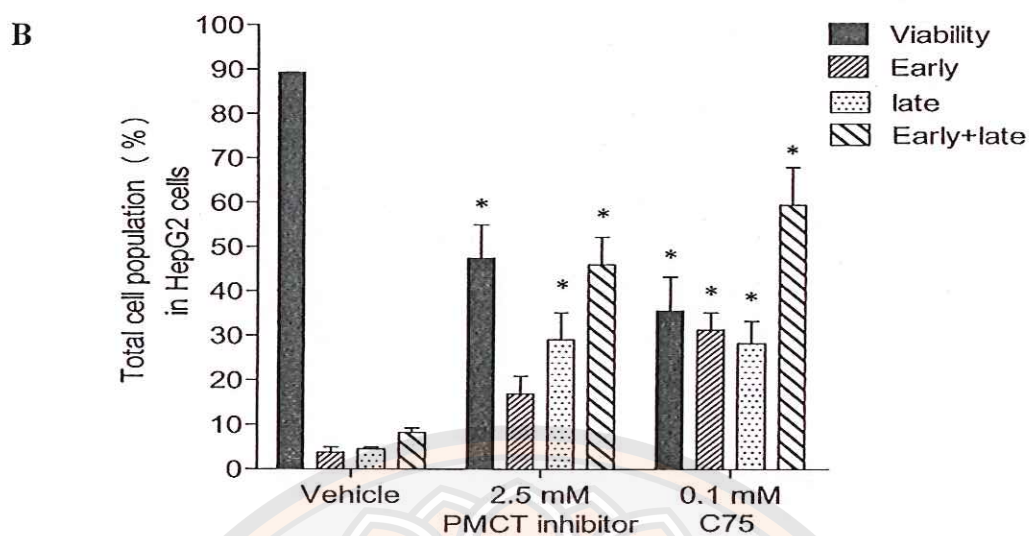


**Figure 15 Apoptosis was induced by PMCT inhibitor in HepG2 cells.**

(Cells were incubated with 2.5 mM of PMCT inhibitor or 0.1 mM C75 as a positive control for 24 h (A) Representative flow cytometry scatterplots were depicted using double stained with Annexin V/Alexa Fluor<sup>®</sup>488 and propidium iodide (PI) to determine the distribution of viable, early or late stage and necrotic cells.)



(B) The percentage of cells related to the whole cell populations (set as 100%) was expressed by bar charts showing the proportion of viable, early, late, and total apoptotic cells. The control was defined as cells treated with a medium or vehicles without an inhibitor. Data indicated mean  $\pm$  SEM from at least three independent experiments performed in triplicates. \*  $p < 0.05$  significantly different from the control.

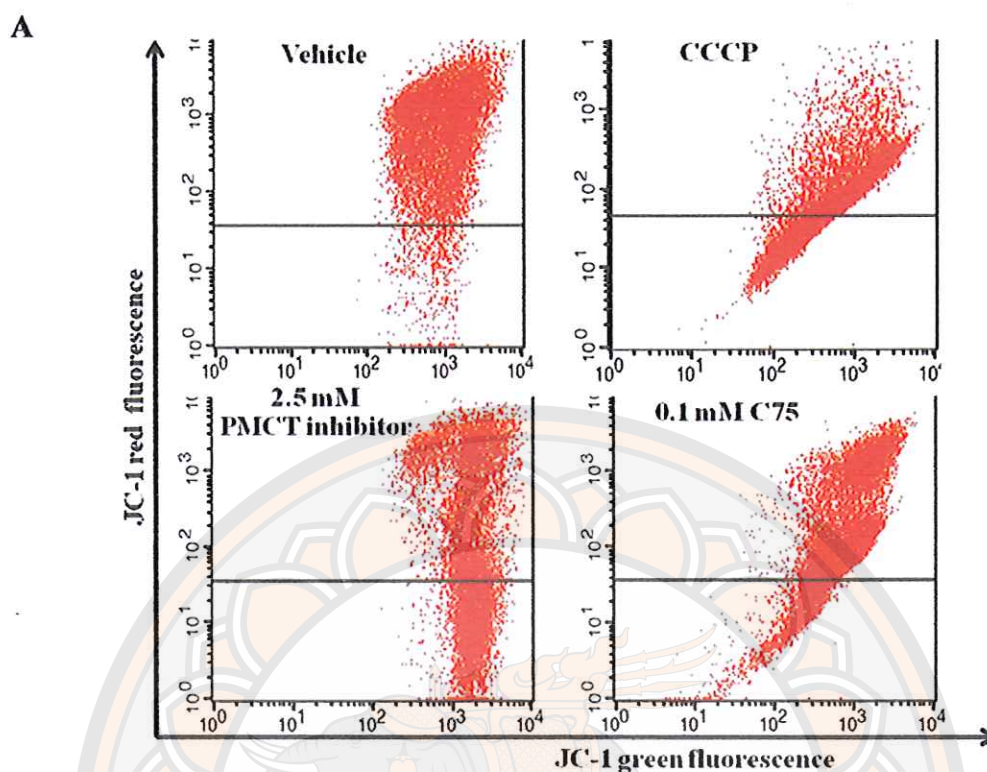
Figure 15 (cont.)



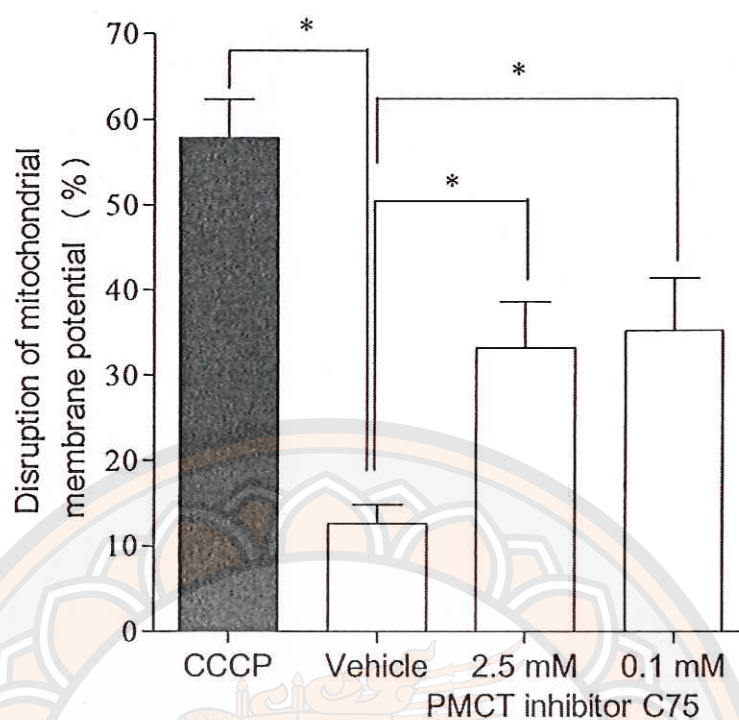
### 3. The effect of PMCT inhibitor on mitochondrial membrane potential ( $\Delta\Psi_m$ )

Depolarization of the mitochondrial membrane is a special characteristic of the initiation event of the intrinsic apoptotic pathway. This study examined PMCT inhibitor-induced apoptosis in HepG2 cells was involved to the disruption of  $\Delta\Psi_m$ . The JC-1 fluorescence dye was used as an indicator of  $\Delta\Psi_m$  status. In normal cells, the mitochondria has high membrane potential, JC-1 forms complexes in mitochondria, which emit a red fluorescence accumulated in the mitochondria. The loss depolarization of mitochondrial membrane potential in apoptotic cells, JC-1 remains in the monomeric form accumulated in the cytoplasm, which emits green fluorescence. The relative  $\Delta\Psi_m$  value was obtained by calculating the ratio between levels of red to green fluorescence. A relative decrease in the red/green fluorescence intensity ratio was therefore considered as depolarization of  $\Delta\Psi_m$  as shown in figure 16A. Flow cytometric analysis of control group stained with JC-1, showed only 13.58% of green and 86% of red fluorescence intensity (Figure 16B), indicating cells were in the high  $\Delta\Psi_m$ . Cells treated with PMCT inhibitor ( 2.5 mM ) were presented an increase in green fluorescence intensity to 33.18% when compared with the control. Cells were treated with CCCP at 50  $\mu$ M were used as a positive control to induce and increase of green fluorescence intensity. They indicated a decrease in  $\Delta\Psi_m$ .

As shown in figure 16C, HepG2 cells were determined in perturbations of  $\Delta\Psi_m$  using JC-1 dye staining and the sample were analyzed by confocal microscopy. The bar chart presented percentage of disruption of mitochondrial potential. The intensity of green fluorescence were increased to 734.5% when compared to control group (Figure 16D).



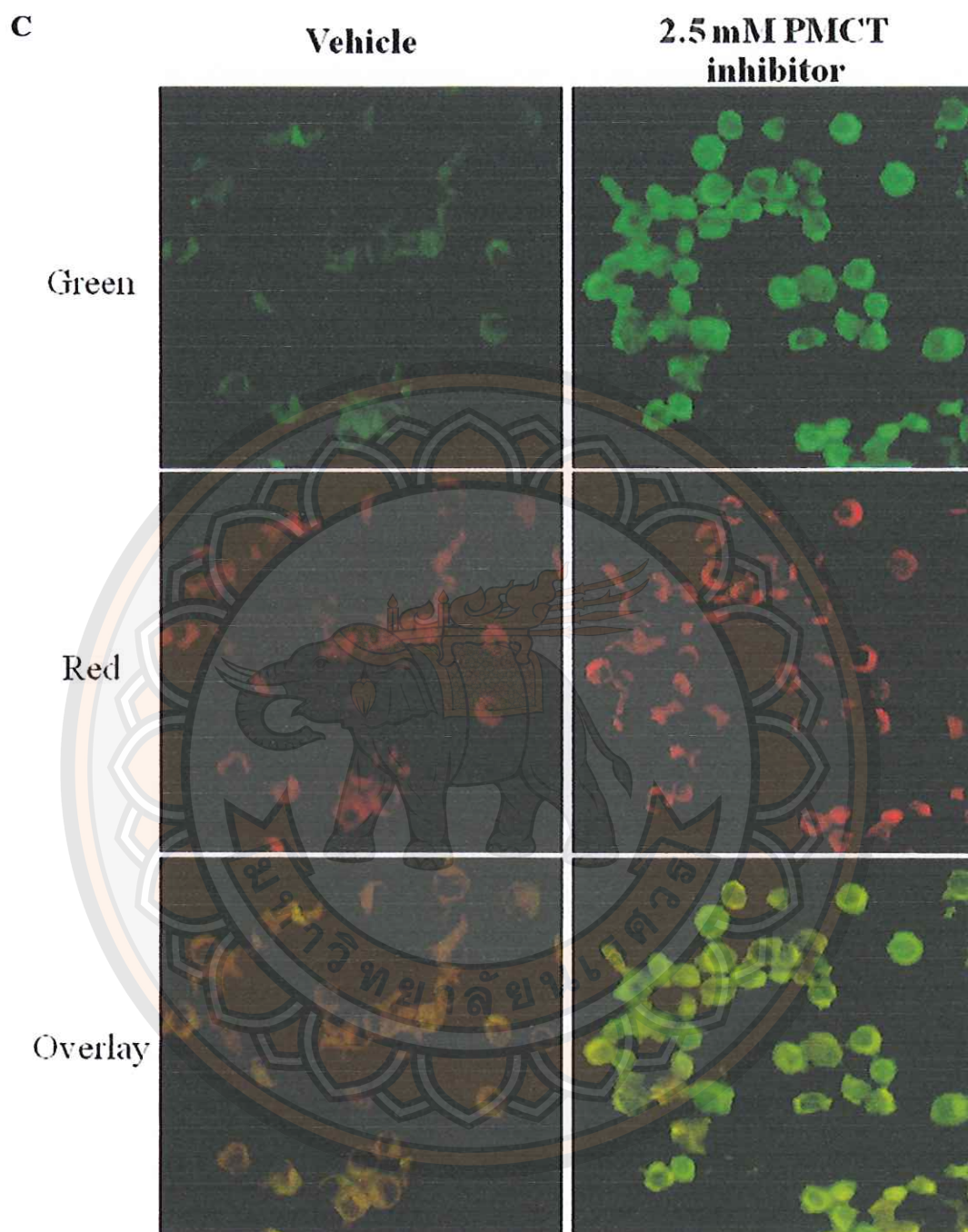
**Figure 16** PMCT inhibitor induced the disruption of mitochondrial membrane potential in HepG2 cells. (Cells were incubated at 2.5 mM of PMCT inhibitor for 24 h. Then, stained with JC-1 fluorescence dye and detected by flow cytometry. The control defined as cells were treated with a medium or vehicles without an inhibitor. (A) The mitochondrial transmembrane potential was evaluated by calculating the relative level of red (J-aggregate form) to green (J-monomeric form) fluorescence intensity. Cell distribution in the upper shows a high potential and lower quadrant areas was considered as cells had an energized mitochondrial and low mitochondrial membrane potential states.)

**B**

(B) Flow cytometry analysis of the percentage of disruption of the mitochondrial potential relative to the whole cell populations is expressed in bar charts. Cells were incubated with CCCP as a positive control of the depolarization of the mitochondrial membrane. PMCT inhibitor could significantly induced disruption of the mitochondrial potential in HepG2 cells when compared control.

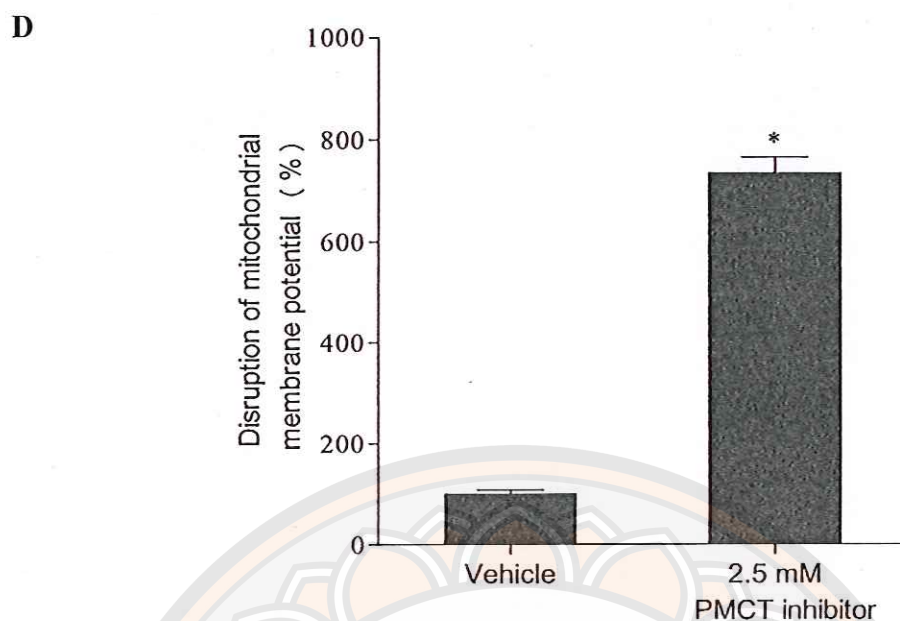
Figure 16 (cont.)





**(C) Mitochondrial membrane potential was determined by confocal laser scanning microscopy in cells stained with JC-1 dye. Cells were treated PMCT inhibitor increase green fluorescence intensity, expression a loss of mitochondrial membrane potential.**

**Figure 16 (cont.)**



**(D)** The percentage of cells showed mitochondrial depolarization, which was determined by confocal microscopy and fluorescence intensity was quantified using the ImageJ software. Data indicated mean  $\pm$  SEM, \*  $p < 0.05$  significantly different from the control.

Figure 16 (cont.)

#### 4. The effect of PMCT inhibitor on caspase-8 activity

To determine the apoptotic pathway induced by PMCT inhibitor, caspase-8 activities were evaluated after treated with 2.5 mM PMCT inhibitor for 24 h. The effect of PMCT inhibitor on the caspase-8 activity of HepG2 cells was analyzed by caspase-8/FLICE Fluorometric assay kit. The results showed the percentage of caspase-8 activity in HepG2 cells treated with 2.5 mM PMCT inhibitor was 130% and 146% in C75-treated cells when compared to control group. These findings indicated that PMCT inhibitor enhanced caspase-8 activity and induced apoptosis in HepG2 cells through extrinsic pathway.

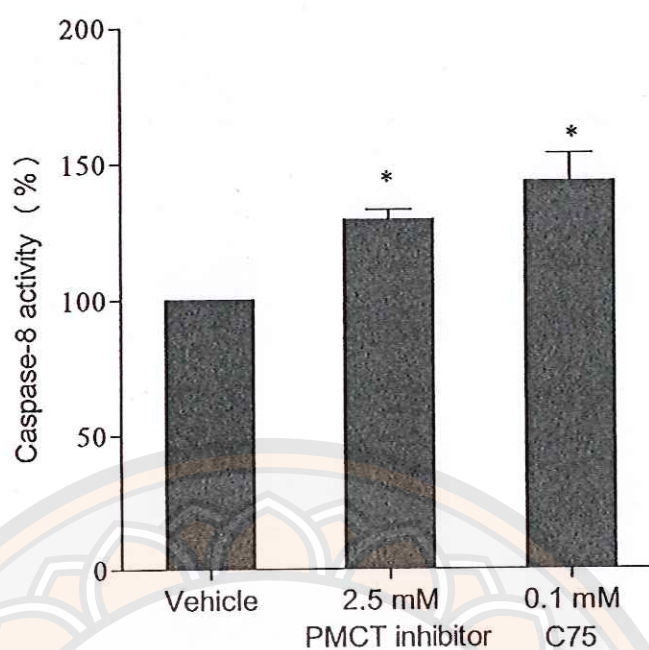


**Figure 17** PMCT inhibitor activated caspase-8 activity in HepG2 cells. (After incubation of 2.5 mM of PMCT inhibitor for 24 h, cells were harvested and determined by caspase-8/FLICE fluorometric kit. The control defined as cells treated with a medium or vehicles without an inhibitor. Data represented mean $\pm$ SEM from at least three independent measurements performed in triplicates. \*  $p < 0.05$  significantly different from the control.)



## **Part II : The mechanism of PMCT inhibitor on HepG2 cells apoptosis.**

### **1. The effect of PMCT inhibitor on ROS generation**

To evaluate the effect of PMCT inhibitor-induced generation of reactive oxygen species (ROS). HepG2 cells were treated with PMCT inhibitor (2.5mM) for 24 h. and the untreated and treated cells were stained with the fluorescent dye 5-(and-6)-chloromethyl-2',7'-dichlorodihydrofluorescein diacetate, acetyl ester (CM-H<sub>2</sub>DCFDA). This probe diffused through cell membrane and was hydrolyzed by intracellular esterase to dichlorodihydrofluorescein. That was oxidized to dichlorofluorescein, a fluorescent product. HepG2 cells were stained with CM-H<sub>2</sub>DCFDA. The percentage of ROS level was investigated by flow cytometry and data expressed in bar chart, as shown in figure 18A. After treatment with PMCT inhibitor, the level of Ros generation in HepG2 cells were increased to 1316.7% when compared to control group and to 1478 % in C75-treated group. As shown in Figure 18B, to observe the characteristics of apoptotic nuclei and ROS level, HepG2 cells were stained with DAPI and CM-H<sub>2</sub>DCFDA and they were assayed by confocal microscopy. In the control group, cells showed a round shape and homogenous nuclear staining. In contrast, the treated cells were expressed the apoptotic features, such as staining brightly and condensed chromatin. The ROS level are shown in green channel, cells were treated with 2.5 mM PMCT inhibitor increased the fluorescence intensity when compared to control group. As shown in figure 18C, fluorescence intensity was quantified using imageJ software showed 100% of control group and 247% of fluorescence intensity in 2.5 mM PMCT inhibitor treated group. This result implies that PMCT inhibitor-induced ROS production and suggest that effect to apoptosis in HepG2 cells.

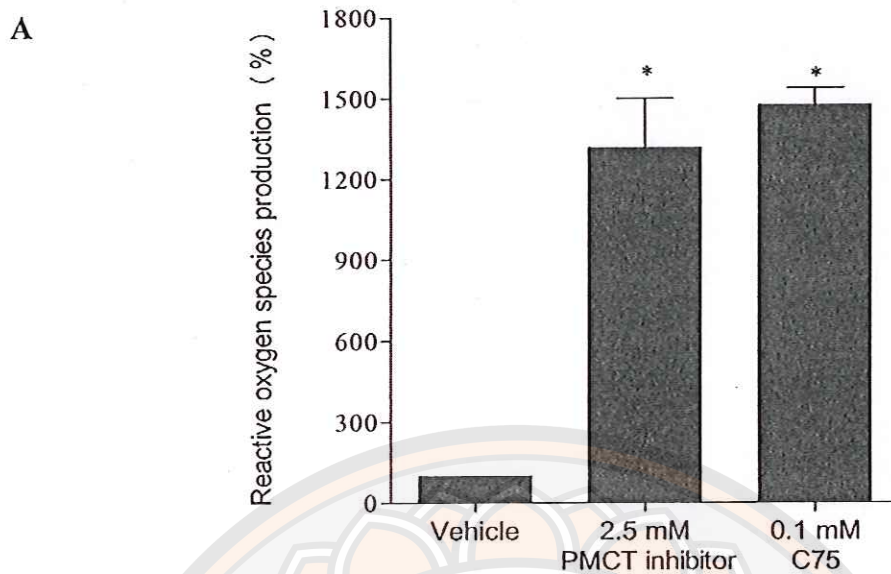
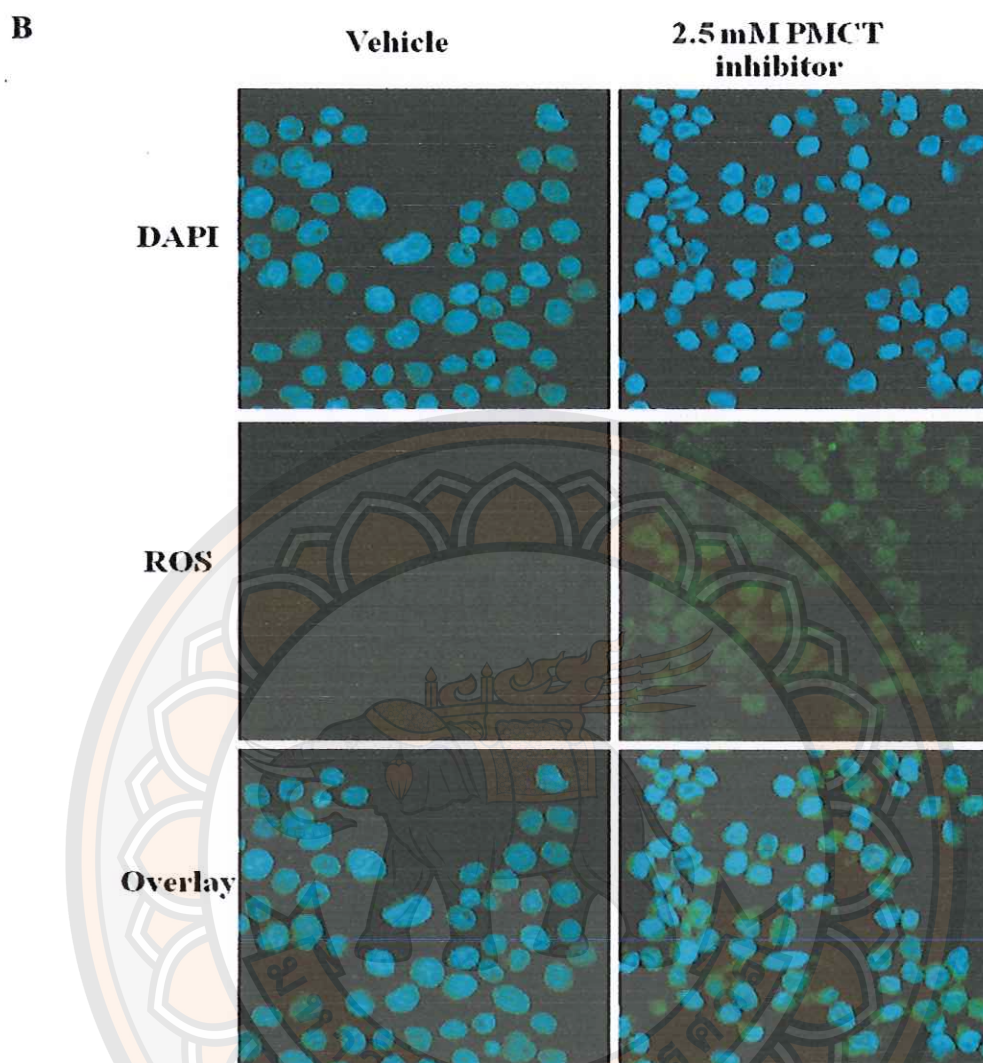


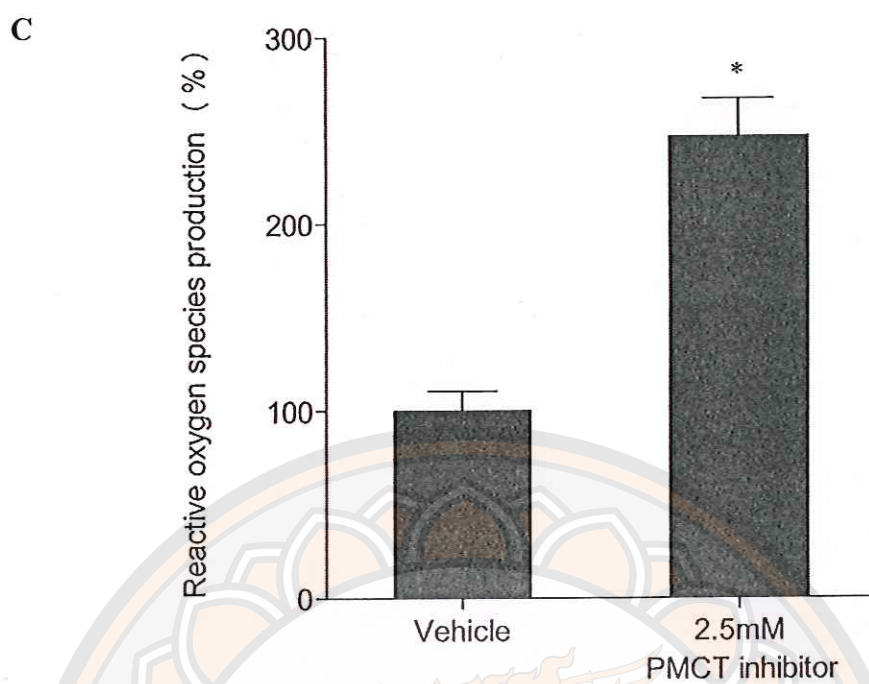
**Figure 18** PMCT inhibitor increased ROS level in HepG2 cells. (After incubation of 2.5 mM of PMCT inhibitor for 24 h cells were stained with CM-H<sub>2</sub>DCFDA (A)The percentage of ROS level was analyzed by flow cytometry. The control was defined as cells treated with a vehicles without an inhibitor. The figure shows ROS production significantly increase in treated group.)



(B) Cells were observed under a confocal laser scanning microscope after stained with DAPI and CM-H<sub>2</sub>DCFDA. The blue channel showed DAPI stained nuclei and the green channel showed CM-H<sub>2</sub>DCFDA-expressed dichlorofluorescein. The green fluorescence intensity of treated group was increased when compared control. It means PMCT inhibitor induced production of ROS.

Figure 18 (cont.)





(C) Green fluorescence intensity (ROS) was quantified using imageJ software. Data represented mean  $\pm$  SEM, \*  $p < 0.05$  significantly different from the control.

Figure 18 (cont.)

## 2. The effect of PMCT inhibitor on intracellular citrate level

The intracellular citrate is the starting material for the *de novo* fatty acid, triglycerol, and cholesterol synthesis for cancer cells survival. This study evaluated that decreased intracellular citrate induced by PMCT inhibitor was responsible for induction of apoptosis in HepG2 cells. As shown in figure 19, the percentage of intracellular citrate after cells were treated with 2.5 mM of PMCT inhibitor for 24 h. It was decreased to 53.22% compared to control group. This finding suggested that PMCT inhibitor decreased citrate level which in turn led to suppression of *de novo* fatty acid synthesis, resulting in apoptosis in HepG2 cells.

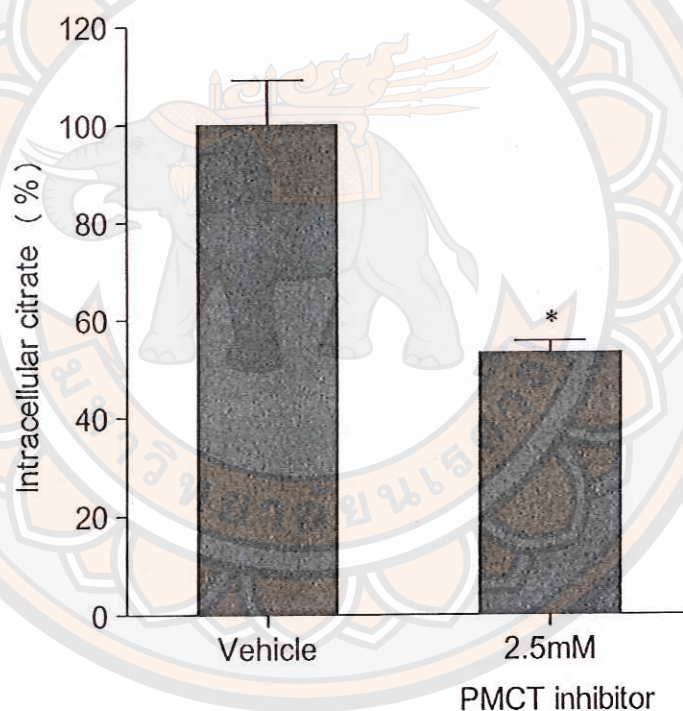


**Figure 19** PMCT inhibitor decreased citrate level in HepG2 cells. (After incubation of 2.5 mM of PMCT inhibitor for 24 h, cells were harvested and determined by citrate assay quantification kit. The control defined as cells were treated with a medium or vehicles without an inhibitor. Data represented mean $\pm$ SEM from at least three independent measurements performed in triplicates. \*  $p < 0.05$  significantly different from the control.)

### 3. The effect of PMCT inhibitor on protein expressions

It has been reported that the overexpression of FASN protects immortalized liver cancer cells from apoptosis, thus this study hypothesized that suppression of FASN could induce apoptosis in HepG2 cells. This study investigated the inhibitory effect of PMCT inhibitor on the expressions of FASN, ACC and ACLY proteins that led to suppression the *de novo* fatty acid synthesis caused cytotoxic and induced apoptosis in HepG2 cells. Cells were incubated with 0.5 mM and 2.5 mM PMCT inhibitor for 24 h. As shown in figure 20A, Equal amounts of total protein were analyzed by Western blotting. There was no alteration in the abundance of all three protein expressions compared with the control.

As shown in figure 20B, cells were stain nuclei with DAPI and they were incubated with antibody and observed under a confocal microscope. The blue channel showed a apoptotic feature in treated cells, the green channel displayed the fluorescence intensity of antibody labeled Alexafluor-488 dye. These data showed that no difference in brightly fluorescence compared with the control. As shown in figure 20C, The resulting ratio FASN/ $\beta$ -Actin represented no significantly difference in protein expressions. These studies demonstrated that PMCT inhibitor decreased fatty acid synthesis and induced apoptosis in HepG2 cells without changes in the abundance of *de novo* fatty acid synthesis protein expressions.



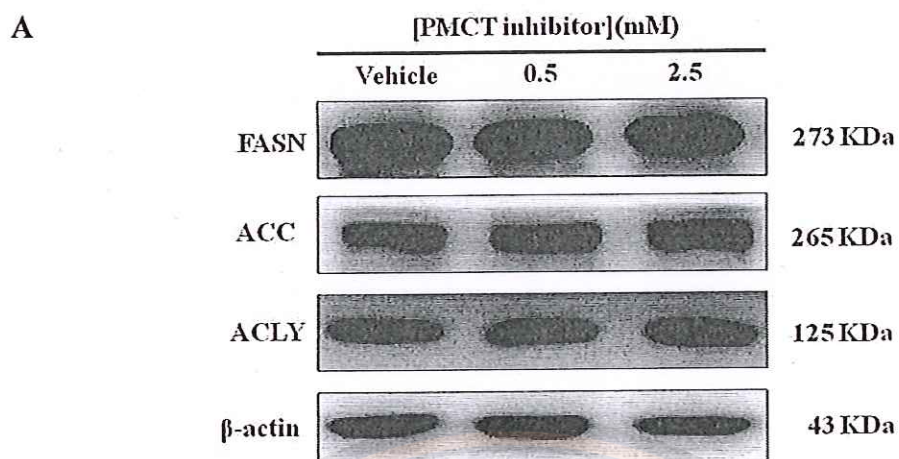
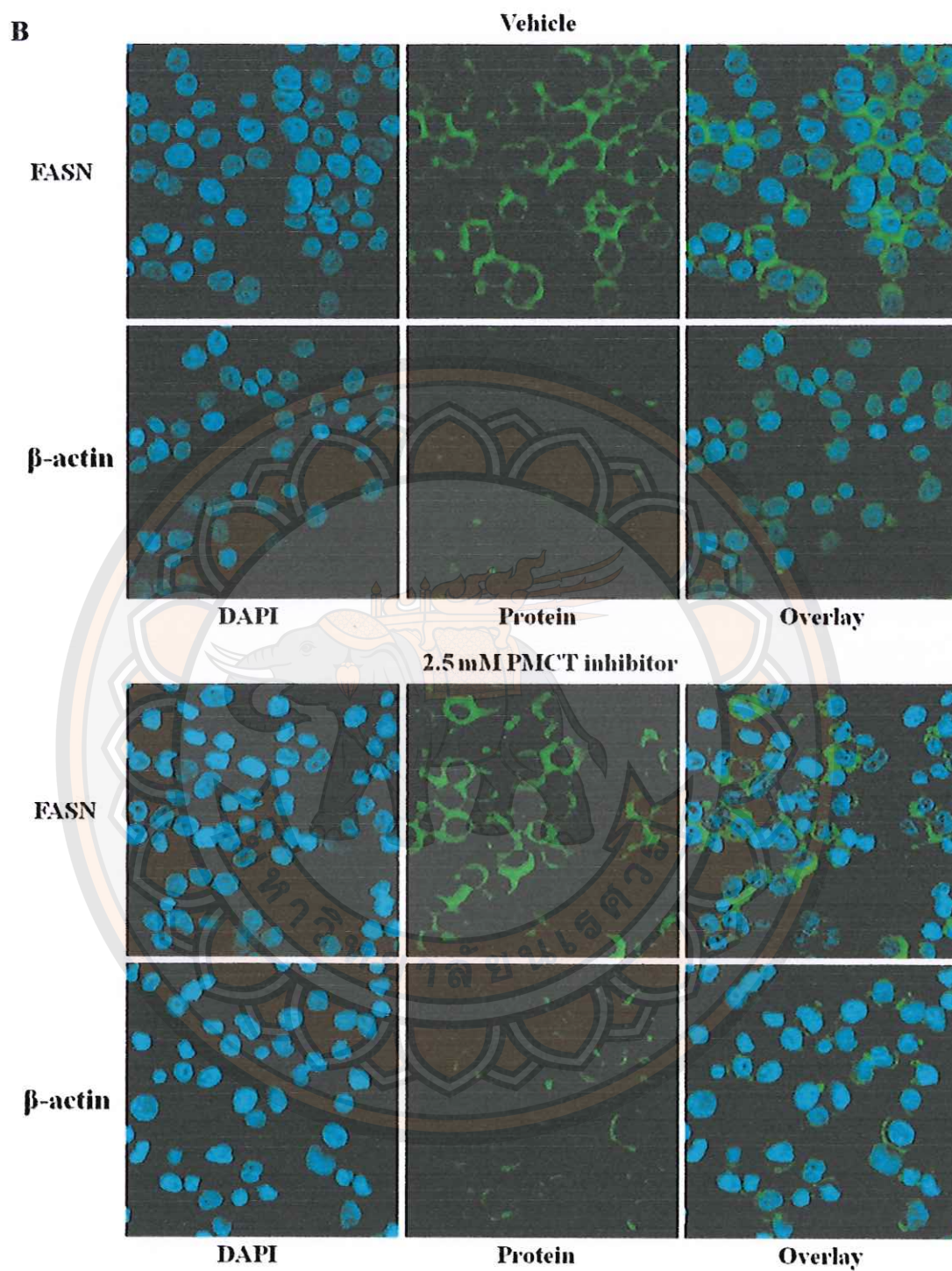
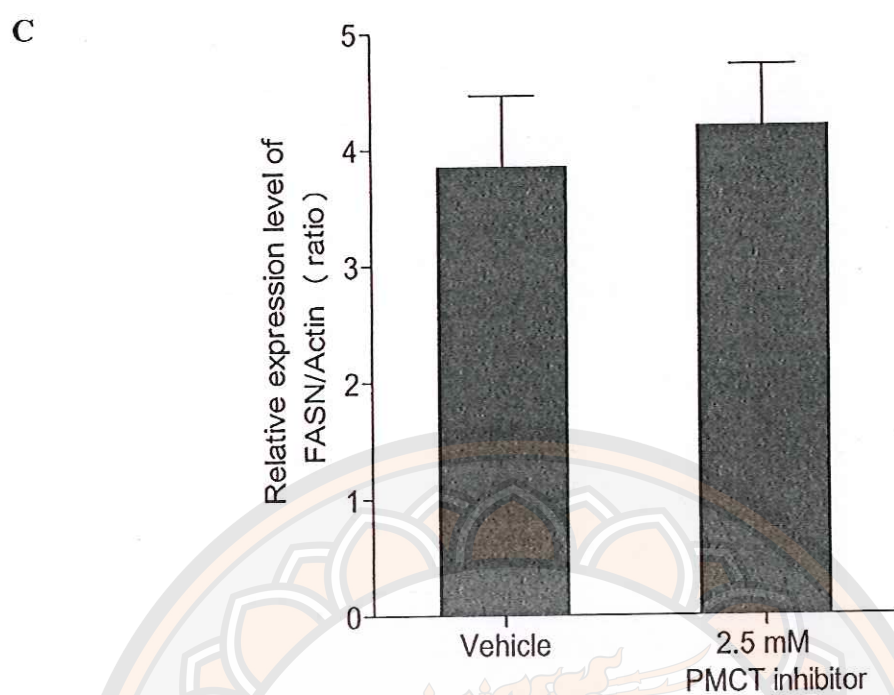


**Figure 20** The effects of PMCT inhibitor on FASN, ACC, ACLY protein expressions in HepG2 cells. (Cells were treated with PMCT inhibitor for 24 h. (A) Protein expressions were detected by Western blotting. The control defined as cells treated with a medium or vehicles without an inhibitor. The band result of proteins were representative of those obtained from at least three independent experiments.  $\beta$ -actin was used as an internal control for integrity and equal amount of protein loading and transferring.)



(B) Cells were measured protein expression by confocal laser scanning microscopy. The treated and untreated cells were no alteration of luminescence.

Figure 20 (cont.)



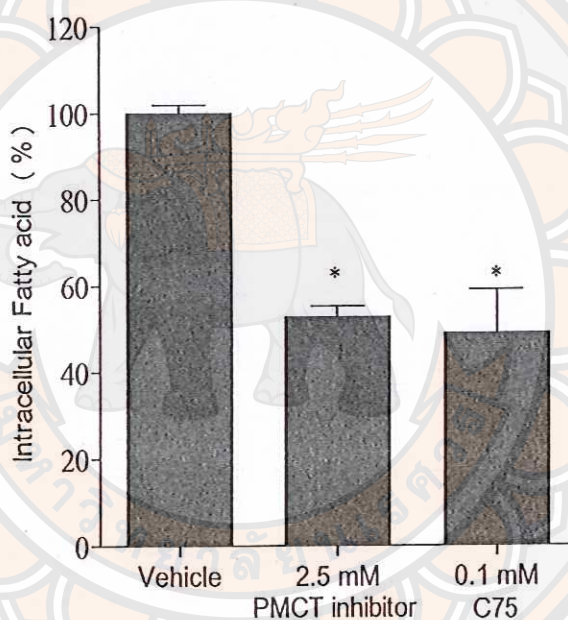
(C) The relative expression level of FASN/ $\beta$ -actin ratio displayed in bar chart. The data showed no difference between control and treated group.

Figure 20 (cont.)



#### 4. The effect of PMCT inhibitor on intracellular free fatty acid level

This study evaluated that PMCT inhibitor suppressed an enzymatic activity of FASN in the synthesis of fatty acid without changes in the abundance of FASN protein expression, could lead to apoptosis in HepG2 cells. The intracellular free fatty acid level was detected after cells treated with 2.5 mM of PMCT inhibitor for 24 h. As shown in figure 21, the percentage of intracellular free fatty acid was decreased to 52.37% compared to 100% of the control group. This study demonstrated that PMCT inhibitor induced apoptosis. It involved in a reduction of level of *de novo* fatty acid synthesis in HepG2 cells.



**Figure 21** PMCT inhibitor decreased FASN activity in HepG2 cells. (After incubation of 2.5 mM of PMCT inhibitor for 24 h, cells were harvested and determined by intracellular fatty acid assay quantification kit. The control defined as cells treated with a medium or vehicles without an inhibitor. Data represented mean  $\pm$ SEM from at least three independent measurements performed in triplicates. \*  $p < 0.05$  significantly different from the control.)

### 5. The effect of PMCT inhibitor on intracellular triglyceride level

Triglyceride is a product of *de novo* fatty acid synthesis. The intracellular triglyceride level was evaluated after cells were treated with 2.5 mM of PMCT inhibitor for 24 h. As shown in figure 22, the percentage of intracellular free fatty acid decreased to 32.73% compared to 100% of the control group. This study demonstrated that PMCT inhibitor decreased a triglyceride, a product of *de novo* fatty acid synthesis in HepG2 cells. This finding suggested that PMCT inhibitor suppressed *de novo* fatty acid synthesis and lead to apoptosis.

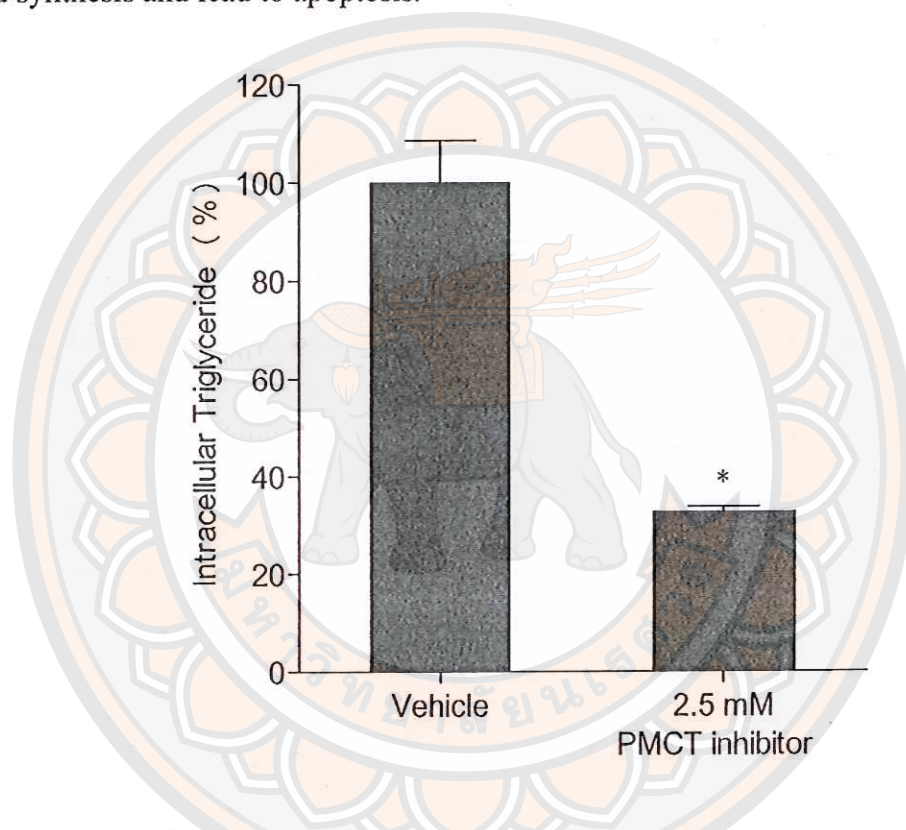


**Figure 22** PMCT inhibitor decreased triglyceride level in HepG2 cells. (After incubation of 2.5 mM of PMCT inhibitor for 24 h, cells were harvested and determined by triglyceride assay quantification kit. The control defined as cells treated with a medium or vehicles without an inhibitor. Data represented mean $\pm$  SEM from at least three independent measurements performed in triplicates. \* $p < 0.05$  significantly different from the control.)



## 6. The effect of malonyl-CoA on apoptosis

TOFA (5-tetradecyloxy-2-fluoric acid) is a ACC (Acetyl-CoA carboxylase- $\alpha$ ) inhibitor, blocking the carboxylation of acetyl-CoA to Malonyl CoA. To understand the mechanism of apoptosis of PMCT inhibitor, we measured the effect of TOFA on fatty acid synthesis and survival of HepG2 cells. Apoptosis was quantified by JC-1 dye staining, which was detected mitochondrial membrane potential using flow cytometry. Cells were pretreated with TOFA for 1 h and then exposed to 2.5 mM PMCT inhibitor for 12 h. As shown in figure 23A, TOFA was nontoxic to HepG2 cells and rescues cells from PMCT inhibitor-induced apoptosis. The percentage of the control group stained with JC-1 showed only 8.64% of green intensity, indicating cells were in the high  $\Delta\Psi_m$ . Cells with depolarization of  $\Delta\Psi_m$  induced by 2.5 mM of PMCT inhibitor for 12 h. They were presented an increase of green fluorescence intensity to 21.64%. After treatment of 2.5 mM PMCT inhibitor combine with 10  $\mu\text{g/ml}$  of TOFA, the green fluorescence intensity reduced to 14.95%. Moreover, C75 showed a decreased of green fluorescence intensity from 34.42% to 17.79%. No significantly alteration showed in figure 23B. This finding suggested that TOFA was not toxic and rescue cells from apoptosis in the fatty acid synthesis inhibition. In order to know whether cell apoptosis was related to fatty acid level or not, we measured the effect of fatty acid synthesis inhibitor including TOFA, PMCT inhibitor and C75 on the fatty acid level in HepG2 cells. As shown in figure 23C, PMCT inhibitor, C75, TOFA and including combination of TOFA and PMCT inhibitor or C75 showed a significantly reduced fatty acid level compared to control cells. This results indicated that fatty acid starvation from fatty acid synthesis inhibitor, was not the major source of cytotoxicity. Accumulation of malonyl-CoA, resulting from inhibition of fatty acid synthesis might established cytotoxicity and led to apoptosis in HepG2 cells.



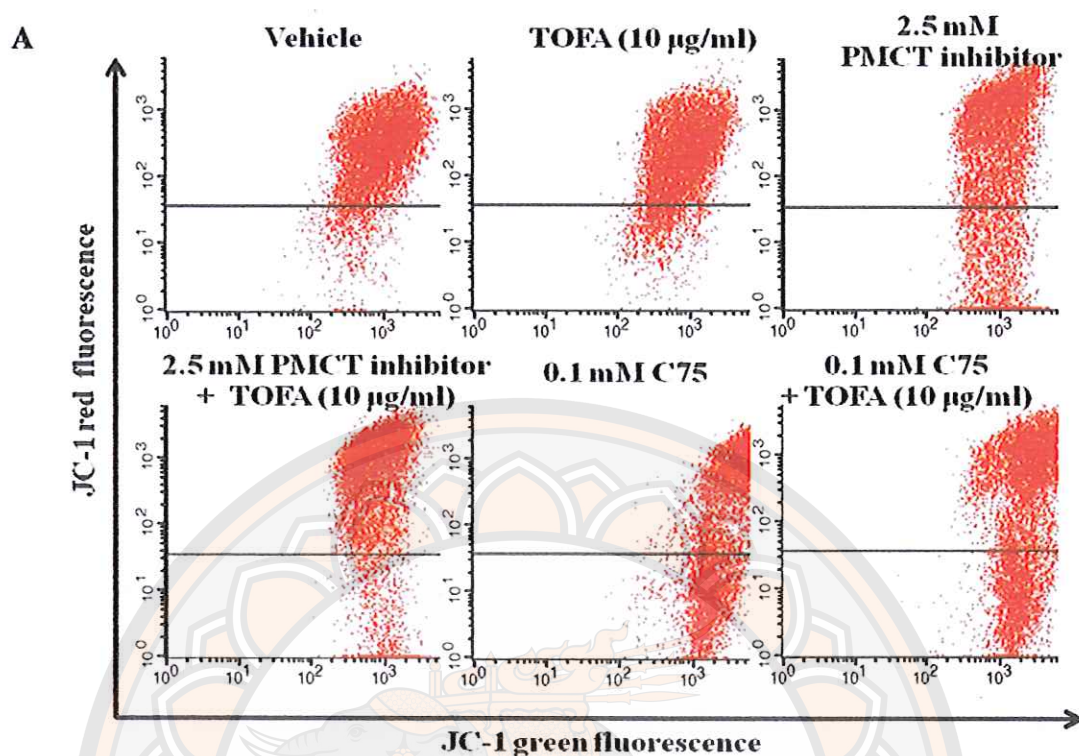
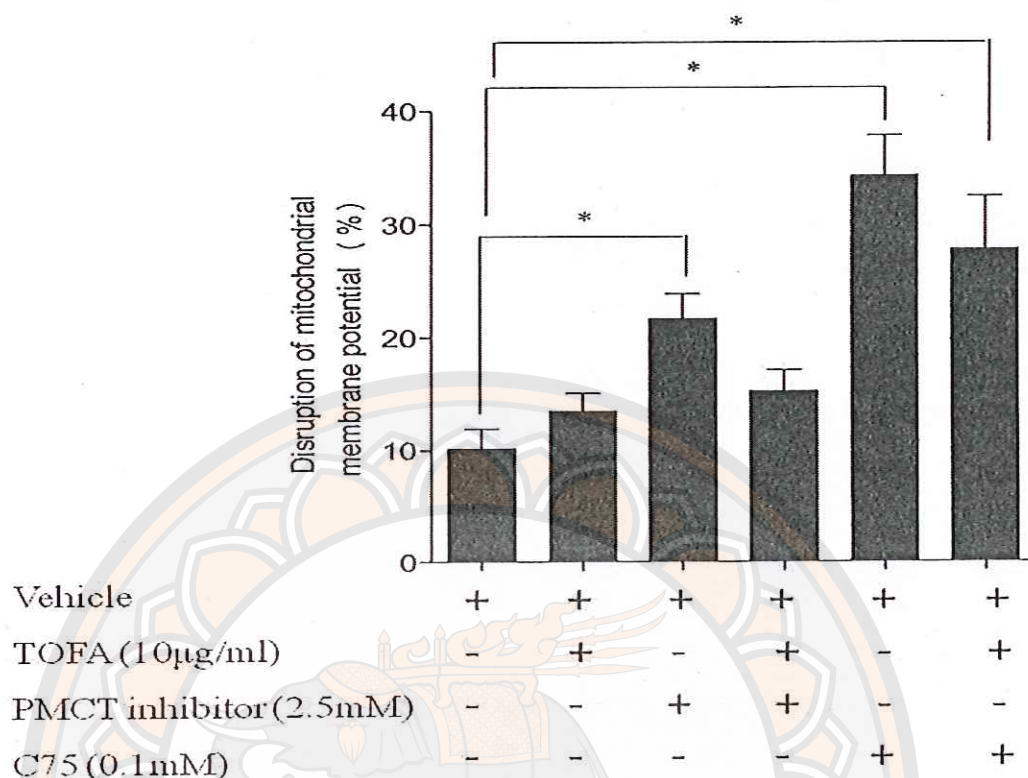


**Figure 23** Effect of PMCT inhibitor, C75 and TOFA on mitochondrial membrane potential and fatty acid level. (After treated cells with 2.5mM PMCT inhibitor or C75 only and TOFA combined with PMCT inhibitor or C75 for 12 h, cells were detected fatty acid synthesis and survival of HepG2 cells. (A) Cells were measured the mitochondrial membrane potential by JC-1 dye staining. A scatterplot represented a flow cytometry data.)

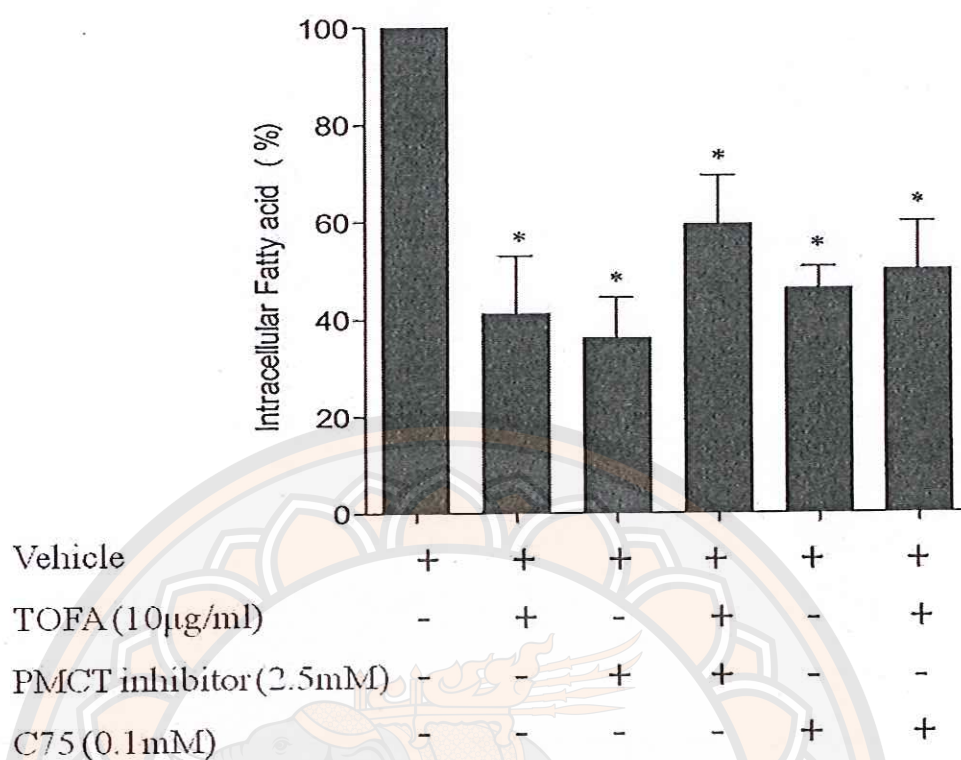
B



(B) From the flow cytometry experiment, The percentage of disruption of mitochondrial membrane potential was increased by PMCT inhibitor and C75 treatment in HepG2 cells compared to control. In contrast, cells were treated TOFA only and TOFA combined PMCT inhibitor was no alteration compared to control. It meant TOFA rescue cells from apoptosis. However, TOFA combined C75 was decreased a loss of mitochondrial membrane potential with no significantly compared to control.

Figure 23 (cont.)

C



(C) The percentage of intracellular fatty acid expressed in bar charts showing a reduction of fatty acid level in cells which were treated fatty acid synthesis inhibitor including PMCT inhibitor, C75 and TOFA. Data indicated mean  $\pm$  SEM from at least three independent experiments performed in triplicates. \*  $p < 0.05$  significantly different from the control.

Figure 23 (cont.)



### 7. The effect of PMCT inhibitor on CPT-1 activity

Carnitine palmitoyltransferase 1 (CPT-1) is an enzyme that enters a long-chain fatty acids into mitochondria for  $\beta$ -oxidation. It is a site for intracellular regulation of fatty acid metabolism, with malonyl-CoA acting as a physiological inhibitor. To examine the effect of PMCT inhibitor on CPT-1 activity, HepG2 cells were treated with TOFA (10  $\mu$ g/ml), PMCT inhibitor (2.5 mM), C75 (0.1 mM) and 0.2% DMSO for 24 h. CPT-1 activity was measured by mitochondrial extraction and adding reaction mix as described in material and method. As shown in figure 24, TOFA had no effect on CPT-1 activity (101.14% compared to 100% control). The percentage of CPT-1 activity of C75 treated cells was increased to 114.57%. This result supported that C75 directly stimulates CPT-1 activity increasing fatty acid oxidation in previous study. In contrast, cells were treated PMCT inhibitor reduced CPT-1 activity from 100% control to 57.23%. It meant PMCT inhibitor suppressed fatty acid synthesis and increased malonyl-CoA, inhibited CPT-1 activity and may no activation of  $\beta$ -oxidation in HepG2 cells.

## CHAPTER V

### DISCUSSION AND CONCLUSIONS

#### **Part I: The effect of PMCT inhibitor on apoptosis in HepG2 cells**

In this study, we investigate the inhibitory effect of PMCT inhibitor on proliferation of HepG2 cells in a dose-dependent manner. This results show that PMCT inhibitor significantly decreases cell viability on HepG2 cells similar effects of several natural chemical such as quercetin (Ana Belén, et al., 2006) capsaicin (Shang, et al., 2009) and curcumin (Fan, et al., 2014). This finding indicates that PMCT inhibitor causes cytotoxic effect on HepG2 cells. In addition, apoptosis assay was measured by flow cytometry, the result showed the percentages of apoptotic cells in both of early and late stages increased with PMCT inhibitor treatment. It means PMCT inhibitor can induces apoptosis in HepG2 cells.

Moreover, We investigated the pathways of cell apoptosis to understand how cancer cell respond to PMCT inhibitor. Intrinsic apoptotic pathway investigated by the alteration of mitochondrial membrane potential. The results show significant on increases in the loss of mitochondria membrane potential when cells were treated with PMCT inhibitor, demonstrating PMCT inhibitor could changes the potential of mitochondria and induces process of intrinsic apoptotic pathway. Furthermore, PMCT inhibitor can activated the activity of caspase-8, which is effector protein induced by death receptors in extrinsic apoptotic pathway. This investigator suggests that PMCT inhibitor induces apoptosis through the intrinsic and extrinsic pathway. PMCT inhibitor maybe have an effect on HepG2 cells same as 5-fluorouracil, which a chemotherapeutics drugs. In the previous study reported that the activation of caspase-8 and caspase-3 mediates 5-fluorouracil induced apoptosis in HepG2 cells. (Yi and Yang, 2003).



## Part II: The mechanism of PMCT inhibitor on HepG2 cells apoptosis.

Mitochondria are both source and target of reactive oxygen species (ROS), which could induce apoptosis in several cancer cell in many different cell system. ROS such as superoxide ( $O^{\cdot-}$ ) and hydrogen peroxide ( $H_2O_2$ ) play a key role in a cell death in cancer cells (Simon, 2000). In recent study have reported that piperine promoted minimal superoxide anion production and more hydroxyl radical production, which induces apoptosis in rectal cancer cells (Yaffe, 2013). Ample evidence showed that apoptosis of colon cancer cells through a p53-independent pathway could be regulated by the decrease of mitochondrial membrane potential and intracellular ROS accumulation (Wang, et al., 2013). It has been report to confirm that ROS causes the loss of mitochondria transmembrane permeabilization, thereby causing of the cytochrome c release and the caspase-9 and -3 activation. Moreover, ROS contributes to further activation of p53 trough activation of p38 kinase and induces apoptosis in HepG2 cells (Huang, 2008). We also found that the PMCT inhibitor greatly enhanced production of intracellular ROS and this result relates to the loss of mitochondrial membrane potential in HepG2 cells. This finding suggests that PMCT inhibitor could induced ROS generation and lead to loss of mitochondrial membrane potential, which is prior of apoptotic process.

However, In recent study have indicated that induction of apoptosis in HepG2 cells by ROS production led to endoplasmic reticulum stress (ERS), which a condition of unfolded protein accumulation in the endoplasmic reticulum. ERS could increased the level of intracellular cellular calcium ( $[Ca^{2+}]_i$ ), which a second messenger and regulator of cell apoptosis. Furthermore, the blocking of ERK1/2 pathway was regulated by ROS-activated ERS, affect to  $Ca^{2+}$  release. It means that HepG2 cells could be apoptosis trough a ROS-ERS- $Ca^{2+}$  mediated ERK pathway (Wang, 2013).

Moreover, we investigated that PMCT inhibitor-induced apoptosis was associated with inhibition of *de novo* fatty acid synthesis. Thus, we also assumed that the inhibition of fatty acid synthesis by PMCT inhibitor may be a mechanism of apoptosis in HepG2 cells.



It has been reported that a reduction of activity of NaCT or INDY (I'm not dead yet) originally discovered in *Drosophila* causes a decrease of body size and fat content which leads to increase of average life-span. It means that the inhibition of PMCT activity extending life-span involves prevention obesity, decrease fatty acid and cholesterol biosynthesis (Sun, 2010). This study also found that PMCT inhibitor can decreased intracellular citrate, fatty acid and triglyceride levels in HepG2 cells. In contrast, PMCT inhibitor showed no alteration of abundance expression of FASN, ACC, and ACLY, which are *de novo* fatty acid synthesis enzyme proteins. This finding suggest that PMCT inhibitor inhibited *de novo* fatty acid synthesis pathway without protein expressions modify. However, we assumed that PMCT inhibitor may be affect to activity of protein enzymes.

The many experimental studies have suggested that treatment with pharmacologic inhibitor of FASN such as C75 induced cell growth inhibition and apoptosis in cancer cells (Ho, et al., 2007). The FAS gene in cancer cell significantly up-regulated by hypoxia, which attend by reactive oxygen species (ROS) generation. Hypoxia significantly up-regulated sterol regulatory-element binding protein (SREBP-1), the major transcriptional regulator of the FAS gene. SREBP-1 activated via phosphorylation of Akt followed by activation of hypoxia-inducible factor 1 (HIF-1) (Furuta, et al., 2008). It has been reported that C75, which is FASN inhibitor induce apoptosis trough down-regulate phosphorylation or expression of effector such as PI3K, AKT and mTOR (Tomek, 2011). Moreover, It has been reported that a FASN inhibitor could induced apoptosis trough blocked the activation of the oncogene HER2 and downstream signaling pathways ERK1/2 MAPK and PI3K/AKT (Puig, et al., 2009).

Many study have established that decrease of fatty acid levels lead to apoptosis in cancer cells. Apoptosis may relate to the depletion of fatty acid products such as phospholipid. The major phospholipid in eukaryote cells is phosphatidylcholine, which is synthesized from the endogenous fatty acid synthesis. It is the precursor for other major phospholipid biosynthesis in proliferating cells. (Ridgway, 2013). Thus, the inhibition of *de novo* fatty acid affected to synthesis of cell membrane during cell proliferation and lead to apoptosis (Jackowski, et al., 2000).

Furthermore, inhibition of fatty acid synthesis contributes to an accumulation of malonyl-CoA by reducing the inhibitory effect of the newly synthesized fatty acid on ACC enzyme activity (Mason, 2012). The high malonyl-CoA levels induced cytotoxicity appears to be involved with an inhibition of carnitine palmitoyltransferase-I (CPT-1) activity, preventing the oxidation of newly synthesized fatty acids (Puig, 2009). CPT-1 oxidized fatty acids into the mitochondrial matrix for  $\beta$ -oxidation and for sphingolipid ceramide synthesis. An accumulation of ceramide after inhibition of CPT-1 by malonyl-CoA plays a vital role in apoptosis induction. In addition, several studies reported that ceramide analogues and ceramidase inhibitors could induced rapid cell death through activation of various proapoptotic molecules in cancer but not normal cells, such as caspases and cytochrome *c* (Selzner, et al., 2001) or BNIP3, TRAIL, and DAPK2 (Bandyopadhyay, 2006). However, it has been reported that CPT-1 blockade by etomoxir did not rescue cells from C75 cytotoxicity. In contrast, ACC inhibitor by TOFA can protected cells from C75 induced apoptosis, suggesting that high level of malonyl-CoA likely plays an important role in C75 induced cytotoxicity, but not through CPT-1 (Zhou, 2007).

In this present study also shows that TOFA (ACC inhibitor) was nontoxic to HepG2 cells even fatty acid level was decreased. In contrast, PMCT inhibitor and C75 decreased fatty acid level and induced apoptosis. However, TOFA could rescues cells from PMCT inhibitor-induced apoptosis even fatty acid level was decreased. This findings indicate that a lower of fatty acid level lead to malonyl-CoA accumulation and induced apoptosis. In contrast, the inhibition of malonyl-CoA by TOFA was rescued cell from apoptotic. Thus, malonyl-CoA likely plays an important role in PMCT inhibitor-induced apoptosis in HepG2 cells and fatty acid starvation was not the major cause of apoptosis.

In addition, this study found that PMCT inhibitor suppress CPT-1 activity but stimulates in C75 treatment group. This finding suggest that C75 is directly activates CPT-1 activity (Nicot, et al., 2004). In contrast, PMCT inhibitor induces apoptosis and inhibited CPT-1 activity via accumulation of malonyl-CoA in HepG2 cells.

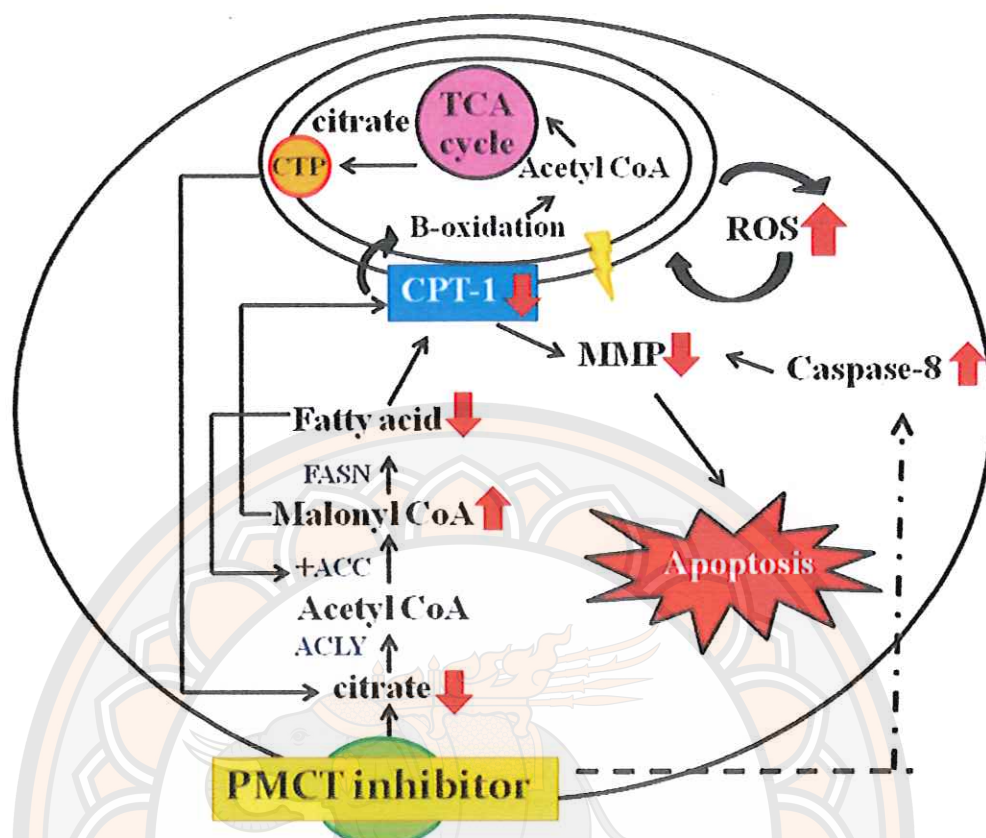


The diagram illustrates the metabolic pathways of fatty acid oxidation and ketone body metabolism. Fatty acid enters the mitochondrion and is converted to Malonyl CoA by FASN. Malonyl CoA is then converted to Acetyl CoA by ACC. Acetyl CoA enters the TCA cycle via B-oxidation, producing Acetyl CoA and Citrate. Citrate is converted to CTP by CPT-1. CTP is then converted to Citrate by CPT-2. Citrate is converted to Acetyl CoA by CPT-3. Acetyl CoA is then converted to ROS by CPT-4. The diagram also shows the conversion of Citrate to Acetyl CoA by CPT-5. The background features a watermark of a Thai elephant and the text 'มหาวิทยาลัยเทคโนโลยีพระจอมเกล้าธนบุรี' (Mahavithayalai King Pra Jomklao Thaburi).

**Figure 25** Summary of the proposed mechanism for the apoptosis induced by PMCT inhibitor in HepG2 cells. ((A) Citrate is substrate for *de novo* fatty acid synthesis pathway in cancer cell.)



B



(B) The results in PMCT inhibition, It could reduces citrate, decreased fatty acid and leads to accumulation of malonyl-CoA, resulting apoptosis in HepG2 cells. In addition, PMCT inhibitor promoted ROS generation, which induces apoptosis through intrinsic pathway via disrupted mitochondrial membrane potential, Moreover, caspase-8 activity was increased in HepG2 cells. It indicated that PMCT inhibitor could induced apoptosis through extrinsic pathway too.

Figure 25 (cont.)



## REFERENCES

มหาวิทยาลัยจุฬาลงกรณ์

## REFERENCES

- Ana Belén G.-S., María A. M., Laura B., Luis G. and Sonia R. (2006). Quercetin Induces Apoptosis via Caspase Activation, Regulation of Bcl-2, and Inhibition of PI-3-Kinase/Akt and ERK Pathways in a Human Hepatoma Cell Line (HepG2). **J Nutr**, 136, 2715-2721.
- Bandyopadhyay S., Zhan R., Wang Y., Pai S. K., Hirota S., Takano Y., et al. (2006). Mechanism of apoptosis induced by the inhibition of fatty acid synthase in breast cancer cells. **Cancer Research**, 66, 5934-5940.
- Bialecki E. and Di Bisceglie A. (2005). Diagnosis of hepatocellular carcinoma. **HPB:Official Journal of The International Hepato Pancreato Biliary Association**, 7, 26-34.
- Biswas S., Lunec J. and Bartlett K. (2012). Non-glucose metabolism in cancer cells is it all in the fat? **Cancer Metastasis Rev**, 31, 689-698.
- Boatright K. M. and Salvesen G. S. (2003). Mechanisms of caspase activation. **Current Opinion in Cell Biology**, 15, 725-731.
- Crack P. J. and Taylor J. M. (2005). Reactive oxygen species and the modulation of stroke. **Free Radical Biology and Medicine**, 38, 1433-1444.
- De Schrijver E., Brusselmans K., Heyns W., Verhoeven G. and Swinnen J. V. (2003). RNA interference-mediated silencing of the fatty acid synthase gene attenuates growth and induces morphological changes and apoptosis of LNCaP prostate cancer cells. **Cancer Res**, 63, 3799-3804.
- Elmore S. (2007). Apoptosis: A Review of Programmed Cell Death. **Toxicologic Pathology**, 35, 495-516.
- El-Serag H. B. (2011). Hepatocellular Carcinoma. **New England Journal of Medicine**, 365, 1118-1127.
- Fan H., Tian W., Ma X. and Ma X. (2014). Curcumin induces apoptosis of HepG2 cells via inhibiting fatty acid synthase. **Target Oncol**, 9, 279-286.
- Fei Y. J., Liu J., Inoue K., Zhuang L., Miyake K., Miyauchi S., et al. (2004). Relevance of NAC-2, an Na<sup>+</sup>-coupled citrate transporter, to life span, body size and fat content in *Caenorhabditis elegans*. **Biochem**, 379, 191-198.



- Fiorentino M., Zadra G., Palescandolo E., Fedele G., Bailey D., Fiore C., et al. (2008). Overexpression of fatty acid synthase is associated with palmitoylation of Wnt1 and cytoplasmic stabilization of beta-catenin in prostate cancer. **Lab Invest**, 88, 1340-1348.
- Fleury C., Mignotte B. and Vayssiere J. L. (2002). Mitochondrial reactive oxygen species in cell death signaling. **Biochimie**, 84, 131-141.
- Furuta E., Pai S. K., Zhan R., Bandyopadhyay S., Watabe M., Mo Y. Y., et al. (2008). Fatty Acid Synthase Gene Is Up-regulated by Hypoxia via Activation of Akt and Sterol Regulatory Element Binding Protein-1. **Cancer Research**, 68, 1003-1011.
- Gelebart P., Zak Z., Anand M., Belch A. and Lai R. (2012). Blockade of fatty acid synthase triggers significant apoptosis in mantle cell lymphoma. **PLoS One**, 7, 33738-33747.
- Ho T. S., Ho Y., Wong W. Y., Chi M., Chiu L. and Eng-Choon O. V. (2007). Fatty acid synthase inhibitors cerulenin and C75 retard growth and induce caspase-dependent apoptosis in human melanoma A-375 cells. **Biomed Pharmacother**, 61, 578-587.
- Huang J., Wu L., Tashiro S.-i., Onodera S. and Ikejima T. (2008). Reactive Oxygen Species Mediate Oridonin-Induced HepG2 Apoptosis Through p53, MAPK, and Mitochondrial Signaling Pathways. **Journal of Pharmacological Sciences**, 107, 370-379.
- Icard P., Poulain L. and Lincet H. (2012). Understanding the central role of citrate in the metabolism of cancer cells. **Biochimica et Biophysica Acta (BBA) Reviews on Cancer**, 1825, 111-116.
- Inoue K., Zhuang L., Maddox D. M., Smith S. B. and Ganapathy V. (2002). Structure, function, and expression pattern of a novel sodium-coupled citrate transporter (NaCT) cloned from mammalian brain. **J Biol Chem**, 277, 39469-39476.
- Jackowski S., Wang J. and Baburina I. (2000). Activity of the phosphatidylcholine biosynthetic pathway modulates the distribution of fatty acids into glycerolipids in proliferating cells. **Biochim Biophys Acta**, 1483, 301-315.

- Jose C., Bellance N. and Rossignol R. (2011). Choosing between glycolysis and oxidative phosphorylation: a tumor's dilemma? **Biochim Biophys Acta**, 1807, 552-561.
- Koukourakis M., Giatromanolaki A., Harris A. L. and Sivridis E. (2006). Comparison of metabolic pathways between cancer cells and stromal cells in colorectal carcinomas: a metabolic survival role for tumor-associated stroma. **Cancer Research**, 66, 632-637.
- Koukourakis M., Pitiakoudis M., Giatromanolaki A., Tsarouha A., Polychronidis A., Sivridis E., et al. (2006). Oxygen and glucose consumption in gastrointestinal adenocarcinomas: correlation with markers of hypoxia, acidity and anaerobic glycolysis. **Cancer Sci**, 97, 1056-1060.
- Lin V. C., Tsai Y. C., Lin J. N., Fan L. L., Pan M. H., Ho C. T., et al. (2012). Activation of AMPK by pterostilbene suppresses lipogenesis and cell-cycle progression in p53 positive and negative human prostate cancer cells. **J Agric Food Chem**, 60, 6399-6407.
- Mashima T., Seimiya H. and Tsuruo T. (2009). De novo fatty-acid synthesis and related pathways as molecular targets for cancer therapy. **British Journal of Cancer**, 100, 1369-1372.
- Mason P., Liang B., Li L., Fremgen T., Murphy E., Quinn A., et al. (2012). SCD1 inhibition causes cancer cell death by depleting mono-unsaturated fatty acids. **PLoS One**, 7, 33823-33830.
- Nicot C., Napal L., Relat J., Gonzalez S., Llebaria A., Woldegiorgis G., et al. (2004). C75 activates malonyl-CoA sensitive and insensitive components of the CPT system. **Biochem Biophys Res Commun**, 3, 660-664.
- Pandey P., Okuda H., Watabe M., Pai S. K., Liu W., Kobayashi A., et al. (2011). Resveratrol suppresses growth of cancer stem-like cells by inhibiting fatty acid synthase. **Breast Cancer Res Treat**, 130, 387-398.
- Paumen M., Ishida Y., Muramatsu M., Yamamoto M. and Honjo T. (1997). Inhibition of carnitine palmitoyltransferase I augments sphingolipid synthesis and palmitate-induced apoptosis. **J Biol Chem**, 272, 3324-3329.



- Pizer E. S., Thupari J., Han W. F., Pinn M. L., Chrest F. J., Frehywot G. L., et al. (2000). Malonyl-coenzyme-A is a potential mediator of cytotoxicity induced by fatty-acid synthase inhibition in human breast cancer cells and xenografts. **Cancer Research**, 60, 213-218.
- Puig T., Turrado C., Benhamu B., Aguilar H., Relat J., Ortega-Gutiérrez S., et al. (2009). Novel Inhibitors of Fatty Acid Synthase with Anticancer Activity. **Clin Cancer Res**, 15, 7608-7615.
- Resendis-Antonio O., Checa A. and Encarnación S. (2010). Modeling Core Metabolism in Cancer Cells: Surveying the Topology Underlying the Warburg Effect. **PLoS ONE**, 5, 12383-12393.
- Ridgway N. D. (2013). The role of phosphatidylcholine and choline metabolites to cell proliferation and survival. **Crit Rev Biochem Mol Biol**, 48, 20-38.
- Rodriguez-Enriquez S., Cárreno-Fuentes L., Gallardo-Perez J. C., Saavedra E., Quezada H., Vega A., et al. (2010). Oxidative phosphorylation is impaired by prolonged hypoxia in breast and possibly in cervix carcinoma. **Int J Biochem Cell Biol**, 42, 1744-1751.
- Rogina B. (2000). Extended Life-Span Conferred by Cotransporter Gene Mutations in *Drosophila*. **Science**, 290, 2137-2140.
- Scott D., Richardson A. D., Filipp F. V., Knutzen C. A., Chiang G. G., Ronai Z. A., et al. (2011). Comparative metabolic flux profiling of melanoma cell lines: beyond the Warburg effect. **J Biol Chem**, 286, 42626-42634.
- Selzner M., Bielawska A., Morse M. A., Rudiger H. A., Sindram D., Hannun Y. A., et al. (2001). Induction of apoptotic cell death and prevention of tumor growth by ceramide analogues in metastatic human colon cancer. **Cancer Research**, 61, 1233-1240.
- Shang P. H., Jung C. C., Chih C. W., Chi T. C., Nou Y. T., Ho Y. T., et al. (2009). Capsaicin-induced Apoptosis in Human Hepatoma HepG2 Cells. **ANTICANCER RESEARCH**, 29, 165-174.
- Smolkova K., Plecita-Hlavata L., Bellance N., Benard G., Rossignol R., Ježek P., et al. (2011). Waves of gene regulation suppress and then restore oxidative phosphorylation in cancer cells. **Int J Biochem Cell Biol**, 43, 950-968.



- Simon H. U., Haj-Yehia A. and Levi-Schaffer F. (2000). Role of reactive oxygen species (ROS) in apoptosis induction. **Apoptosis**, 5, 415-418.
- Sun J., Aluvila S., Kotaria R., Mayor J. A., Walters D. E., Kaplan S. R., et al. (2010). Mitochondrial and Plasma Membrane Citrate Transporters: Discovery of Selective Inhibitors and Application to Structure/Function Analysis. **Molecular and cellular pharmacology**, 2, 101-110.
- Wang C. L., Liu C., Niu L. L., Wang L. R., Hou L. H., Cao X. H., et al. (2013). Surfactin-Induced Apoptosis Through ROS-ERS-Ca<sup>2+</sup>-ERK Pathways in HepG2 Cells. **Cell Biochemistry and Biophysics**, 67, 1433-1439.
- Wang C., Xu C., Sun M., Luo D., Liao D. F. and Cao D. (2009). Acetyl-CoA carboxylase- $\alpha$  inhibitor TOFA induces human cancer cell apoptosis. **Biochem Biophys Res Commun**, 385, 302-306.
- Warburg O. (1956). On the origin of cancer cells. **Science**, 123, 309-314.
- Wörns M. A. and Galle P. R. (2010). Future perspectives in hepatocellular carcinoma. **Dig Liver Dis**, 42, 302-309.
- Yaffe P. B., Doucette C. D., Walsh M. and Hoskin D. W. (2013). Piperine impairs cell cycle progression and causes reactive oxygen species-dependent apoptosis in rectal cancer cells. **Experimental and Molecular Pathology**, 94, 109-114.
- Yi T. B. and Yang L. Y. (2003). Caspase-8 in apoptosis of hepatoma cell induced by 5-fluorouracil. **Hepatobiliary Pancreat Dis Int**, 2, 98-101.
- Yoon S., Lee M. Y., Park S. W., Moon J. S., Koh Y. K., Ahn Y. H., et al. (2007). Up-regulation of acetyl-CoA carboxylase  $\alpha$  and fatty acid synthase by human epidermal growth factor receptor 2 at the translational level in breast cancer cells. **J Biol Chem**, 282, 26122-26131.
- Zheng J. (2012). Energy metabolism of cancer: Glycolysis versus oxidative phosphorylation. **Oncology Letters**, 4, 1151-1157.
- Zhou W., Han W. F., Landree L. E., Thupari J. N., Pinn M. L., Bililign T., et al. (2007). Fatty acid synthase inhibition activates AMP-activated protein kinase in SKOV3 human ovarian cancer cells. **Cancer Research**, 67, 2964-2971.

Zhou W., Simpson P. J., McFadden J. M., Townsend C. A., Medghalchi S. M.,  
Vadlamudi A., et al. (2003). Fatty acid synthase inhibition triggers apoptosis  
during S phase in human cancer cells. **Cancer Research**, 63, 7330-7337.





## APPENDIX



### Preparation of phosphate-buffered saline (PBS)

Reagent	Amount (for 1X solution)
NaCl	8 g
KCl	0.2 g
Na <sub>2</sub> HPO <sub>4</sub>	1.44 g
KH <sub>2</sub> PO <sub>4</sub>	0.24 g

PBS can be made as dissolve the reagents listed above in 800 mL of H<sub>2</sub>O. Adjust the pH to 7.4 with HCl, and then add H<sub>2</sub>O to 1 L. Store PBS at room temperature.

Source: [http://cshprotocols.cshlp.org/content/2006/1/pdb.rec8247.full?text\\_only=true](http://cshprotocols.cshlp.org/content/2006/1/pdb.rec8247.full?text_only=true)

### Protein extraction by MPER (Mammalian Protein Extraction Reagent)

HepG2 cells were plated and exposed to PMCT inhibitor at corresponding concentration and time intervals. Cells will be washed with PBS and then will be harvested by treatment with 0.25% trypsin-EDTA. Then cells will be lysed and extract the total protein using M-PER according the to the manufacturing instruction below;

Pellet the suspension of the cells after trypsinization step. The supernatant will be discard and cells will be washed by PBS buffer (pH 7.4). cells will be centrifuged again at 2500 x g for 10 minutes and add the appropriate amount of M-PER reagent to the cell pellet. For  $1 \times 10^6$  cells, add 100  $\mu$ l of M-PER. Then shake gentry for 10 minutes. Remove cell debris by centrifugation at 14,000 x g for 15 minutes. At the end, transfer the protein supernatant to a new tube for further analysis.

**Note:** before adding the M-PER reagent into the cell pellet, protease inhibitor should be added into the M-PER reagent before use.

Source: <https://www.thermofisher.com/order/catalog/product/78501>

### The protein concentration measurement by Pierce™ BCA Protein Assay Kit

Microplate Procedure (Sample to WR ratio = 1:8)

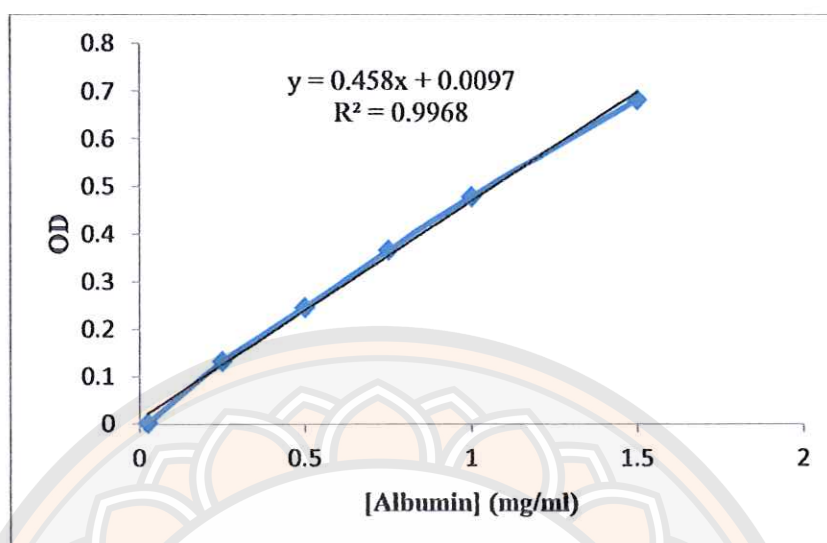
1. Pipette 20  $\mu$ L of each standard or unknown sample replicate into a microplate well
2. Add 160  $\mu$ L of the WR to each well and mix plate thoroughly on a plate shaker for 30 seconds.
3. Cover plate and incubate at 37°C for 30 minutes.
4. Cool plate to RT. Measure the absorbance at or near 590 nm on a plate reader.

**Note:** To prepare WR by mixing 50 parts of BCA Reagent A with 1 part of BCA Reagent B (50:1, Reagent A:B)

#### Preparation of diluted albumin (BSA) Standards

Final BSA Concentration	Volume of BSA (from stock)	Volume of dH <sub>2</sub> O	Total Volume of Diluted Standard
1.5 mg/ml	60 $\mu$ l	20 $\mu$ l	80 $\mu$ l
1 mg/ml	40 $\mu$ l	40 $\mu$ l	80 $\mu$ l
0.75 mg/ml	30 $\mu$ l	50 $\mu$ l	80 $\mu$ l
0.5 mg/ml	20 $\mu$ l	60 $\mu$ l	80 $\mu$ l
0.25 mg/ml	10 $\mu$ l	70 $\mu$ l	80 $\mu$ l
0.025 mg/ml	1 $\mu$ l	79 $\mu$ l	80 $\mu$ l

### The standard curve of BCA standard



Source: <https://www.thermofisher.com/order/catalog/product/23225>

### Preparation the SDS-polyacrylamide gel

	Lower gel (8%)	Upper gel (4%)
1. 30% acrylamide :Bis	2.7 ml	650 µl
2. Gel buffer pH 8.8 (Tris-HCl 1.5M)	2.5 ml	-
3. Gel buffer pH 6.8 (Tris-HCl 0.5 M)	-	1,250 µl
4. 10% SDS	100 µl	50 µl
5. Distilled water	4.7 ml	3,050 µl
6. TEMED	5 µl	5 µl
7. 10% APS (ammonium persulfate)	50 µl	25 µl



### Citrate assay

Citrate of HepG2 cells will be detected by the citrate assay kit (US Biological, MA, USA). Citrate is formed by the addition of oxaloacetate to the acetyl group of acetyl-CoA derived from the glycolysis. Citrate can be transported out of mitochondria and convert back to acetyl-CoA for fatty acid synthesis. In this assay, citrate will be converted to pyruvate via oxaloacetate. The pyruvate will be quantified by converting a nearly colorless probe to an intensely colored at 570 nm. According to the manufacturing instruction, the assay protocol is mentioned below;

#### 1. Standard curve preparations for fluorometric assay:

10  $\mu$ l of the citrate standard will be added to 990  $\mu$ l of deionized water ( $\text{dH}_2\text{O}$ ), mix well and then further dilute by adding 10  $\mu$ l to 90  $\mu$ l of  $\text{dH}_2\text{O}$  to dilute the citrate standard to 0.1 nmol/ $\mu$ l. 0, 2, 4, 6, 8, and 10  $\mu$ l will be added into a series of standard wells on a 96 well plate. The assay buffer will be added to adjust the volume to 50  $\mu$ l/well to generate 0, 0.2, 0.4, 0.6, 0.8, and 1.0 nmol/well of the standard.

#### 2. Sample preparation:

Cells ( $2 \times 10^6$ ) will be homogenized in 100  $\mu$ l of citrate assay buffer. The cell lysate will be centrifuged at 15,000 g for 10 min to remove cell debris. 1-50  $\mu$ l of sample will be added into duplicate wells of a 96 well plate and the assay buffer will be added to adjust volume of each well to 50  $\mu$ l.

Develop: Sufficient amount of reagent will be mixed. For each well, prepare a total 50  $\mu$ l reaction mix containing :

	Sample	Background Control*
Citrate assay buffer	44	46
Citrate enzyme mix	2	0
Developer	2	2
Citrate Probe**	2	2

\*Sample may contain oxaloacetate or pyruvate which can generate a background and need to be subtracted from the sample background signal.

\*\*For the fluorometric assay, citrate probe will be diluted 10X with DMSO to reduce fluorescent background.

50  $\mu$ l of the reaction mix will be added to each well containing the citrate standard and test sample. The plate will be incubated for 30 minutes at room temperature, protected from light. Measure the fluorescent at EX/EM 535/587 nm.

To calculate the citrate concentration: background will be corrected by subtracting the value of the 0 nmol/ $\mu$ l Citrate standard from all reading. Then the value of the Sample background control will be subtracted from the test sample. The standard curve was then plotted. The corrected sample readings will be applied to the standard curve to get citrate amount in the sample wells. The citrate concentrations in the test samples can be calculate as

$$C = Ay/Sv \text{ (nmol/}\mu\text{l ; or }\mu\text{mol/ml; or mM)}$$

Ay is the amount of citrate (nmol) in the sample from the standard curve.

Sv is the sample volume ( $\mu$ l) added to the sample well.

Citric acid molecular weight: 191 g/mol

### **Free fatty acid quantification assay**

The Free Fatty Acid Quantification Kit (US Biological ,MA, USA) used for detecting the long-chain free fatty acids. Free fatty acid is synthesized by the catalyzing of fatty acid synthase enzyme from Acetyl-CoA, malonyl-CoA and NADPH. Fatty Acids are converted to their CoA derivatives, which are afterwards oxidized with the concomitant generation of color or fluorescence then quantified by colorimetric method (spectrophotometry at OD = 570 nm). According to the manufacturing instruction, the assay protocols are mentioned below;

#### **1. Reagent Preparation:**

- Free fatty acid Probe : Dissolve in 220  $\mu$ l DMSO. Aliquot and store at -20  $^{\circ}$ C until the next used, protect from light and moisture.

- Enzymes: Dissolve ACS (acyl-CoA synthetase) reagent, and enzyme mix individually with 220  $\mu$ l assay buffer each by pipetting up and down. Aliquot and store at -20  $^{\circ}$ C until use.



## 2. Standard Curve Preparation for the fluorometric assay

The palmitic acid Standard will be diluted to 0.1 nmol/ $\mu$ l by adding 10  $\mu$ l of the standard to 90  $\mu$ l of assay buffer, mix well then add 0, 2, 4, 8, 8, 10  $\mu$ l into each well. into 96-well plate. Adjust volume to 50  $\mu$ l/well with assay buffer to generate 0, 0.2, 0.4, 0.6, 0.8, and 1.0 nmol/well of the Fatty acid standard.

## 3. Sample Preparation

After treatment, HepG2 cells  $1 \times 10^6$  cells can be extracted by homogenization with 200  $\mu$ l of chloroform-Triton X-100 (1% Triton X 100 in pure chloroform) in a microhomogenizer. The extract will be spun for 5-10 minutes at high speed in a microcentrifuge. The organic phase (lower phase) will be collected after centrifugation, air dry at 50  $^{\circ}$ C to remove chloroform and vacuum dry for 30 minutes to remove trace chloroform. The dried lipids will be dissolved in 200  $\mu$ l of Fatty acid assay buffer by vortexing extensively for 5 minutes and use 1-50  $\mu$ l of the extracted sample per assay.

Add 2  $\mu$ l ACS reagent into all the standard and sample wells. Mix well; incubate the reaction at 37  $^{\circ}$ C for 30 minutes

4. Reaction Mix Preparation: Mix enough reagents for the number of assays to be performed: For each well, prepare a total 50  $\mu$ l Reaction Mix containing:

- 44  $\mu$ l assay buffer
- 2  $\mu$ l Fatty acid Probe
- 2  $\mu$ l ACS Enzyme Mix
- 2  $\mu$ l Enhancer

Add 50  $\mu$ l of the reaction Mix to each well containing the standard or test sample. Incubate the reaction for 30 minute at 37  $^{\circ}$ C, protect from light. Measure the fluorescence at Ex/Em = 535/590 nm in a micro plat reader.

## 5. Calculations the amount of free fatty acid

Plot standard curve nmol/well vs. fluorescence reading. Next apply the sample readings to the standard curve to obtain Fatty acid amount in the sample wells.

Fatty Acid Concentration =  $Fa/Sv$  (nmol/  $\mu$ l or mM)

Fa is the Fatty acid amount (nmol) in the well obtained from standard curve.

Sv is the sample volume ( $\mu$ l) added to the sample well.



### Triglyceride Quantification assay (US Biological ,MA, USA)

Triglycerides (TG) are the main constituent of vegetable oil, animal fat, LDL and VLDL, and play an important role as transports of fatty acids and glycerol, after which both can serve as substrate for energy producing and metabolic pathways. TG is one of the product from the fatty acid synthesis pathway. It is formed by combining glycerol with three molecules of fatty acid .In the assay, TG are convert to free fatty acids and glycerol. The glycerol is then oxidize to generate a product which reacts with the probe to generate color (spectrophotometry at 570 nm) and fluorescence (Ex/Em=535/587 nm).

#### 1. Reagent Preparation:

- Triglyceride Probe is ready to use as supply. It will be warmed by placing in a 37°C bath for 1-5 minutes to thaw the DMSO solution before use.
- Triglyceride Standard is frozen storage and it may cause the standard to separate from the aqueous phase. To re-dissolve the standard, kept the cap tightly closed. Then place in a hot water bath (~80-100 °C) for 1 minute or until the standard looks cloudy. Then mix by vortexing for 30 seconds. The heating and vortexing were repeated one more time.
- Triglyceride Enzyme Mix: Dissolve the Triglyceride Enzyme mix in 220 µl of Triglyceride assay buffer. Aliquot and store at – 20 °C until the next used.
- Lipase: Dissolve lipase in 220µl Triglyceride assay buffer, mix well. Aliquots the lipase and store at – 20 °C until the next used.

#### 2. Standard Curve Preparation for the fluorometric assay

Dilute the Triglyceride Standard to 0.01-0.1 mM with Triglyceride assay buffer. Take each concentration of Triglyceride Standard 50 µl into duplicate wells of a 96 well plate.

#### 3. Sample Preparation:

HepG2 cells will be treated with various concentration of PMCT inhibitor.  $1 \times 10^6$  cells can be extract by homogenization in 1 ml 5% Triton-X100 in water. Then slowly heat the sample to 80-100 °C in a water bath for 2-5 minutes or until the Triton X- 100 become cloudy. Slowly cool down to room temperature and repeat the heating one more time to solubilize all triglyceride into solution. The supernatant will be centrifuged for 5 minutes to remove any insoluble materials and dilute 10 fold with

dH<sub>2</sub>O before the assay. Add lipase 2 µl in to each standard and sample well, mix well and incubate for 20 minutes at room temperature to convert triglyceride to glycerol and fatty acid.

4. Triglyceride Reaction Mix: Mix enough reagent for the number of samples and standards to be performed. For each well, prepare a total 50 µl Reaction Mix containing:

- 46 µl Triglyceride Assay buffer
- 2 µl Triglyceride Probe\*
- 2 µl Triglyceride Enzyme Mix\*

For the fluorescent assay, dilute the probe and enzyme mix 10x with DMSO and assay buffer respectively to reduce the background readings.

Add 50 µl of the reaction mix to each well containing the triglyceride standard, test sample and controls. Mix well. Incubate at room temperature for 30-60 minutes. Protect from light. Measure at Ex/Em = 535/590 nm for Fluorescence assay in a microtiter plate reader.

The amount of triglyceride will be calculated by plot the standard curve nmol/well vs. fluorescence reading and apply the sample readings to the standard curve. Triglyceride amount in the sample wells can be calculated:

$$C = Ts/Sv \text{ nmol/}\mu\text{l or } \mu\text{mol/ml or mM}$$

Ts is triglyceride amount from standard curve (nmol)

Sv is the sample volume (before dilution) added in sample wells (µl)



### The calculation of fluorescence intensity

CTCF = Integrated Density – (Area of selected cell X Mean fluorescence of background readings)

Note : CTCF stand for corrected total cell fluorescence

	Area	Mean	STDEV	Max	IntDen	RawIntDen	CTCF	%
1	860	7.833	4.437	24	6736	6736	6669.2	158.4
2	680	6.1	4.327	22	4148	4148	4095.2	97.3
3	640	5.589	5.243	20	3577	3577	3527.3	83.8
4	588	8.665	6.398	25	5095	5095	5049.3	119.9
5	421	8.501	6.273	28	3579	3579	3546.3	84.2
6	690	6.612	4.972	25	4562	4562	4508.4	107.1
7	508	8.388	4.693	22	4261	4261	4221.6	100.3
8	451	6.171	4.502	21	2783	2783	2747.9	65.3
9	448	7.199	5.911	24	3225	3225	3190.2	75.8
10	577	7.972	6.172	26	4600	4600	4555.2	108.2
Mean	586.3	7.303	5.293	23.7	4256.6	4256.6	4211.1	100
SD	136.75	1.123	0.823	2.452	1117.042	1117.042		
Min	421	5.589	4.327	20	2783	2783		
Max	860	8.665	6.398	28	6736	6736		

### Background

	Area	Mean
1	638	0.154
2	708	0.011
3	592	0.068
BG average		0.078

Source: <http://sciencetechblog.com/2011/05/24/measuring-cell-fluorescence-using-imageJ/>